ISSN1000-9620

Marine Science Bulletin

Volume 1 • Number 1 1999

LIBRARY
Pacific Islands Fisheries Science Center
NOAA Fisheries
Honolulu, Hawai'i

ISSN 1000-9620
01>
9 771000 962001

NATIONAL MARINE DATA AND
INFORMATION SERVICE OF CHINA

NOAA
U.S. DEPARTMENT OF COMMERCE
NATIONAL OCEANIC AND ATMOSPHERIC ADMINISTRATION

LIBRARY
APR 2 3 2002
National
Atmospheric
U.S. Dep

MARINE SCIENCE BULLETIN

Vol. 1 No. 1 May 1999

CONTENT

Wave-induced Seabed Response and Influence on Stability of Structures
..... *Bie Shean*(别社安) and *Zhao Zidan*(赵子丹)(1)
Characteristics of Water Type Distribution and Seasonal Variations in the Southern East China Sea ..... *Miao Yutian*(苗育田) and *He Dehua*(何德华)(11)
El Nino Effect on SST, Wave and Sea State in the Nansha Islands Waters
..... *Ke Dongsheng*(柯东胜) and *Xu Shigeng*(许时庚)(25)
The Impacts of Sea Level Rise on the Coastal Areas to the West of the Bohai Bay
..... *Liu Zhenxia*(刘振夏) and *Xia Dongxing*(夏东兴)(30)
On the Solution of the Boundary Layer Equation for the Laminar Boundary Layer between Parallel Streams ..... *Li Xinming*(李心铭) and *Zhen Li*(41)
On Sustainable Development of Marine Resources in Bohai Area .....
..... *Jiang Tieming*(蒋铁民)(58)
On the Rational Utillization of Coastal Resources of the Shandong Province
..... *Zhao Quanji*(赵佺基) (64)
Oceanographic Condition in the Distribution Areas of Anchovy Engraulis Japonicas in the Yellow Sea and East China Sea ..... *Chen Jufa*(陈聚法) (68)
Sporopollen Assemblage Characteristics of Surface Sediments in Offshore Area of the Western Bohai Sea ..... *Xu Jiasheng*(徐家声) and *Sun Tingzhi*(孙庭智)(83)

Wave-Induced Seabed Response and Influence on Stability of Structures

Bie Shean and Zhao Zidan
Tianjin University, Tianjin, 300072

Abstract Wave-induced transient response of displacements, effective stresses and pore pressure in saturate seabed are solved by a consolidation finite element method. The influence of the responses to the stability of seabed and coastal structures is shown by an improved slice method with circular arc slip surface. Dynamic elastic consolidation theory and linear permeability theory are employed in the solution of seabed response. The seabed can be consisted of layered soil with arbitrary boundaries. The acting wave can be regular or irregular. Irregular wave pressure acting on the surface of seabed is calculated by linear superposition method. Wave-induced excess stress on the slip surface is considered in the stability analysis. The spatial and temporal variations of pore pressure in sandy seabed compare well with experiment. Calculations for a vertical breakwater show that the safety factor of seabed and structure will decrease if wave-induced seabed response is considered. The scope of decrease is mainly related to wave amplitude and permeability of seabed soil. The influence of wave-induced seabed response on the stability of seabed and coastal structures can not be completely neglected.

Keywords: wave, seabed response, pore pressure, dynamic elastic consolidation FEM, stability analysis.

Ⅰ. Introduction

There are two types of wave load acting on seabed soil. One is that waves act on structure and the wave load spread into seabed soil through structure. The other is that the spatial and temporal variations of wave pressure acting on the surface of seabed cause seepage in seabed, and the seepage force acts on seabed soil. It is possible that coastal and offshore structures (e.g. breakwater, offshore platform, pipeline under seabed, etc.) loss their stability under the combination of these loads. In the design of engineering, only the first type of wave load has been taken into account and wave-induced seepage force has not been considered. In other words, the influence of wave-induced pore pressure in seabed on the displacements and stresses of seabed soil is not regarded. Engineering facts and local observations show that the failure of some coastal and offshore structures is related to excess pore pressure in seabed to a large extent (Zen, 1993). Therefore, many researchers and scholars have paid close attention to problems about wave-induced seabed response and its influence on stability of seabed and structures, and have studied for decades.

In the research of problems about the response of wave-induced pore pressure in porous medium, many different models have been studied since 1940's. A considerable advance had been made by

Yamamoto et al (1978) and Madsen (1978) employing the consolidation theory of Biot (1941). In the studies of Yamamoto et al (1981, 1983), Okusa (1985), Siddharthan (1987), Zhang (1993), Stephen (1995), Tsai (1995), etc., inertia and damping, finite thickness of porous deposit, nonlinear soil properties, residual pore water pressure have been considered (Zhao, 1995). But most of researches are based on mathematical and analytical method just considering the action of harmonic wave. The conditions in real engineering are complex. For example, seabed soil is layered or in different fields with different soil properties, acting wave is irregular, structures laid on seabed may influence the distribution of pore pressure. Therefore, numerical approaches must be employed for engineering.

Coastal and offshore structures have possibility of failure due to the instability of seabed under the action of storm waves. There are two types of failure for seabed soil: (a) Liquefaction in sandy seabed; (b) Significant deformation and stresses cause the loss of strength. This paper focuses on the problem (b) above. Limit equilibrium theory and deformation analysis theory are usually applied in the study of the second problem. Basing on the study of wave-induced pore pressure response (Okusa, 1985), Okusa (1987) had applied an advanced slice method analyzing the stability of seabed with gentle seafloor under the action of waves. The method is simple and easy to be understood. But the disadvantage of the method is similar with that of the general slice method. The forces between soil slices have been neglected.

In this paper, a consolidation finite element method (FEM) is presented to solve the transient response of seabed, and an improved slice method with circular arc slip surface is developed to analyze the stability of seabed and coastal structures. Dynamic elastic consolidation theory and linear permeability theory are employed to get a solution for the response of pore pressure, displacements and effective stresses in a saturated seabed with arbitrary boundary conditions under the action of regular and irregular waves. Irregular wave pressure acting on the surface of seabed is calculated by linear superposition method. The pore pressure calculated by theory will compare with the result measured in model test. Some calculations that show the influence of wave-induced seabed response to the stability of seabed and structures will be stated.

Ⅱ. Wave-induced Response of Seabed

2.1 *Governing Equations*

In homogenous soil, two dimensional force equilibrium equations under strain conditions are

$$\frac{\partial \sigma_x}{\partial x} + \frac{\partial \tau_{xy}}{\partial y} + \frac{\partial p}{\partial x} + X - \rho \frac{\partial u}{\partial t^2} - \eta \frac{\partial u}{\partial t} = 0 \tag{1a}$$

$$\frac{\partial \sigma_y}{\partial y} + \frac{\partial \tau_{xy}}{\partial x} + \frac{\partial p}{\partial y} + Y - \rho \frac{\partial v}{\partial t^2} - \eta \frac{\partial v}{\partial t} = 0 \tag{1b}$$

in which σ_x, σ_y and τ_{xy} are the components of effective stress, p is the wave-induced pore pressure in excess of the hydrostatic condition, ρ is the mass density of soil, η is the coefficient of damping, u

and v are the components of displacement, X and Y are the body forces in the x and y directions respectively. The relative motion between pore water and soil skeleton is neglected in the inertia term of equilibrium equations.

Based on Biot's consolidation theory, the two dimensional governing equation for the pore pressure of incompressible pore fluid in a compressible porous medium can be written as

$$\frac{k}{\gamma_w}\left(\frac{\partial p}{\partial x^2}+\frac{\partial p}{\partial y^2}\right)-\frac{\partial}{\partial t}\left(\frac{\partial u}{\partial x}+\frac{\partial v}{\partial y}\right)=0 \tag{2}$$

in which k is the permeability coefficient of soil, (w in the unit weight of the pore water.

Equation (1) and (2) are the differential form based on dynamic elastic consolidation theory and linear permeability theory for the solution of transient response of seabed. In the real engineering, the permeability of seabed soil is very small, and wave period is from 6 second to 10 second, so the pore water flows slowly. In this case, it is suitable that pore water is assumed to be Darcy flow and the relative motion between pore water and soil skeleton is neglected.

Considering boundary conditions at mud-line and impermeable border, the response of pore pressure and seabed soil can be solved from (1) and (2) by employing FEM.

2.2 *Pressure of Irregular Wave*

The free-surface equation of an irregular wave can be expressed as

$$\eta(x,t)=\sum_{n=1}^{N}a_n\cos(k_nx-\omega_nt+\varepsilon_n) \tag{3}$$

where $\eta(x,t)$ denotes the wave surface at position x and time t, a_n, k_n, ω_n and ε_n are amplitude, wave number, angular frequency and initial phase of the n-th constituent wave respectively, N is the number of constituent waves. a_n, ω_n and ε_n of every constituent wave can be calculated by the modeling of wave spectrum or wave surface. ω_n and k_n satisfy the linear dispersion equation, $\omega_n^2=k_ng\tanh(k_nd)$, here g is the acceleration of gravity, d is the depth of water.

Under the action of irregular wave, wave pressure can be calculated by linear superposition method. At the depth of z, the wave pressure p is

$$\frac{p}{\rho g}=\sum_{n=1}^{N}a_n\frac{\cosh(k_nz)}{\cosh(k_nd)}\cos(k_nx-\omega_nt+\varepsilon_n) \tag{4}$$

and on the surface of seabed, p_b is

$$\frac{p_b}{\rho_g}=\sum_{n=1}^{N}a_n\frac{1}{\cosh(k_nd)}\cos(k_nx-\omega_nt+\varepsilon_n) \tag{5}$$

where ρ is the water mass density.

Similarly, at the depth of z, the pressure p of an irregular wave in front of vertical wall can be written as

$$\frac{p}{\rho g}=\sum_{n=1}^{N}\frac{\cosh(k_n z)}{\cosh(k_n d)}[\alpha_n\cos(k_n x-\omega_n t+\varepsilon_n)+\alpha_n K_r\cos(k_n x+\omega_n t+\varepsilon_n)] \tag{6}$$

and on the surface of seabed, p_b is

$$\frac{p_b}{\rho g}=\sum_{n=1}^{N}\frac{1}{\cosh(k_n d)}[\alpha_n\cos(k_n x-\omega_n t+\varepsilon_n)+\alpha_n K_r\cos(k_n x+\omega_n t+\varepsilon_n)] \tag{7}$$

in which Kr is the coefficient of reflection.

Wave pressure under more complex conditions can be gotten from other approximate method.

2.3 *Boundary Conditions and FEM Solution*

The FEM equations are established by weight-residual method according to (1) and (2). In which displacements and pore pressure in nodes are unknown. The seabed field is meshed by 4-node or 8-node element.

The boundary condition of displacement in this case is treated as in general solid mechanics FEM. For the pore water, there are two types of boundary, one is permeable in which the pore pressure is known. The other is impermeable in which the boundary condition is $\frac{\partial p}{\partial n}=0$. The surface of seabed is permeable, and the pore pressure equal to the bottom wave pressure. The other boundary of seabed is assumed to be impermeable. If there is an impermeable structure laid on seabed, the interface boundary is impermeable. While the structure is calculated, the general solid FEM is applied. Only displacement is unknown, and the pore pressure need not be considered.

In general, the length of calculation field of seabed is taken as 5 to 9 times wave length. When the thickness of seabed is infinite, the depth of calculation field is taken as 3 to 5 times wave water depth. If the permeable seabed is thinner and the action of wave can influence the distribution of stress in impermeable seabed, the impermeable seabed must be calculated.

Wilson-θ step-by-step integration method is employed to solve the transient response problem. For consolidation problem, it is important that how to take the time step. If the time step is bigger, the accuracy of solution may be lower. For smaller time step, the solution may be error because the difference between elements in the coefficient matrix of equations may be very large when the time step is smaller. Calculations show that if the time step Δt satisfy $T/50\leqslant\Delta T\leqslant T/20$ (T is the wave period), the solution will be good.

Ⅲ. Stability Analysis

It is assumed that seabed and structure slide along a circular are failure surface (Figure 1). The slice method is applied to analyze the stability of seabed and structure. Wave-induced response of seabed solved above is an excess action. The static forces acting on the slice i ($ABFE$) in Figure 1 are:

$$\text{Sliding force } T_i=W_i\sin\alpha_i \tag{8}$$

$$\text{Resisting force } R_i = W_i' \cos\alpha_i \tan\varphi + L_{AB} \cdot c \tag{9}$$

where W_i' is the submerged weight of the slice i, α_i is the slope angle of the slip plane AB, anti-clockwise positive, L_{AB} is the length of AB, φ' and c' are the effective inner friction angle and cohesion of the soil near the slip plane AB, respectively.

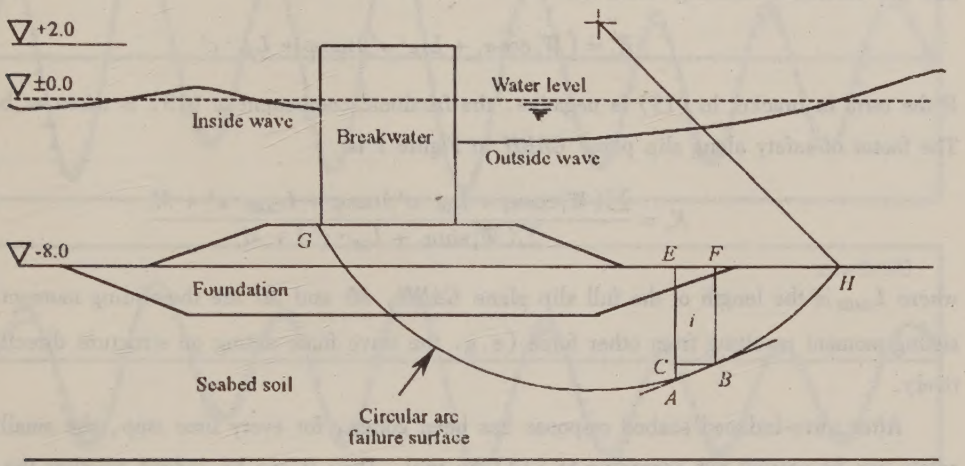

Fig.1 Wave-induced rotational failure of seabed and structure

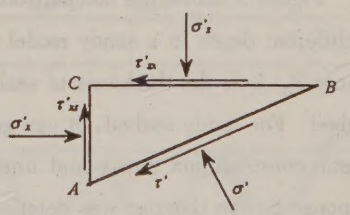

Fig.2 Wave-induced effective stresses in seabed

Wave-induced effective stresses on the small segment ABC on slip plane AB in Figure 1 are shown in Figure 2. They are

$$\sigma' = \sigma_x' \sin^2\alpha_i + \sigma_z' \cos^2\alpha_i - \tau_{xx}' \sin\alpha_i \cos\alpha_i \tag{10}$$

$$\tau' = (\sigma_x' - \sigma_z')\sin\alpha_i \cos\alpha_i + \tau_{xx}' (\sin^2\alpha_i - \cos^2\alpha_i) \tag{11}$$

where σ' and τ' are the normal stress and shear stress on the slip plane AB respectively, σ_x', σ_z' and τ_{xz}' are the excess effective stresses of seabed soil under the action of wave.

Therefore, the combined sliding forces on slice i considering the wave-induced stresses are

$$T_i = W_i' \sin\alpha_i + L_{AB} \cdot \sigma') \tan\varphi + L_{AB} \cdot c' \tag{12}$$

and the combined resisting forces are

$$R_i' = (W_i' \cos\alpha_i + L_{AB} \cdot \sigma') \tan\varphi + L_{AB} \cdot c' \tag{13}$$

If the term in bracket in (13) is negative, the frictional component of (13) is taken as being zero. The factor of safety along slip plane *GABH* in Figure 1 is

$$K_s = \frac{\sum (W_i' \cos\alpha_i + L_{AB} \cdot \sigma') \tan\varphi + L_{GABH} \cdot c' + M_t}{\sum (W_i' \sin\alpha_i + L_{AB} \cdot \tau') + M_r} \tag{14}$$

where L_{GABH} is the length of the full slip plane *GABH*, *Mt* and *Mr* are the sliding moment and the resisting moment resulting from other force (e.g. the wave force acting on structure directly), respectively.

After wave-induced seabed response has been gotten, for every time step, the smallest factor of safety can be carried out according to (14) by trial. Then it can be judged whether the seabed and structure are safe and when they are instable.

Ⅳ. Calculation

4.1 *Verification*

Figure 3 shows the comparisons of calculated and measured (Bie, 1997) pore pressure response at different depth in a sandy model seabed under the action of an irregular wave. They agree well. In Figure 3, h is the thickness of seabed, $z/h = 0$ denotes the top of seabed and $z/h = 1$ the bottom of seabed. For sandy seabed, it can get a good solution for wave-induced response by employing dynamic elastic consolidation theory and linear permeability theory. The study about the wave-induced seabed response by the theories was detailed in author's another paper (Bie, 1998).

4.2 *Example*

The stability of a vertical wall breakwater (Figure 1) is analyzed by the general slice method and the way in which the influence of wave-induced seabed response has been considered, respectively. The stability of the breakwater and seabed mainly depend on the properties of seabed soil and wave load. Table 1 shows some calculation parameters in three sets of seabed, in which E, k, γ_w, φ', c' are the elastic modulus, permeability, unit weight, effective inner friction angle and effective cohesion, respectively. For the convenience of results comparison, a harmonic wave is adopted. The wave period is 8.0 second, the wave length is about 64.9 meter under the condition of 8.0 meter of water depth according to the linear wave theory. The amplitude H_w of wave in front of vertical wall is taken

as 1.0m, 2.0m and 3.0m respectively.

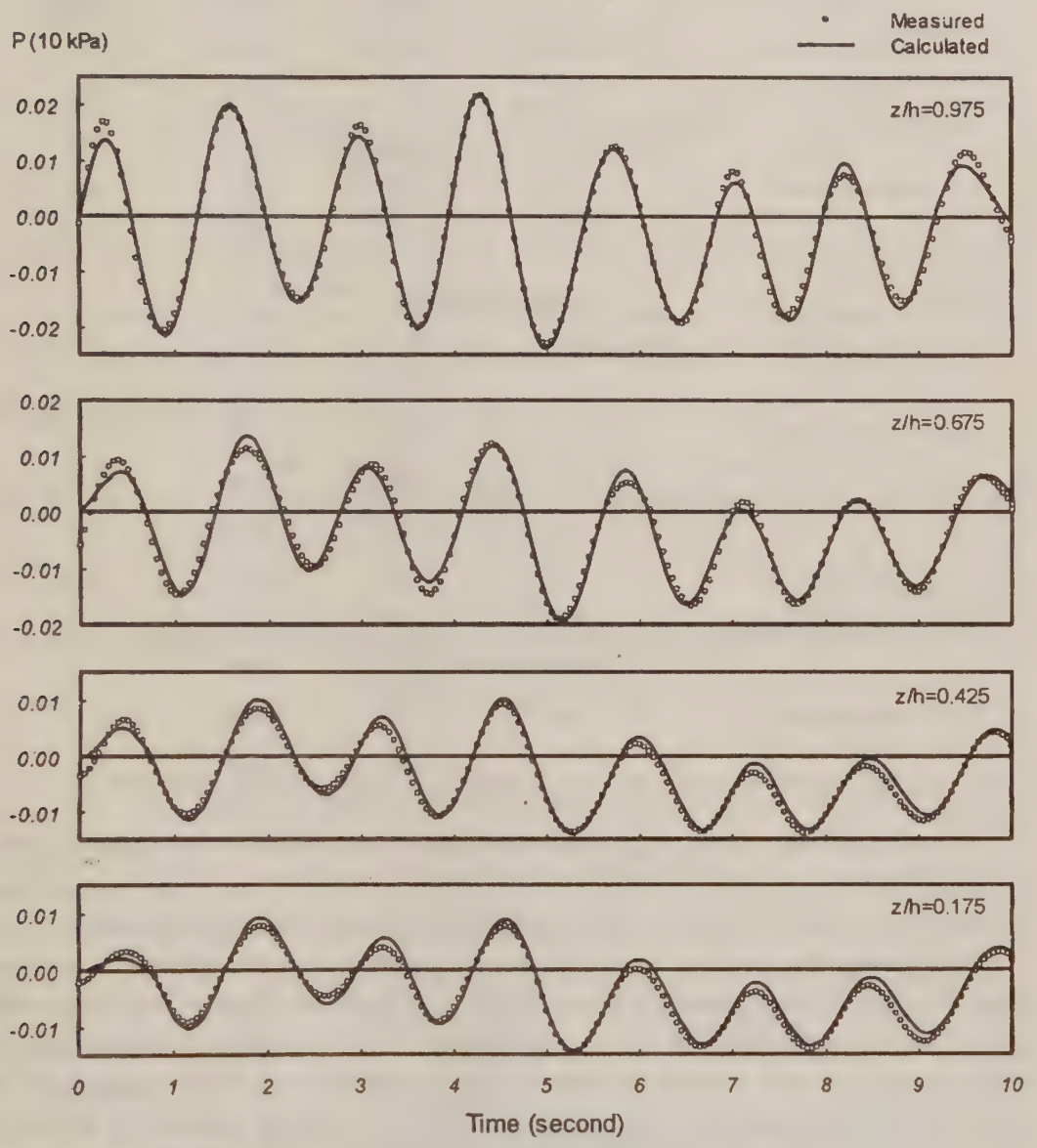

Fig.3 Comparisons of pore water pressure in homogeneous sandy seabed

Table 2 shows some safety factors of stability analysis, in which K_{s0} and K_s represent the results by the two ways mentioned above, the general method and the paper method, respectively. P_k is the percent of the difference of K_{s0} and K_s. Figure 4, Figure 5 and Figure 6 show the variations of safety factor in a wave period for three seabeds, respectively.

Tab 1. Properties of Seabed Soil

Name of Properties	Unit	Sandy seabed I	Sandy seabed II	Muddy seabed III
Elastic modulus E	10^6 N/m^2	25.0	25.0	10.0
Permeability k	10^{-6} m/s	100.0	10.0	1.0
Unit weight r_w	10^3 N/m$_3$	19.0	19.0	18.0
Inner friction angle φ'	(°)	28.0	28.0	14.0
Cohesion c'	103 N/m2	0.0	0.0	8.0

Tab 2. Comparison of Results

Seabed	$H_w(m)$	K_{z0}	K_z	P_k
Sandy seabed I	1.0	1.485	1.443	2.8
	2.0	1.470	1.397	5.2
	3.0	1.456	1.344	7.7
Sandy seabed II	1.0	1.485	1.463	1.5
	2.0	1.470	1.433	2.5
	3.0	4.456	1.403	3.6
Muddy seabed III	1.0	1.101	1.092	0.8
	2.0	1.091	1.074	1.5
	3.0	1.080	1.057	2.1

It is found that when a wave trough comes near the breakwater, the safety factor decreases. When the trough goes away, the safety factor is recovered. When a wave crest comes near the breakwater, the safety factor increases. The phase of safety factor lags behind the phase of acting wave.

The influence of wave-induced seabed response to the stability of seabed and structure can not be completely neglected. Under the action of wave with 3.0m of amplitude, the safety factor of the seabed I (sandy seabed with bigger permeability) has decreased by 7.7%, the seabed II (sandy seabed with smaller permeability) by 3.6% and the seabed III (muddy seabed with more smaller permeability) by 2.1%. The better permeability in sandy seabed, the more the safety factor decreases. If the accumulation of pore pressure is not considered, the influence of muddy seabed is less than that of sandy seabed.

In general, designed safety factor is greater than 1.1. For most engineering, even if the influence is considered, the real safety factor will be greater than 1.0. The seabed and structure is stable yet. If the designed safety factor is just greater than 1.0, under the action of a storm wave and in consideration of the influence, the safety factor will be smaller than 1.0. In this case, the seabed and structure will be unstable.

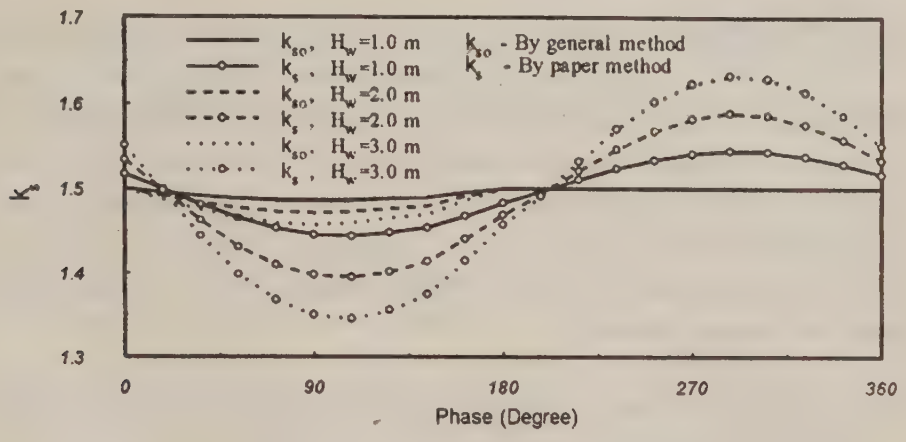

Fig.4 Variations of safety factor in a wave period (Sandy seabed I)

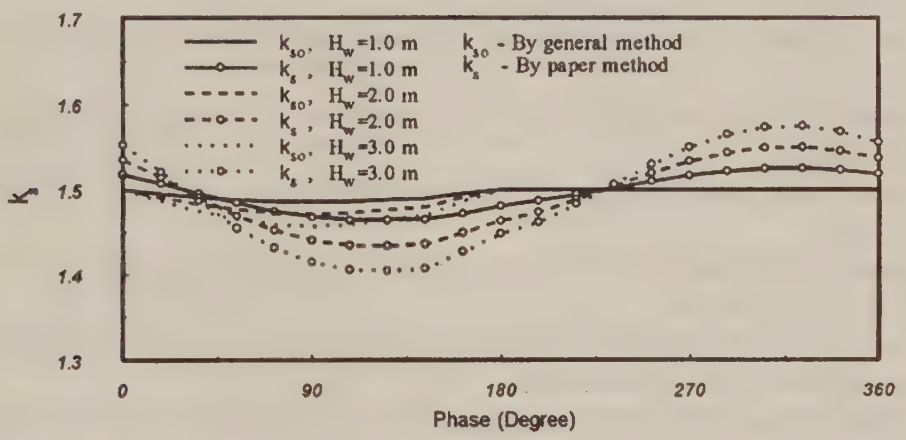

Fig.5 Variations of safety factor in a wave period (Sandy seabed II)

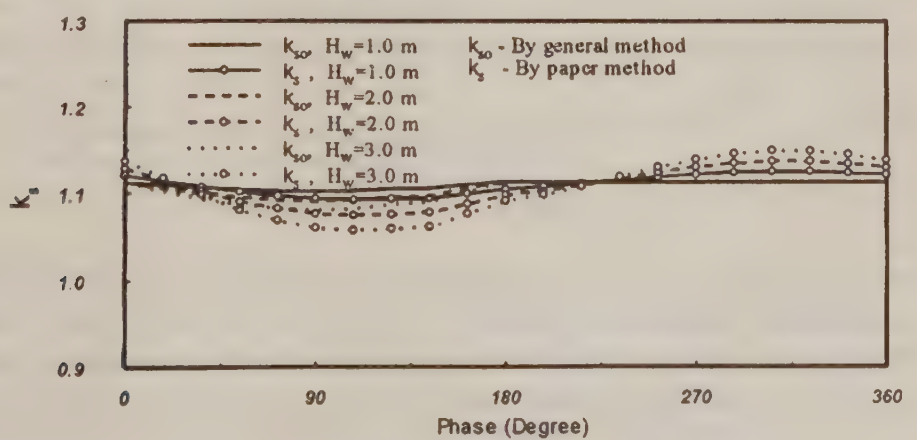

Fig.6 Variations of safety factor in a wave period (Muddy seabed III)

V Conclusions

A dynamic elastic consolidation finite element method is used for solving seabed response under the action of regular and irregular waves, and an improved slice method considering wave-induced seabed response is applied to analyze the stability of seabed and structures. The responses of pore pressure by theory and model test compare well. The calculations for a breakwater show that the influence of wave-induced seabed response to the stability of seabed and structures can not be completely neglected. The better permeability of seabed and bigger amplitude of wave, the more the safety factor of the seabed and structures decreases.

Bie Shean and Zhao Zidan (1998). Pore pressure response to random waves in sandy seabed. *Harbour Engineering*, No. 2, pp.13-18 (In Chinese).

Bie Shean and Zhao Zidan et al. (1997). Model test of wave-induced pore pressure in sandy seabed. Marine Science Bulletin, Vol.16, No.5, pp.55-65 (In Chinese).

Biot M A (1941). General theory of three-dimensional consolidation. *Journal of Application Phys*, Vol.12, pp.155-164.

Madsen O S (1978). Wave-induced pore pressure and effective stresses in a porous bed. *Geotechnique*, Vol.28, No.4, pp.377393.

Okusa S (1985). Wave-induced stresses in unsaturated submarine sediments. *Geotechnique*, Vol.35, No.4, pp.517-532.

Okusa S and Yoshimura (1987). Wave-induced instability in sandy submarine sediments. *Soils and Foundations*, Vol. 27, No.4, pp.62-72.

Siddharthan R (1987). Wave-induced displacements in seafloor sands. Int. *Journal for Numerical and Analysis Methods in Geomechanics*, Vol.11, pp.155-170.

Stephen D Thomas (1995). A finite element model for the analysis of wave induced stresses, displacements and pore pressures in a unsaturated seabed II:model verification. *Computers and Geotechnics*, Vol.17, pp.107-132.

Tsai C P et al. (1995). Standing wave induced pore pressures in a porous seabed. *Ocean Engineering*, Vol.22, No.6, pp.505-517.

Yamamoto T et al. (1978). On the response of a poro-elastic bed to water waves. *Journal of Fluid Mechnics*, Vol.87, No.1, pp.193206.

Yamamoto T et al. (1981). Wave-induced pore pressures and effective stresses in inhomogeneous seabed. *Ocean Engineering*, Vol.8, pp.1-16.

Yamamoto T et al. (1983). On the response of a Coulomb-damped poroelastic bed to water waves. *Marine Geotechnology*, Vol.5, No.2, pp.3-129.

Zen K and Yamazaki H (1993). Wave-induced liquefaction in a permeable seabed. Report of the Port and Harbour Research Institute, Vol.31, No.5, pp.155192.

Zhang Gengde and Gu Xiaoyun (1993). Wave-induced response in finite thickness sandy seabed. *Journal of Mechnics*, Vol.25, No:1, pp.56-68 (In Chinese).

Zhao Zidan and Bie Shean (1995). Review of study on wave-induced response and stability in sandy seabed. *Marine Science Bulletin*, Vol.14, No.4, pp.85-104 (In Chinese).

Characteristics of Water Type Distribution and Seasonal Variations in the Southern East China Sea*

Miao Yutian, Yu Honghua, He Dehua and Wang Chunsheng
Second Institute of Oceanography, SOA, Hangzhou 310012

Abstract By using the data of Summer and Winter 1987, Spring and Autumn 1988 obtained by the R/V "Shijian" during the China-Japan Joint Research Program on Kuroshio, the paper makes an analysis and research on the water type distribution and its variations in the studied sea area. The results of which are mainly as follows: (1) The Class IV mixing water whose property is similar to that of the continental coastal water is located in the northeast sea area, along the coast of the continent in autumn and winter while extending to the open sea in spring and summer. (2) The boundary between the Kuroshio water and the shelf mixing water (called the left boundary of the Kroshio water) is approximately located in between the 100m and 200m isobaths in various seasons and various layers, and mostly near the 200m isobath. In the sea area northeast of Taiwan, the Kuroshio water is to the west most in spring and then in winter. In summer, it is to the east most while, in autumn, it is in between its positions in summer and winter. At the bottom in summer and from surface to bottom in spring, the Kuroshio water mainly comes from the sea area to the northeast of Taiwan while part of it from the Taiwan Straits. Near the R_1, the intrusion of Kuroshio water into the shelf is the strongest in winter and the boundary is to the west; in summer, the intrusion is the weakest in the most cases and the authumn is in between the above two cases. (3) There is crisscross intrusion between the Kuroshio water and the shelf mixing water. The Kuroshio water is mingled with the mixing water of Classes Ⅰ and Ⅱ, while the shelf mixing water with isolating water of Kuroshio. (4) Along the continental slope, an upwelling phenomenon of Kuroshio water is often seen, but sometimes, slipping down of the shelf mixing water is also found to occur along the slope. (5) The water type distribution from southeast to northwest does not exactly follow the order of Classes K, Ⅰ, Ⅱ, Ⅲ, and Ⅳ; sometimes a transitional zone of water type may occur, its position varying with time and place.

Keywords: Southern East China Sea, water type distribution, seasonal variation

Ⅰ. Introduction

Past research findings indicate that the main water types in the Southern East China Sea are roughly divided into the high-salinity Kuroshio water and the low-salinity continental water as well as the mixing water between them. And that their range of distribution shows obvious annual and seasonal

* This is a project funded by the National Natural Science Fund numbered 4957275

variations, thus presenting a complicated and changeable marine environment [1 2 3]. The change of such a marine environment would directly affect marine fishery, the living of marine life and its distribution range, so the research on the distribution of water types and its variations is of important practical value and scientific significance.

Ⅱ. Data and Methods

This paper reviews the distribution of water types. And its variation by using the data obtained By the R/V "Shijian" in July-August, 1987 (summer), December, 1987 (winter), May-June, 1988 (spring) and October-November, 1988 (autumn) as well as a number of observations on the s S2 and R1 during the China-Japan Joint Research Program on Kuroshio. The distribution of survey sections and station locations is shown in Fig. 1 as follows:

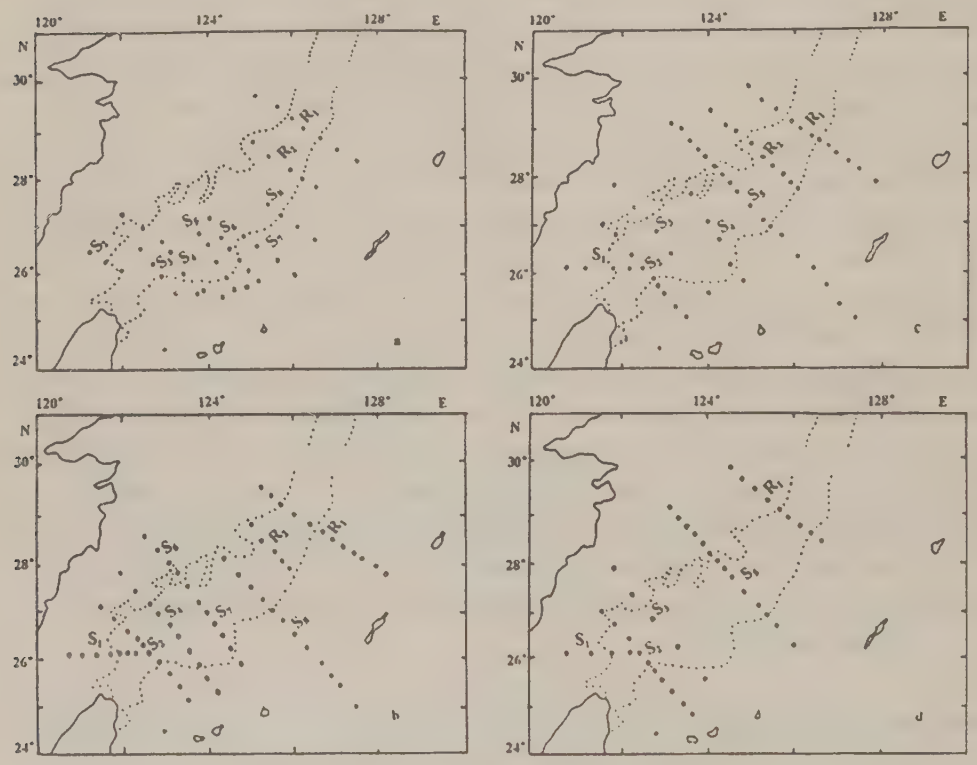

Fig.1 Distribution of Survey Sections and Station Locations

a. July-August, 1987 (summer) **b. December, 1987 (winter)**

c. May-June, 1988 (spring) **d. October-November, 1988 (autumn)**

The water type composition adopts the improved water-type analysis method based on the T-S point-cluster classification and grading proposed by Japanese scholars Tsutomu Sahara and Yoichi

Hanzawa[1,2]. The gist of this method is: Based on the T-S elements in the surveyed area and in the light of the Sections T-S and the general distribution trend, the water types in the surveyed area are divided into the high-temperature and high-salinity Kuroshio water (K). And the continental coastal water (CCW) with salinity lower than 30.50 as well as the mixing modification water (M) of the East China Sea continental shelf. That is further divided into Classes Ⅰ, Ⅱ, Ⅲ and Ⅳ, among which, Class Ⅰ refers to a mixing water with T-S property similar to that of the Kuroshio water, i.e., with little modification in relation to the Kuroshio water. Class II refers to mixing water whose T-S property is modified in relation to the Class I water and with greater modification than the Kuroshio water. Class III is an intermediate mixing water in between the Kuroshio water (K) and the continental coastal water (CCW). And Class IV is mixing modification water whose T-S property is similar to that of the continental coastal water. In order to find out the mixing and modifying process of the water of various classes, and to trace the details of its mixing and modification, the Kuroshio water (K) and the mixing modification water of the East China Sea continental shelf are further divided into four grades. The water with conditional density (δt) smaller than 23.7 is taken as Grade Ⅰ, the one with $\delta t = 23.7$as Grade Ⅱ, the one with $\delta t = 25.7 - 27.0$ as Grade Ⅲ and the one with $\delta > 27.0$ as Grade Ⅳ, among which k-1, k-2, k-3 and k-4 correspond to the surface water, subsurface water, mid-water and deep-water of Kuroshio respectively. The diagram of specific division is shown in Fig.2.

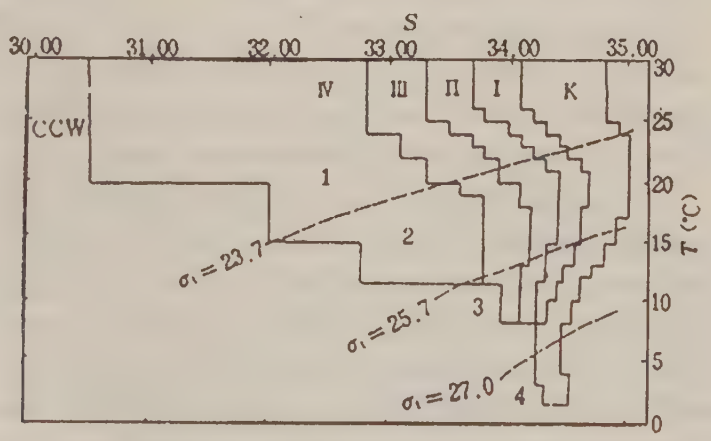

Fig.2 Diagram of T-S Point Cluster Classification and Grading

The above mentioned improved method of water-type classification and grading seems to be more visible, convenient and feasible than other methods in differentiating the water-type composition in the East China Sea. It can not only clearly reveal the plane and sectional distribution characteristics of various water types, but also distinctively differentiate the characteristic phenomena occurring in various water types such as transition layer, frontal surface and the heteromorphic isolating water left over in the various water types which has not been able to mix or modify in time.

Ⅲ. Distribution of Water Types

1. *Plane Distribution of Water Types*

In summer, the seawater generally warms up and there exists only Grade I water of various classes of water near the surface in the entire studied sea area. The left boundary of the Kuroshio water is roughly identical with the position of the 200m isobath. The mixing water of the continental shelf is located on the left side of the 200m isobath. And along the direction of the Kuroshio from the northeast of Taiwan are distributed water of Classes Ⅰ-1, Ⅱ-1, Ⅲ-1 and Ⅳ-1 (see Fig.3a). At the 50m layer, the Class Ⅳ-1 water whose T-S property is similar to that of the continental coastal water no longer exists, k-1, Ⅰ-2 and Ⅱ-1 are arranged successively from southeast to northwest and individual stations there exists the water of Class Ⅲ-1. In the direction tending towards the shore, there is less and less composition of open seawater while more and more that of the coastal water, and the modification character tends to become more obvious. The sea area to the north of Taiwan is entirely occupied by the water of Class Ⅰ-1 and the Kuroshio water has extended to the left side of the 200m isobath. On the S_2 to the northeast of Taiwan and the R_2-R_1, in the north of the surveyed are, the force of the Kuroshio water intruding into the continental shelf is stronger than that in the surface (see Fig. 3b). The distribution of water types at the bottom is complicated as compared with that at the surface or the 50m layer, where apart from four grades of Kuroshio water, i.e., k-1, k-2, k-3 and k-4. There is the mixing water of the continental shelf-Classes Ⅰ-1, Ⅰ-2, Ⅱ-2, Ⅲ-1 and Ⅲ-2. The crisscross intrusion phenomenon among various water types is obvious: (1) The Kuroshio water is mingled with the water of Classes Ⅱ-1, Ⅱ-2 and Ⅰ-4. (2) And the mixing water of the continental shelf with the Kuroshio water k-1 at the Section $S_{2\text{-}4}$ has a distribution trend of coming from the Taiwan Straits (see Fig.3c).

In winter, the temperature of the near-surface seawater universally drops. In the surveyed area, except that the Kuroshio water has the Grade 1 water, other water types are all in the Grade 2 water. The Kuroshio water has crossed the 200m isobath and intruded extensively into the continental shelf. The Kuroshio water and the Class Ⅰ mixing water whose property is similar to that of the Kuroshio water have occupied the wide survey area with depth larger than 100m. The mixing water of Class Ⅳ has receded to the continental coastal zone and range of the mixing water of Class Ⅱ-Ⅲ has obviously been reduced as compared with that in summer. The water types are distributed from southeast to northwest in the order of k-1, k-2, Ⅰ-2, Ⅱ-2, Ⅲ-2 and Ⅳ-2, and the Kuroshio water type is mingled with the isolating mixing water of Class Ⅰ-2. At the 50m layer in winter, due to the intensification of vertical connective mixing, the water-type distribution is very similar to that at the low layer except that the Kuroshio water recedes more to the open see than that at the surface layer and the distribution range of the Class Ⅰ-2 water enlarges. At the bottom, except that k-3 and k-4 of lower temperature occur in the Kuroshio water, the distribution of water types in other stations is basically identical with that at the 10m or 50m layer (see Fig.4).

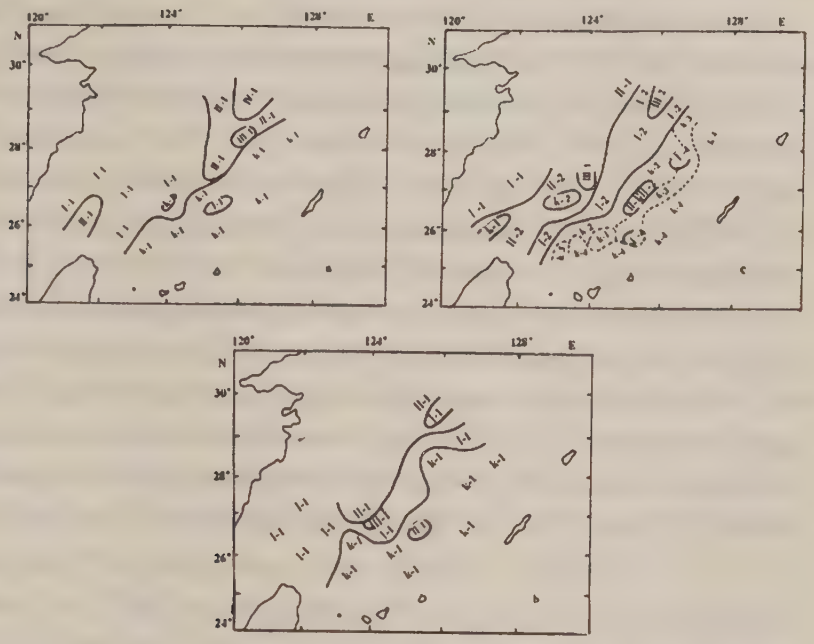

Fig.3 Distribution map of water types in Jul.-Aug.

a. 10m layer b. 50m layer c. bottom

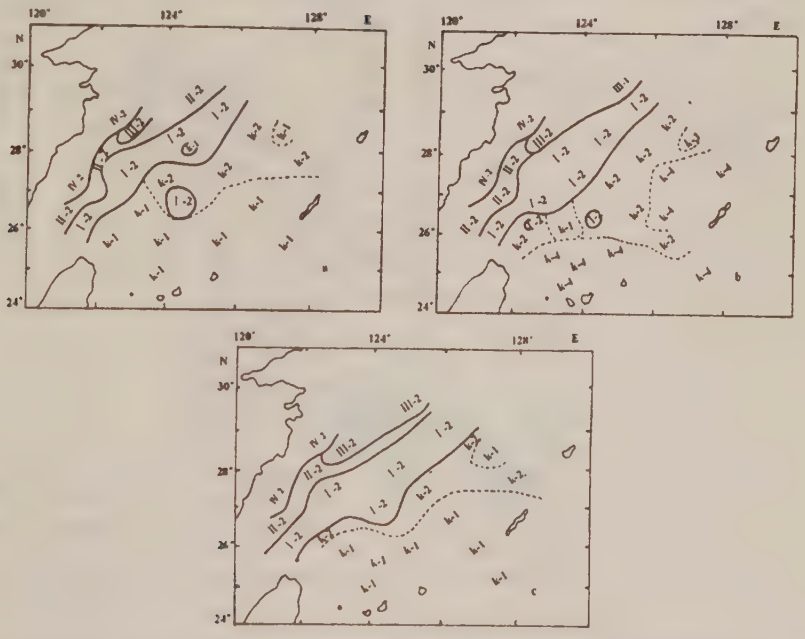

Fig.4 Distribution map of water types in December, 1987

a. 10m layer b. 50m layer c. bottom

In spring, as in summer, there exist only the Grade 1 water of various classes in the surface. The range of the Class Ⅳ-1 water is obviously larger than that in winter, extending from northwest to southeast in a tongue shape, whose front is directly connected with the Kuroshio water, and a strong water-type transitional zone is formed in between (see Fig.5). The Kuroshio water has intruded into the left side of the 200m isobath, and, especially off the north of Taiwan, it goes westward right to the S_{1-2} station. The Kuroshio water in the sea area north of Taiwan mainly comes from the sea area to the east of Taiwan Island and part of it from the Taiwan Straits. At the 50m layer, there is the Grade 2 water of various classes in addition to the Grade 1 water and at the S_{1-2} station in the northwest of Taiwan, isolating water has been separated from the Kuroshio water. The range of Ⅳ-2 water has been reduced, which has receded to the northwest of the surveyed area which the range of the Class Ⅱ water has enlarged. On the Class Ⅳ, and there exists a water type transitional zone between them. The water type at the bottom is complicated as compared with that at the surface or the 50m layer, where there exists the water of Classes Ⅰ-2, Ⅱ-2, Ⅲ-1 and Ⅲ-2 apart from the four grades of the Kuroshio water. i.e., k-1, k-2, k-3 and k-4. At the S_{1-2} station in the northwest of Taiwan Island, there still exists the Kuroshio water k-1. It is clear from above that in spring of 1988, the Kuroshio water in the sea area north of Taiwan Island comes in part from the Taiwan Strait from surface to bottom while in summer of 1987, the Kuroshio water coming from the Taiwan Straits only exists at the bottom.

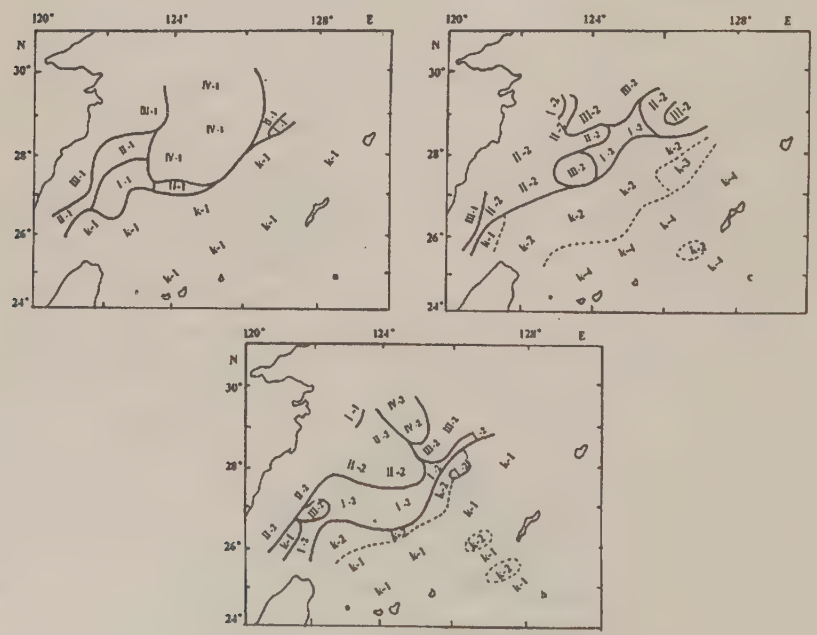

Fig.5 Distribution map of water types in May-June, 1988

a. 10m layer b. 50m layer c. bottom

In autumn, during the observation, the Ⅳ-1 mixing water of the surface has receded to the coast of the continent and the left boundary of the Kuroshio water is approximately identical with the position of the 200m isobath. Within the surveyed area are arranged successively from southeast to northwest the water of Classes k-1, Ⅰ-1, Ⅰ-2, Ⅱ-1, Ⅱ-2, Ⅲ-1 and Ⅳ-1, of which Class Ⅲ-1 increases in range as compared with that in other season. At the 50m layer, the Kuroshio water in the northeast of Taiwan obviously intrudes into the continental shelf and there occurs upwelling of the subsurface water of Kuroshio. At $S_{2\text{-}3}$ and $S_{3\text{-}3}$, the Kuroshio water k-2 appears the range of the Class Ⅲ-1 water decreases and those of the Classes Ⅰ-1 and Ⅰ-2 water increases while the Class Ⅳ-1 water has disappeared. At the bottom layer, there exist from southeast to northwest the Kuroshio water of k-4, k-3 and k-2, and the continental shelf mixing modification water of Ⅰ-1, Ⅰ-2, Ⅱ-1, Ⅱ-2 and Ⅲ-1. The distribution range of the Kuroshio water in the northern sea area of Taiwan extends westward as compared with that at the 50m layer, where the left boundary of the Kuroshio water has reached the stations $S_{1\text{-}3}$ and $S_{2\text{-}3}$. The distribution range of Kuroshio water on other sections is similar to that at the 50m layer.

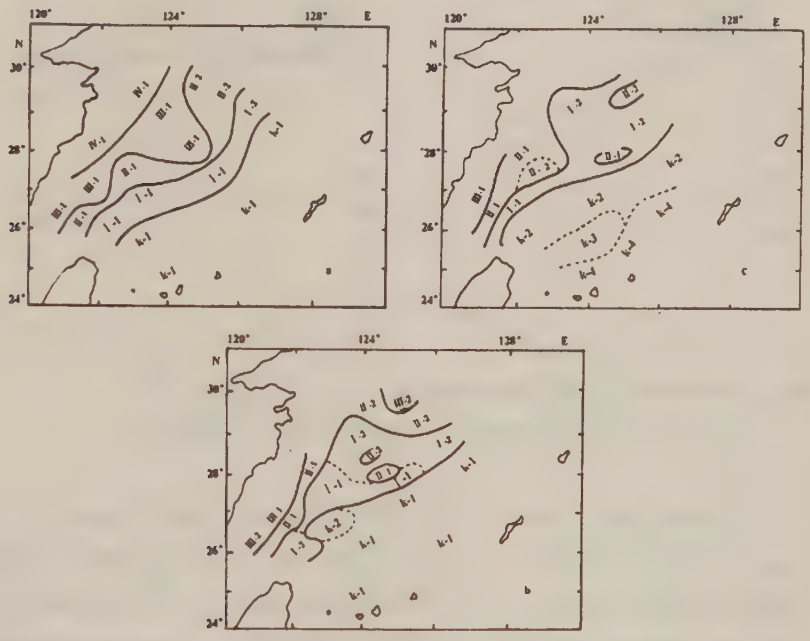

Fig.6 Distribution map of water types in Oct.-Nov., 1988
a. 10m layer b. 50m layer c. bottom

2. *Water Type Distribution on the Sections*

The Sections S_2 and R_1 are takes for example. In summer, as there are few sectional stations in July-August 1987, the observation on June 11-12 1988 is here taken as the early summer condition. It can be seen from Fig.7 that on the left side of the section are arranged from above to below the water

of Ⅳ-1, Ⅲ-1, Ⅱ-1, Ⅰ-1 and the isolating Class k-1 water, the subsurface water of Kuroshio having climbed onto the continental shelf. And on the right side of the section there exist from above to below k-1, k-2, k-3 and k-4. The Kuroshio water is mingled with the mixing water of Classes Ⅰ-1 and Ⅰ I-2 and the k-1 water of the bottom layer at the S_{2-2} station is the Kuroshio water from the Taiwan Straits. On the Section R_1 there exist a number of water types, such as Ⅳ-1, Ⅲ-1, Ⅲ-2, Ⅱ-1, Ⅱ-2, Ⅰ-1, Ⅰ-2, K-1-k-4. At the slope break of the continental shelf there occurs a phenomenon of the Ⅰ-2 water slipping down along slope, but this is not a general rule of the water type distribution on the Section R_1 in summer. For instance, the water-type distribution on the Section PN (whose position is near the Section R) as observed by the Japan Meteorological Agency in the summer of 1987 is obviously different from this observation (see Fig.8), where still occurs a phenomenon of the k-2 water climbing up the slope.

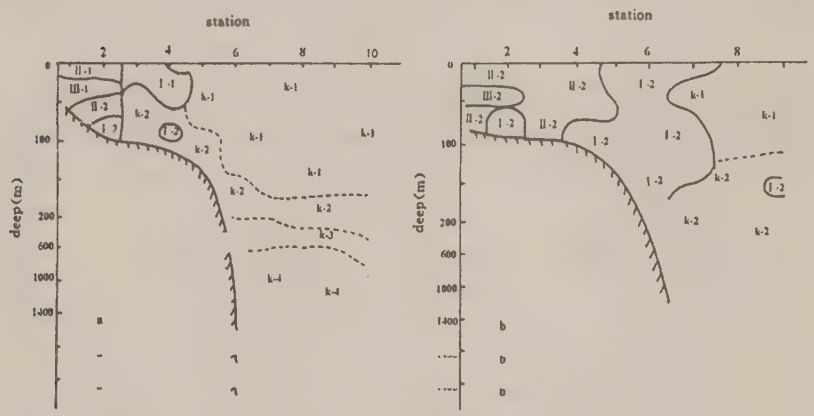

Fig.7 Distribution of water types in summer

a. June 11-12, 1988, **Section S_2 b. Aug.** 5-7, 1987, **Section R_1**

In winter, on the left side of the Section S_2, i.e., at the station S_{2-1} near the coast, there is the Class Ⅳ-2 water from above to below and adjacent to it are the water of Classes Ⅰ-2 and Ⅱ-2. There exists a strong transition zone of water types between them. The Kuroshio water is located on the right side of the section, where exist k-1, k-2, k-3 and k-4. The upper Kuroshio water intrudes into the continental shelf forcefully, the k-1 water extends westwards up to the station S_{2-4} and, near the continental slope, the Kuroshio water is mingled with the isolating water of Class Ⅰ-2. On the Section R_1, Class Ⅳ water dose not exist, and, on the left side of the section, the upper and lower water types are identical and there are from left to right the water of Classes Ⅲ-2 and Ⅰ-2, between which there exists a transitional zone of water types. On the right side of the section, the Kuroshio water k-2 climbs along the slope onto the Class Ⅰ-2 water from above to below and extends leftwards up right to the surface of the stations No.4-6. There is the Class Ⅰ-2 water in the Kuroshio water.

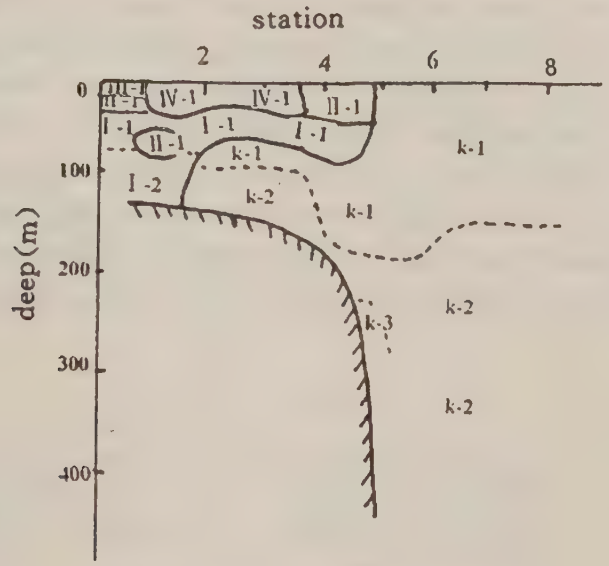

Fig.8 Distribution of water types on the Section PN in summer, 1987

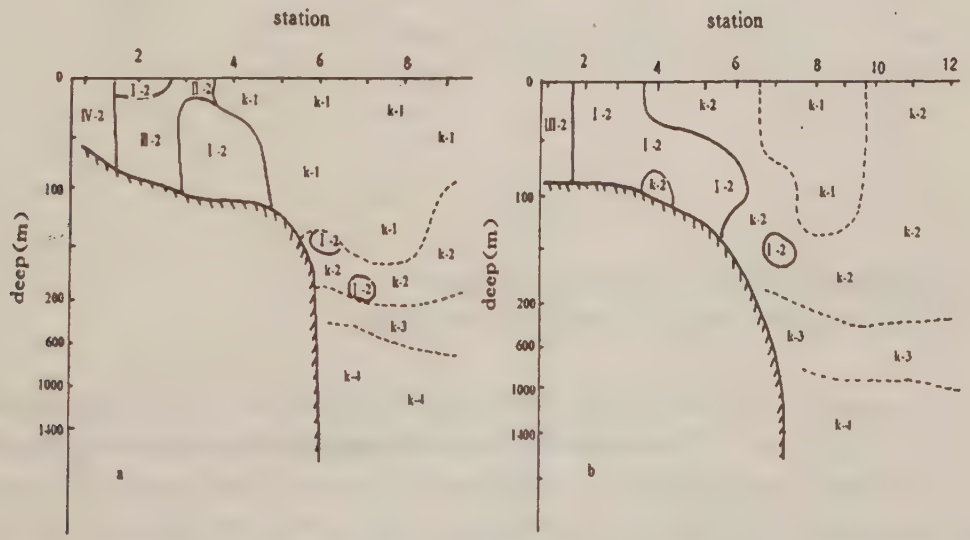

Fig.9 Distribution of water types at the sections in winter

a. Dec.8-10, 1987, Section S_2 b. Dec.24-25, 1987, Section R_1

In spring, the Class Ⅳ water dose not exist on the Section S_2, and, on the left side of the section, are the water of Classes Ⅲ-1, Ⅱ-1 and Ⅱ-2. The Kuroshio water intrudes into the continental shelf forcefully and is directly connected with the Class Ⅱ water at the station S_{2-2}, between which

forms a transitional zone of water types. Besides, in the Kuroshio water, there are isolating mixing water of Classes Ⅰ-2 and Ⅰ-1. In the shelf zone of the Section R1, there exist the mixing water of Classes Ⅳ, Ⅲ and Ⅱ. Near the slope break of the continental shelf, the water types are complicated in the upper layer. There is the water of Classes Ⅰ-1 and Ⅱ-1, below which there is intrusion of the Kuroshio water k-1, and, below the k-1 water, there is crisscross water of the Classes Ⅲ-2, Ⅱ-2 and Ⅰ-2, the last of which tends to slip down along the slope, and on the right side of the section is the Kuroshio water. Such complicated water type variations are just a distinguishing feature of the composition and distribution of water types in the transitional seasons.

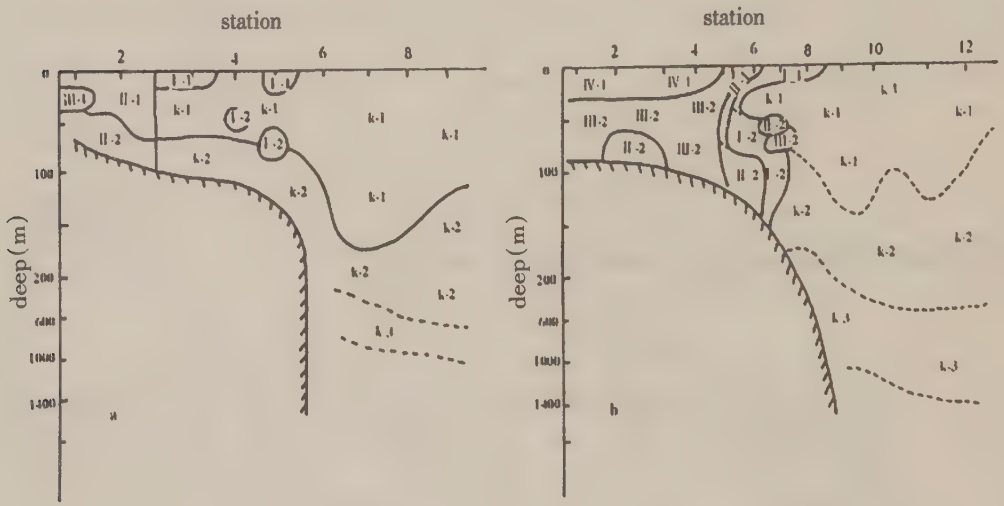

Fig.10 Distribution of water types at the sections in spring

a. May 14-16, 1988 Section S_2 b. May 23-25, 1988 Section R_1

In autumn, in Oct.-Nov., 1988, on the left side of the Section S2 are the water types of Ⅰ-1, Ⅱ-1, Ⅱ-2, Ⅲ-1 and Ⅰ-2 and on the right side are the Kuroshio water types of k-1, k-2, k-3 and k-4. The subsurface water of Kuroshio k-2 climbs onto the 50m layer of the Station No.3 to connect with the water of Classes Ⅱ-1 and Ⅱ-2 at the Station S_{2-2}, between which there is a transitional zone of water types. The continental shelf zone of the R is occupied by Ⅰ-2, Ⅱ-2 and Ⅲ-2, and near the slope break of the continental shelf is the Class Ⅰ-2 water (see Fig.11). But the distribution of water types is not always like this every year. For instance, in October 1990, the distribution of water types is obviously different from the one mentioned above (see Fig.12). It is clear from Fig.12 that the Kuroshio water k-2 has climbed on to the continental shelf, only at the slope break of the continental shelf, the Kuroshio water is mingled with the mixing wafer of Classes Ⅰ-1 and Ⅰ-2.

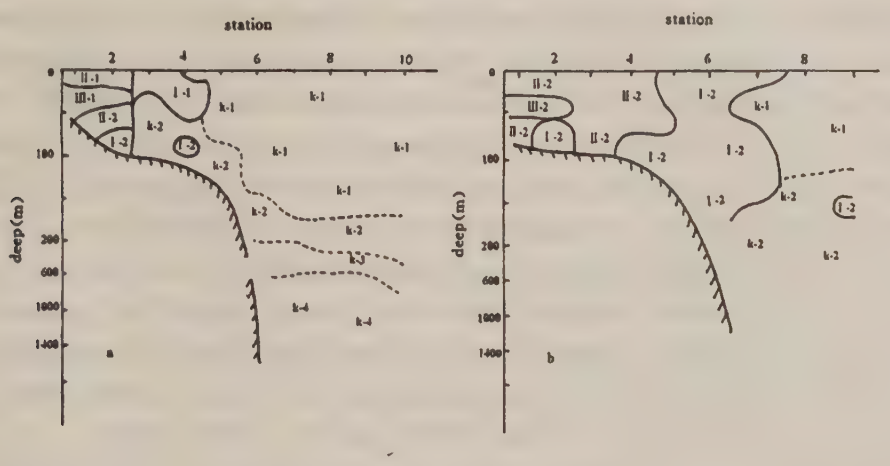

Fig.11 Distribution of water types at the section in autumn

a. Oct.18-23, 1988 Section S_2 b. Nov.23-24, 1988 Section R_1

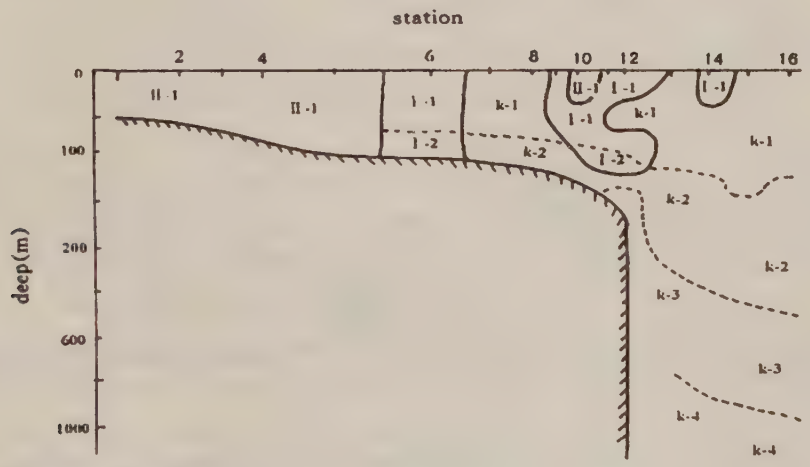

Fig.12 Distribution of water types at the Section R_1 in Oct.-Nov., 1990

Ⅳ. Seasonal Variations in the Position of the Left Boundary of the Kuroshio Water

It can be seen from the analysis above that the distribution range of Kuroshio water varies distinctly with time and place. To find out its seasonal variations, the left boundary of the Kuroshio water is taken here. The positions of the left boundary of Kuroshio water at the 10m, 50m, 100m and bottom layers in four seasons are given respectively in Fig.13. From which it is clear that the left boundary of Kuroshio water at different water layers and in different seasons is roughly located between the 100m

and 200m isobaths, but at different water layers in different sea areas, it has obvious seasonal variations. The distribution of the positions of the left boundary of Kuroshio at different water layers in the sea area to the northeast of Taiwan indicates that in spring the boundary of Kuroshio water is nearest to the west side. That is probably because in spring 1988, from above to below, part of the Kuroshio comes from the Taiwan Straits. Next is winter while in summer the position of the left boundary of Kuroshio water is to the east most and its position in autumn is in between those in winter and summer. The seasonal variations in the position of the Kushio boundary in other sea areas are not so regular like those in the northeastern sea area of Taiwan. The situation at the 10m layer is more or less like this: except in the northeastern waters of Taiwan, the Kuroshio water intrudes into the continental shelf most forcefully in winter and the position of its left boundary is close to the 100m isobath while, in other seasons, the left boundary of Kuroshio water is around the 200m isobath. At the 50m layer, the boundary positions of the Kuroshio water are similar in all seasons except in the northeastern waters of Taiwan and at the Section R_2, i.e. on the left side of the 200m isobath. At the 100m layer, the Kuroshio water intrudes into the continental shelf forcefully in spring at the middle continental shelf and its

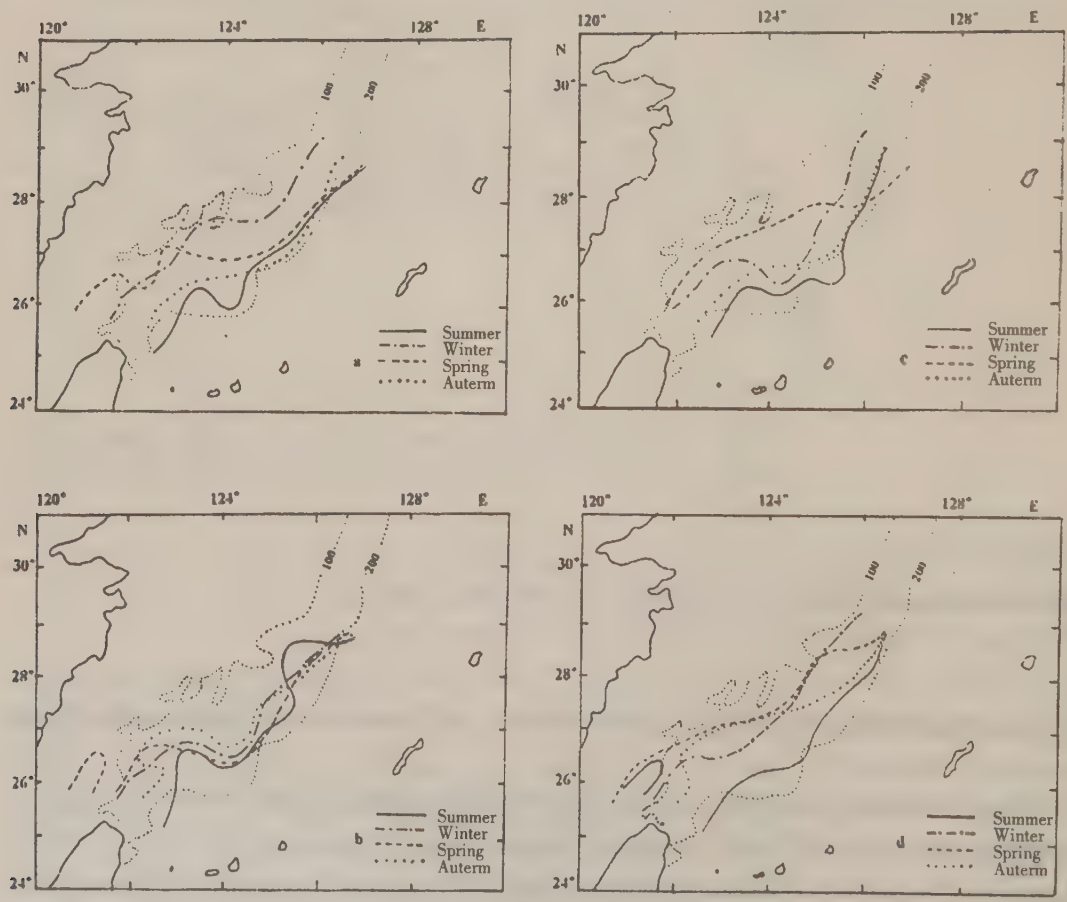

Fig.13 Seasonal variations in the position of the left boundary of Kuroshio water

a. 10m b. 50m c. 100m d bottom

boundary position reaches around the 100m isobath, while, near the Section R_1 in the east of the surveyed area, it recedes eastwards beyond the 200m isobath. In winter, the position of the boundaryswings greatly to the left or right, at the Section R_1, it is close to the 100m isobath while, in the middle section of the surveyed area, it is near to the 200m isobath. In autumn, the position of the boundary of Kuroshio water is close to the left side of the 200m isobath while in summer it swings to the left or right side of the 200m isobath. The condition at the bottom layer is like this: in summer, the boundary position of Kuroshio water is to east most, swinging around the 200m isobath, in the northeast of the surveyed area, the boundary position is near the 100m isobath in winter while in spring and autumn, like in summer, it is close to the 100m isobath. In other sea areas, the position of the boundary of Kuroshio basically is the west most in spring, then in autumn and in between in winter.

Ⅴ. Concluding Remarks

It is clear from the above analysis that the distribution of water types in the studied sea area is complicated and changeable and it is hand to find a universal law. The discussion in this paper is only limited to the actual measurements indicate that:

1. The Class Ⅳ mixing water whose property is similar to that of the continental coastal water is distributed along the shore of the continent in autumn and winter and, in spring and summer. Its distribution range extends to the open sea, being located in the northeastern waters of the surveyed area.
2. The boundary between the Kuroshio water and the continental shelf mixing water (called the left boundary of the Kuroshio water) is approximately located between the 100m and 200m isobaths in different seasons and at different layers and, in most cases, near the 200m isobath, but depicts obvious variations at all times and places. In the northeastern waters of Taiwan, the Kuroshio water is to the west most in spring, then in winter, and in summer it is to the east most while in autumn it is in between its positions in summer and winter. At the bottom in summer and from surface to bottom in spring, the Kuroshio water mainly comes from the sea area to the northeast of Taiwan while part of it from the Taiwan Straits. Near the Section R_1 in the northeast of the surveyed area, the intrusion of Kuroshio water into the continental shelf is strongest in winter. And the boundary is to the west; in summer, the intrusion is weakest in most vases and the boundary is to the east; and the situation in spring and autumn is between the above two cases.
3. In the studied sea area, there is crisscross intrusion between the Kuroshio water and the continental shelf mixing water. The Kuroshio water is mingled with the mixing water of the Classes Ⅰ and Ⅱ, while the continental shelf mixing water with isolating water of Kuroshio.
4. An upwelling phenomenon of Kuroshio water along the slope is often found near the continental slope, but sometimes, on the contrary, slipping down of the continental shelf mixing water along the slope is also found to occur.
5. The distribution of water types from southeast to northwest is not always exactly in the order of

water of the Classes k, I, II, III and IV, but, sometimes, there occurs a transitional zone of water types, whose position varies with time and place.

Miao Yutian, Su Jilan and Yu Honghua, 1987, General Survey of the Mixing of Water Types in the East China Sea in Summer, Collection of Papers on Kuroshio Investigation and Research, China Ocean Press, 204-217.

Miao Tutian, Su Jilan and Yu Hongtua, 1987, Mixing Features of Water Types in the East China Sea in Winter, Collection of Paper on Kuroshio Investigation and Research, China Ocean Press, 218-227.

Miao Yutian and Yu Honghua, 1989, Spatial and Temporal Variations of Water Mass mixing Characteristics in the East China Sea, Proceedings of the Japan-China Hoint Symposium of the Cooperator Study on the Kuroshio, Tokyo, Japan.

Tsutomu Sahara and Yoichi Hanzawa, 1979, Distribution of Water Types in the East China Sea, *Sea and Air*, 54,4, 135-148.

El Nino Effect on SST, Wave and Sea State in Nansha Islands Waters

Ke Dongsheng, Xu Shigeng and Jiang Yuejin
South China Sea Branch, SOA, Guangzhou, 510300

Abstract Based on the SST and wave data observed by vessels passing through the Nansha Islands waters, this paper analyses El Nino event's effect on hydrological factors in the above waters. The paper concludes (1) SST in the Nansha Islands water varies with that of the Eastern Equatorial Pacific Ocean in synchronous phase, but varies with that of the Western Equatorial Pacific Ocean in opposite phase; (2) the sea state in Nansha Islands waters is rough, the frequency of great wave increases in the year of El Nino, especially in the next year of the year of El Nino. The paper discusses the reasons for the above phenomena.

Keywords: El Nino SST Wave Nansha Island Waters

The Nansha islands waters (this refers to the sea area to the south of 12°N and to the east 106°E, which is hereinafter called The Nansha waters for short) is located in southern part of the South China Sea, sea water of this area exchanges with the Pacific Ocean through the central and northern parts of the South China Sea as well as Sulu sea and their characteristics can affect each other. The Nansha waters belongs to the low latitude area near the equator where tropical circulation systems of various are extremely active, and it is one of the important heat and water vapor origins of East Asia atmospheric motion. Besides the local effect of natural environmental conditions, El Nino event occurring in the equatorial Pacific Ocean will inevitably affect the Nansha waters and its adjacent waters. Based on the data concerned, this paper analyzes El Nino effect on SST (sea surface temperature), wave and sea state in the Nansha water from various angles.

Ⅰ. Choice and Processing of Data

The studies in the past show that one of the important characteristics of El Nino is: SST in the tropicaleast and west Pacific Ocean is abnormal. The response of oceanographic hydrological state to El Nino is firstly water temperature. But the Yongshu oceanographic station is affected by the reef surroundings, the representativeness of water temperature is poor because of annual data absence, and therefore, it is not ideal to use the data of this station for water temperature analysis. In order to reflect exactly the response of the Nansha waters SST to El Nino, this paper employs the longer duration data (the year 1961—1993), more frequent observation (100 times monthly) data and the chosen sea area is: 10°—12°E (hereinafter called sea area Ⅰ for short which stands for the northern The Nansha waters); the another sea area is: 4°—6°N, 106°—108°E (hereinafter called sea area Ⅱ for short which

stands for the southern The Nansha waters), in which the data observed from commercial vessels' weather reports.

1. Based on the SST data observed from commercial vessels' weather report, the annual mean (arithmetic mean), 33 years' mean, annual SST anomaly as well as each month SST anomaly of every year are derived for the above mentioned the sea areas Ⅰ and Ⅱ during the years of 1961—1993.

2. Based on references, E stands for El Nino year and A refers to La Nino year in this paper (ENSO Monitoring Group, 1989).

Ⅱ. El Nino Effect on SST in the Nansha Waters

SST is an important sign of oceanographic thermodynamic condition and an aspect of air-sea coupling system. The study on SST, especially on sea surface abnormal variation becomes a major subject of the global and regional climate at present.

Fig.1 presents the annual mean anomaly of SST in the sea areas Ⅰ and Ⅱ of the Nansha waters. Except for the lower water temperature occurring in the El Nino year (1976), when El Nino occurs in the tropical Pacific Ocean, SST becomes high in The Nansha waters and that year is warmer; when La Nino occurs, SST becomes low and that year is cold. The spectral analysis of water temperature in the sea area Ⅰ presents 7.3a, 3.5a and 2.7a period of SST (the correspondent probability of confidence is 0.82, 0.80 and 0.79 respectively), this period is extremely close to El Nino occurrence. These analytical results are also identical with Chen Qili(1993) and Niu Zhiwang(1994) studies. It can be seen that the SST variation in the Nansha waters is the same as that in the central part of the South China Sea and the Beibu Gulf(Guo Zhongxing 1998), and varies with that of the Eastern Equatorial Pacific Ocean in synchronous phase, but varies with that of the Western Equatorial Pacific Ocean in opposite phase irregularly (sometimes high and sometimes low in individual years).

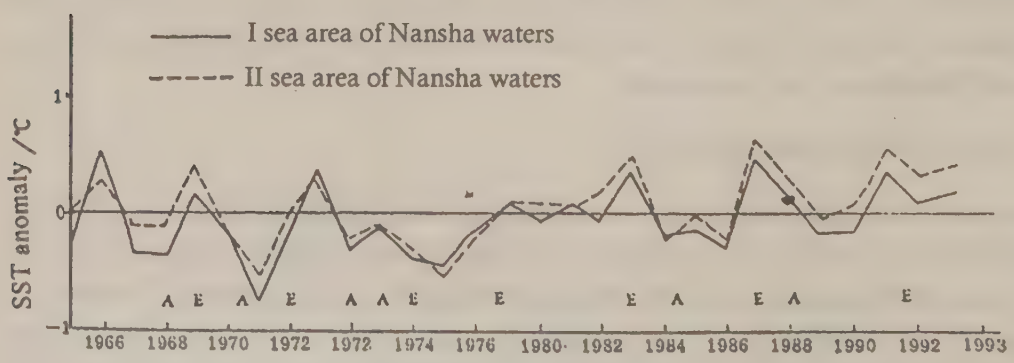
I sea area of Nansha waters
II sea area of Nansha waters
SST anomaly /℃
1
0
-1
A E A E A A E E E A E A E
1966 1968 1970 1972 1972 1974 1976 1980 1982 1984 1986 1988 1990 1992 1993

Note: under the level on the Fig 1 E stands for El Nino year A stands for La Nino

Fig.1 Annual Anomaly of SST in the Nansha waters

For analyzing and verifying the response of SST in Nansha water to El Nino event in the year 1990—1993 in detail and, based on the references, monthly SST anomaly curves for the outer sea off Peru (0°—10°S, 70°—90°W) in the years 1990—1993 are drawn together with those for in the sea areas Ⅰ and Ⅱ of the Nansha waters on Fig.2. This figure indicates that the SST variation in the sea areas Ⅰ and Ⅱ is basically identical with the trend of SST variation in the outer sea off Peru. That El Nino event occurred in May 1991 was strengthened after August entered the full mature period after November. That event reached its prime in March-April in the year period of 1992, then weakened from June and the water temperature tended to became normal in August. By that time, the El Nino event was considered to have vanished. But in April 1993, the El Nino phenomena were reenhanced, and the cold zone of Eastern Equatorial Pacific Ocean was still under the warm state until the end of the year 1993. Certain scholars consider that this is a new El Nino event while other scholars hold that this is only the continuation of the El Nino event of 1991—1992. At the same time, the sea areas Ⅰ and Ⅱ of the Nansha waters showed similar water temperature response to these variation and ocean warming phenomenon occurred too. Fig.2 demonstrates that the sea area Ⅱ got warm in Jul 1997, while the sea area Ⅰ became warm from February. 1991, while was a little early than the Eastern Equatorial Pacific Ocean. But it is found that, the sea areas Ⅰ and Ⅱ of the Nansha waters warmed earlier and began to weaken in July 1991, water temperature became normal in July-August. This ocean warming phenomenon process in the Nansha waters was identical with the trend of the ocean-warming event in the Eastern Equatorial Pacific Ocean. In addition, the sea areas Ⅰ and Ⅱ of the Nansha waters warmed again in April-May 1993. Especially much more obvious is the sea area Ⅰ. Only after October, did the water temperature field of the sea areas Ⅰ and Ⅱ return normal, which was somewhat different from the case of the Eastern Equatorial Pacific Ocean.

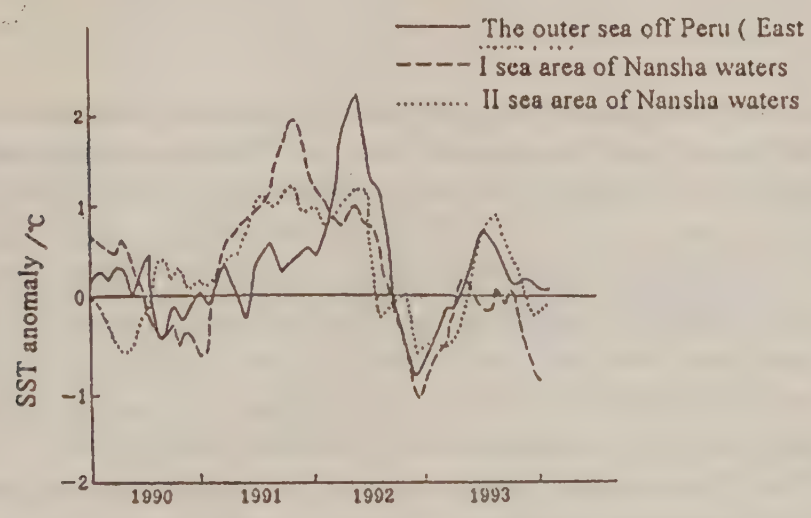

Fig.2 Monthly Anomaly of the SST from 1990 to 1993

Ⅲ. El Nino Effect on Wave and Sea State in the Nansha Water

Based on the analysis on wave data observed at the Yongshu oceanographic station and vessels' reports, the waves in the Nansha waters are mainly affected by monsoon. Generally speaking, from May to September, the southwest monsoon affects the waves mainly, from April to May the wave direction disperses and usually the wave is 1m in height; the SSW direction wave is prevailing from June to September and the monthly mean height of wave is 1.0—1.3m and the mean period is 3—4s, but around 7s for swells. During the southwest monsoon, the frequency of rough sea over 2m is 20% and that of swell is 30-40%. But during the northeast monsoon, the frequency of rough sea is 35—50% and that of swells is 40—70%.

In order to study the effect of El Nino event on the waves in the Nansha waters, it is necessary to analyze the size of waves and the occurrence frequency of various wave scales under the action of wind field. Based on the comparison between the weather reports from ressels passing through the Nansha waters and its adjacent waters with the statistic data observed at Yongshu Jiao. Table 1 presents the occurrence frequency of wave height equal to or over 2m of the first half year (Jan.-Jun.) and the second half year (Jul.-Dec.) from 1990 to 1993. Meanwhile, the table gives the wave statistic results in the vessels reports (including wave and surge).

Tab 1 Rough Sea (Wave Height ≥2m) Occurrence Frequency

Annual	1990	1991	1992	1993	1958-1972
First half year	27	17	19	22	27.5
Second half year	40	54	57	45	42.3
Total	33.5	33.7	38.0	33.5	35

It can be seen that the frequency of rough sea in the first half year of El Nino is low, but increases in the second half year and much more particularly in the next El Nino year. Based on the statistic results for the whole year, the frequently of rough sea is much larger in the year when El Nino occurs than in the normal year. This is because, the SST in the Nansha waters went up rapidly in the first half year of El Nino, while the southwest monsoon was strengthened ahead of time in March and dominated the central and southern parts of the South China Sea. When the southwest monsoon prevailed and there were no tropical storm, wind speed over the Nansha waters weakened the sea state and wave calmed down, and as this period in the El Nino year was longer than that in normal years, and then the frequency of rough sea was low. According to Chen Qili's research findings(Chen Qili, 1992), in the second half of the El Nino year there are much more tropical cyclones occurring in the South China Sea, which in general can affect the Nansha waters (the tropical cyclone location is to the south) and increases the frequency of rough sea in the Nansha waters as well. In the prevailing period of southeast monsoon in autumn and winter, because of the Nansha waters warming in the El Nino year, the tem-

perature gradient and air pressure gradient in the South China Sea are much larger than those in the normal year. These results in the increasing of wind speed, the lengthening of wind duration and the enlarging of frequency of rough sea at the same time. Another note worthy point is that, on Table 1 in the year 1992 (the next year of El Nino event) there were more rough sea occurrences all the year around, especially in the second half year. The reason is that the days of tropical cyclone in the Nansha waters increased in the next year of El Nino event and so did frequency of rough sea.

It ca be seen from the above analysis that the sea state in the Nansha waters is better in the first half year of El Nino year than that in the normal year. Under the control of warmer southwest monsoon the day numbers or frequency of smaller sea state class are generally more than the normal year's in the Nansha waters which is located in the windward of the southwest monsoon.

Ⅳ. Conclusions

The SST in the Nansha waters, like that in the central part of the South China Sea and the Beibu Gulf, varies with the SST in the Eastern Equatorial Pacific Ocean in synchronous phase, but varies with that of in the Western Equatorial Pacific Ocean in opposite phase. The annual variation period of the SST is basically similar to the periodic variation trend of El Nino occurring in the Eastern Equatorial Pacific Ocean, i.e. 7.3a, 3.5a and 2.7a.

The El Nino effects on the wave and sea state in the Nansha waters are mainly as follows: The wave and sea state are better in the first half year of El Nino than in the normal years'. But in the second half year because the days of tropical cyclones increase morn than in the normal year. The days and frequency of rough sea increase morn than the normal year', in particular much more in the next year of El Nino. The annual statistic results indicate that the frequency of rough sea in the South China Sea is larger in the El Nino year than in the normal year.

Chen Qili and Li Jinping, 1992. Tropical Northwest Pacific Ocean Heat Condition's Influence on Tropical Cyclone Activity, *Tropic Oceanology*, 11(3): 89-93.

Chen Qili, 1993. Heat Condition's Effect of Tropical Pacific Ocean on Hydrological Factors in the South China Sea, *Research and Development of the South China Sea*, (3): 1-6.

Enso Monitoring Group 1989. Classification Standard and Index on El Nino Event, *Meteorology*, 15(3): 37-38.

Guo Zhongxing, 1998. SST and Salinity Anomaly during El Nino, *Tropic Oceanology*, 8(4): 52-56.

Niu Zhiwang, 1994. SST Long Periodic Oscillation in the South China Sea and its Relation to El Nino, *Journal of Oceanology*, 16(2): 43-49.

US, 1994. NMC: *Climate Diagnostics Bulletin*, 11: 5-6.

Impacts of Sea Level Rise on the Coastal Areas to the West of the Bohai Bay

Liu Zhenxia, Xia Dongxing, Wang Delin, Li Xuan and Wu Sangyun
First Institute of Oceanography Qingdao 266003

Abstract Based on the assumption of global sea level rising between 30 and 100 cm in the future 100 years by IPCC (1990) in addition to the effect of local ground subsidence, the coastline will retrograde for 50-70 km whose altitudes will be 2.6-3.3m above MSL of Huanghai Sea in the western coastal area of the Bohai bay in 2100. The transgrassive area is about 10,000-11,500 km. If the effect of set-up of storm surge is considered, the transgressive area will reach 16,000 km. Sea level rise which is a serious coastal disaster not only inundates a lot of coastal lowland, but also increases the frequency and intensity of storm tides, and results in the salinization of soils. In vies of this situation we recommend a trinity comprehensive measure of treatment, namely, "building seawall to prevent tides—diverting the Hunaghe River to settle its sediment loads -raising the constructional base".

Keywords: sea level rise, Bohai Bay, coastal area

The warming up of the earth caused by the "greenhouse effect" in the past 50 years has led to the rise of the global sea level. In addition to local ground subsidence owing to natural and man-made factors, the relative sea level rise caused the environments of coastal areas to be worse and worse, such as the retrogradation of coastline, the inundation or contamination of coastal lowlands by sea water, and the destruction or damage of the coastal cities, towns, factories and mines, resulted in the salinization of soils and the shortage of fresh water, increased the frequency and intensity of storm tides and brought about enormous calamity to nearly half of the population living in the agriculturally and industrially developed and culturally concentrated coastal areas all over the world. As a result the rise of sea level and its impacts have become the "hot point" of research of many science branches and have arrested great attention of the governmental departments of the coastal area. Special subjected researches on the mechanism, speed, prediction and response strategies of sea level rise have been carried out by UNEP, SCOPE, IPCC, WMO, US.EPA and other international organizations, governmental departments and scientists from various countries. Most of the researches showed that the global MSL has been rising slowly in the past 100 years, and there is a trend of accelerated sea level rise.

The ground subsidence of western area to Bohai Bay where the third largest city of China- Tianjin and the Tanggu seaport are located is the most serious in China. The impacts of sea level rise on the areas are very terrible. Based on the assumption that the global sea level will rise 30-100 cm in 2100, the relative amplitude of sea level rise and impacts on the western coastal to the area of Bohai Bay are approached and discussed.

Ⅰ. An Outline of the Natural Geography in the Study Area

The study area is on the west coast of the Bohai Sea (116°20′--118°15′E, 38°15′--39°50′N), extending from Nanbu in the north to the Dakouhe River in the south with a coastline of 289 km. In terms of geomorphology, the study area is mainly composed of alluvial-marine deposition plains. The ground of the study area is low and plain in relief, with smoothly low slope gradient. The ground altitude of the west coastal plain of the Bohai Bay varies from 0.5 to 3m, with a slope gradient of 0.01 to 0.02%. In the recent decades, the west coast of the Bohai Bay has been under erosion, resolution in the retrogradation of the natural coastline and the scouring away of the tidal flats.

Tectonically, the study area is largely located in the second subsidence zone of Neocathaysian Structural System, which has been subsiding since the beginning of the Cenozoic Era. The thickness of the Quaternary deposition alone in the coastal plain to the west of the Bohai Bay varies from 350 to 600m. Since the late Pleistocene (about 100 ka BP), three times of seawater transgression have happened in the study area. In Holocene epoch, rivers, lakes and swamps have developed in this area.

The main rivers entering the sea in the study area are Jiyunhe River, New Chaobeihe River, Haihe River, New Yongdinghe River and New Zhangweihe River. The total sediment discharge of all the above rivers is about 900x 10T. In the stage from 3000 B. C., the Haunch River entered the sea at a place near Tianjin and built an old delta system.

The climate in the study area belongs to the continental climate of the East Asia monsoon-type in the Warm-Temperate Zone, characterized by the fact that it is hot and rainy in summer and cold and dry in winter. The mean annual temperature is between 11.2-12.2°C with the precipitation of 560-635mm, and the evaporation capacity is relatively large, and about three times as large as the precipitation.

Except for Nanbu where the tide type is regularly semi-diurnal, the tides along the coasts of this area are irregular semi-diurnal tides, with the tidal ranges varying from 1.5m to 2.5m. The waves in the sea area under consideration are mainly wind waves which are obviously controlled by monsoon. The directions in summer are mainly NE-NNE, while those in winter are mainly NE and NW. The directions of the strong waves and the dominant waves are NE-NNE. Storm surges frequently occur in this area. Set-up more than 2m happen once in 4.6 years.

The study area is an important economic center in the northern part of China. The population of Tianjin is 8 million, and the gross national product in 1990 was 30 billion-yuan. The Tianjin Seaport is the main export-import of Beijing, Tianjin and even the whole North China region. There are oil fields, saltworks and salt chemical industry. Furthermore, aquacultural production and agriculture occupy an important position in regional economy. The annul gross output value of industry and agriculture is over 50 billion yuan.

Ⅱ. Modern and Future Sea Level Changes

1. *Sea Level Changes in Modern Times*

Statistical results of the tidal gauging records from several hundreds of tidal gauging stations around the world showed that the global MSL has risen 10-20cm in the past 100 years, and the speed of sea level rise varies from 0.5 to 3.0mm/a, with an average of 1-2mm/a (IPCC, 1990). Because the amounts and periods of tidal gauging data used by different researchers are quite different, and the gauging stations from which the data are acquired are set at different geographical locations with different influences of vertical movement of the Earth's crust, and the methods of statistical analyses used by different researchers are not the same, some differences exist among the results of statistics made by different researchers. It can be seen obviously in Table 1 that the older and the longer of gauging period of the tidal level records are, the lower the speeds of annual sea-level rise are, and the newer, and shorter of gauging period of the tidal level records are, the higher the rates of annual sea-level rise are, indicating that the sea level rise has been accelerated in the last few decades.

Table 1 **Estimate of Global Sea Level Change**

Rate(mm/a)	Comments	Researchers
>0.5	cryologic estimate	Thorarinsson(1940)
1.1±0.8	many stations, 1907-1939	Gutenburg(1941)
1.2-1.4	combined methods	Kuenen(1950)
1.1-0.4	6 stations, 1807-1943	Lisitzin(1958,1974)
1.2	selected stations, 1900-1950	Fairbridge & Krebs(1962)
1.5	50 American stations	Hicks(1978)
3.0	725 stations, 1935-1975	Emery(1980)
1.2	many stations-regions, 1880-1980	Gornitz et al(1982)
1.5	many stations, 1900-1975	Emery(1980)
1.5±0.15	17 stations, 1903-1969	Barnett(1983)
1.4±0.14	many stations-regions, 1881-1980	Barnett(1984)
2.3±0.23	many stations-regions, 1930-1980	Barnett(1984)
1.15	155 stations, 1880-1986	Barnett(1984)
1.2±0.3	130 stations, 1880-1982	Gornitz & Lebedeff(1987)
1.0±0.1	130 stations, 11 regions, 1880-1982	Gornitz & Lebedeff(1987)
2.4±0.9	40 stations, 1920-1970	Peltier & Tushingham(1989,1990)
1.7±0.13	84 stations, 1900-1980	Trupin & Wahr(1990)
1.5	102 stations,	SOA, China(1990)
1.0-2.0	last 100 years	polar research board(1980)
0.5	last 100 years	Fang Jiaoying et al(1985)
1.4	last 30 yaers	Fang Jiaoying et al(1985)
12±5cm*	since 1900	SCOPE 29 (Molin et al 1986)
10-25cm*	since 1900	US.DOE(Maccracken et al 1985)

The tendency of MSL changes in China is the same as that of the global MSL changes. According to "Reports of Sea Levels in China" published by the State Oceanic Administration of P.R.China

(1989,1990), the sea levels along the coasts of the mainland of China have risen 14 cm on the average in the past 100 years. The statistics of the tide gauging records from 48 long-term tidal gauging stations along the coast of China show that there are 39(1989) or 40(1990) tidal stations (accounting for 81 of 83% of the total number of stations) where sea level has risen, 6(1990) or 7(1989) stations (accounting for 12.5 or 14.6% of the total number of stations) where sea level has fallen, and 2 stations (accounting for 4.5% of the total number of stations) where sea level has kept stable for a long period.

The main reason for the relative sea level lowering of the Yellow Sea may be that the crust of the southeast part of Shandong Peninsula has been uplifted slowly. Estimations of sea level rising rates in the China Seas made by different researchers are different (Table 2). The rate of sea level rise in China in the past 100 years is close to that of the global sea level rise. The annual rate of sea level rise in China varies from 1.0 to 3.5mm. According to statistics of the data from the 48 long-term tidal gauging stations of China, the rate is 1.4mm/a. Since the 1960s the sea level rising rates have become higher, about 2.1-2.3mm/a ion an average, which suggests that the sea level rise has been accelerated. Statistics of the tidal level records of the Tanggu station in the recent 40 years (1950-1989) show that the average rate of the sea level rise is 2.1mm/a (after Zheng Wenzhen, 1991), In general, the sea level changes in the study area has kept in step with those of China and the world.

Table 2 **Estimate of Sea Level Change of the China Seas**

Rate (mm/s)	Stations and period	Sources
2.5	8 stations	Emery & You Fanghu (1981)
3.5	13 stations	Wang Zhihao (1986)
2.3 + 0.9	9 stations 1960-1980	Zhao Mingcai & Zhang Dachu(1986)
2.1	16 stations 1960-1980	Yu Daoyong(1986)
3.0	11 stations	Yang Huairen & Chen Ziqing(1987)
1.0	Changjiang Estuary 1922-1987	Chen Xiqing(1990)
2.5	Changjiang Estuary 1952-1987	Chen Xiqing(1990)
1.0 – 1.2	4 stations of Changjiang Estuary, last 20-35 years	Chen Zongyong et al(1991)
1.4	48 stations	SOA (1989,1990)

2. *Prediction of Sea-level Rise in the Future*

The prediction of the amplitude of sea-level rise in the future is based on the analysis of the causes of sea-level rise, more importantly, on the analysis of the historical data of sea level changes. Most scientists think that the "greenhouse effect" is the main factor contributing to the sea-level rise on the time-scale of decades or ever one hundred years. The State Meteorological Administration(1992) re-

ported that if mankind could not control the emission of greenhouse gases of CO_2, CH, CFC_5 and CO in the future 40 years, the surface temperature of the whole earth will rise about 2.5℃. As the climate becomes warmer, sea water will expand by heating, mountainous glaciers will be melted, and even parts of the ice sheets of Greenland and the west part of the Antarctic will be melted, or splinted into icebergs at the edges of the ice sheets. The thawing water of the glaciers and the ice sheets and also the iceberges will eventually enter the oceans, thus causing the global sea level to rise (Table 3).

Because there are many uncertain factors influencing the climatic warming and sea level rise, the predicted values of sea level rise are scattered quite apart. It is estimated in the recent years that the sea level will rise 50-200cm by the year 2100 AD (Table 4). IPCC (1990) estimated that the rate of sea-level rise in the future would be 3-6 times as high as that in the past 100 years. Under the business-as-usual scenario, the global sea level will rise 31-110cm by the year 2100 AD, most possibly 66 cm. Even if the human beings take various possible measures of prevention to stop the increase of gases in the atmosphere, or to cut them down by the year 2030 A.D, the global sea level will still rise 25 cm in the rest 70 years of the next century because of the lag effects introduced by the thermal inertia of the oceans and the continuing response of land ice to climate changes (IPCC, 1990).

Table 3 Factors Contributing to Sea Level Rise(cm)"Business-as-usual" Scenario-Best Estimate for 2030

	Thermal Expansion	Mountain Glaciers	Greenland	Antarctica	Total
High	14.9	10.3	3.7	0.0	28.9
Best Estimate	10.1	7.0	1.8	-0.6	18.3
Low	6.8	2.3	0.5	-0.8	8.7

(**From IPCC** 1990)

Ⅲ. The Effect of Ground Subsidence

The water-level records made at the tidal gauging stations reflect the changes of the local sea level relative to the benchmarks of the stations, i.e., the relative sea-level changes. Since the land may also be subjected to vertical movements, the benchmarks, which serve as the standards for monitoring sea-level changes, may actually be subjected to vertical movements. So the vertical movement of the ground must be taken into account in the study of the sea-level changes.

Tianjin is one of the most serious regions of ground subsidence in China. The ground subsidence in this region is caused by three factors: (1) tectonic subsidence: Tianjin is tectonically located in the Hebei-Shandong Depression Zone. Under the control of regional tectonics and the differential fault-block movement, the basement has been subsiding in the Tertiary and Quaternary periods at a rate of -3 - -4 mm/a; (2) the compaction of loose sediment layers: The Tianjin region was the old delta of the Huanghe River 1000 years ago, and at present, it is the alluvial plain of the Haihe River, consisting of

5 tributaries, the loose sediment layer which is full of water is of great thickness; (3)the exploitation of ground water: In 1959, the bench marks of Tianjin were found to subside at a rate of -4 to -6 mm/a, which is the rate of subsidence caused mainly by the first two factors, i.e. the natural factors (Huang Liren et al,1991). With the development of the city , more and more ground water has been exploited. In most years, the annual amount of ground-water exploitation was larger than 100 million tons. As a result, the subsidence in Tianjin was speeded up. In the period from 1959 to 1985, 71 km of ground in Tianjin had subsided for 1.5m, with a maximum amplitude 2.63m. The average rate of ground subsidence in the period from 1966 to 1990 is -51 mm/a, with a maximum of -119 mm/a. In 1985, the government of Tianjin began to take measure of controlling the ground subsidence. More than 600 wells have been closed and gradually stopped exploiting ground water. As a result, the rate of ground subsidence decreased year after year. By 1990, the rate of ground subsidence had decreased to -9.9mm/a. Now people in Tianjin are going all out to control ground subsidence in order to decrease the rate to -5 ~ -8mm/ a.

Table 4 **Estimate of Future Global Sea Level Rise(cm)**

Total rise from the 1980s		to(year)	Researchers
Best estimate	Range		
40		2050	Gornitz(1982)
71		2080	Revelle(19830
	56-345	2100	Hoffman(1983)
	26-39	2025	Hoffman(1983)
	58-367	2100	Hoffman(1986)
	10-21	2025	Hoffman(1986)
	10-160	2100	Polar researh board(1985)
80	25-165	2080	Robin(1986)
100	60-230	2100	Thomas(1986)
30	-2-51	2025	Villach(1987)
21	5-44	2030	Raper et al(1990)
20	0-40	2025	Oerlemans (1989)
	28-66	2085	Van der Veen(1988)
18	8-29	2030	IPCC(1990)
44	21-71	2070	IPCC(1990)
66	31-110	2100	IPCC(1990)

The ground subsidence in Tanggu and Hangu, both located close to the Bohai Sea, are even more rapid than in the Tianjin City port. The annual amount of subsidence in Tanggu District was 137 mm in 1984. After the control management for several years, the amount of ground subsidence in this district had decreased to 29 mm by 1988. The rate of subsidence in the study area decreases gradually from the subsidence funnels to both northeast and south directions (Huang Liren, et al, 1991).

Ⅳ. The Landlord Migration of Coastlines and its Impacts

1. *The Possible Positions of the Natural Coastlines in* 2100 *AD*

Sea level rises and lands subsidence manifest in plan as the landlord retrogradation of coastline. All these factors must be taken into account synthetically in predicting the positions of the coastlines in 2100. Because the period of prediction is quite long, some errors may inevitably exist.

As the sea level rise in the study area in the past 100 years has kept pace with the trend and the amplitude of sea level rise in the world, it is feasible to adopt the minimum and maximum amplitudes of MSL rise in 2100 estimated and determined at the conference of IPCC Working Group in 1990, i.e. 30 cm and 100 cm respectively.

The vertical movement of land (including the effects of both natural and man-made factors) is predicted in the mean values. According to the process of ground subsidence in the Tianjin proper in the 20th century and the effect of control management in the recent years, it is reasonable to adopt -7 mm/a as the average annual rate. The rate of subsidence in Tanggu and Hangu districts at present varies from -20 to -30 mm/a, and the rate will possibly still be relatively high in the next 10 years, but later, the rate of subsidence will decrease. So we estimate -15 mm/a the average rate in the two districts to be in the next century. While the rate of subsidence in other places of the Bohai Bay coastal area in the next century is estimated to be -5 mm/a on the average. Of course, the rate of subsidence changes gradually from one region to the adjacent one.

The sum of the amplitude of global sea level change plus that of the vertical movement of the land is the relative sea level change of the area. Because the present natural coastline is located at the position approximately 1.5 m above the MSL of the Yellow Sea, 1.5 m should be added to the above-mentioned predicted relative sea level heights to make out the altitudes of the natural coastlines in 2100 AD which is about 2.6-3.3 m above the MSL.

The study area is severely harmed by storm surge. The potential influence ranges caused by storm surge are determined by adding the storm surge set-up of 2 m to the predicted altitudes of the natural coastlines in 2100. The area under the 4.6-5.3 m contour at present will be possibly influenced by storm surge at that time (Table 5).

Now we can draw the potential lowest and highest coastlines (Fig. 3) and the maximum range under the influence of sea water in case of storm surge in 2100 AD.

2. *The Impacts on Environment*

The impacts of relative sea level rise in the study area are mainly manifested in the following three aspects:

First, coastline retrogradation and land loss. As the coastal area to the west of the Bohai Bay and Tianjin is vast lowlands, the loss and damage caused by the combined effect of sea level rise and ground subsidence will be extremely large. If the amplitude of global MSL rises 30 cm in 2100 AD, the coastline will retrograde for 50 km, reaching the city of Tianjin, which will possibly become a

"Venice in China "in the next century. About 10000^2 km of land will be inundated by seawater, and the Tianjin-Shanghai Railway which is one of the S-N large arteries of transportation of China will also be harmed. If the amplitude of global MSL rises 100 cm, the coastline will retrograde for 70 km, and about 11500 km of land will be inundated.

Table 5 **Sea Level Rise and the Elevation of Coastline in 2100(cm)**

Areas	MSL Rise	Groud subsidence	Relative SLR	Coastline elevation	Potential range of surge
Tianjin city	30	80	110	260	460
	100		180	330	530
Tanggu and Hangu districts	30	160	190	340	540
	100		260	410	610
coast of Bohai Bay	30	60	90	240	440
	100		160	310	510

If the effect of the sea-up of storm surge is added to the combined effect of sea level rise and ground subsidence, the maximum distance of sea water transgression in the coastal area to the west of the Bohai Sea will be more than 100 km, and the area of the land inundated will amount to 16000 km.

Partial elevations of the Tanggu and the Hangu districts are below the spring high water at present. According to the above rates of sea level rise and ground subsidence, the land whose present elevation is below 2.5 m MSl of Huanghai will be lower than the spring high water in the next mid-century. We may imagine that the west coasts of Bohai Bay will be the same as the present coasts of Netherlands after the middle of the 21-century. Except local high lands and artificial buildings, most lands of coastal area will be lower than spring high water and depend on the seawall to preserve and prevent from transgression.

Secondly, the calamities of flooding and water logging will be greatly enhanced. The reasons are as follows: (1) the frequency and intensity of storm surge will increase. Because of the MSL rise, the maximum high tide level that occurs once in 100 years at present will occur once in 20 years or 10 years; (2) The erosional base of rivers and the river beds of the lower-reaches channels will all be raised, resulting in the impediment to the drainage of the rivers in flooding seasons and hance flooding calamities will occur frequently; (3) Most of the available seawalls will become ineffective in preventing the tides. The calamities of flooding and water logging will be especially serious in the Tianjin-Tanggu region. In view of the topography and the development of river systems, the Tianjin-Tanggu region is gradually becoming a water collection basin in North China, in which most of the ground elevation is close to or slightly higher than the present high tide level. The low surface relief is extremely unfavorable for the drainage of flooding water. Once a catastrophic flood occurs, the Tianjin-Tanggu region will inevitably be inundated. The calamity of flooding will be the first disaster in the Tianjin

municipality in the future.

Thirdly, underground invasion of seawater and salinization of soils. Sea level rise means the relative lowering of ground water table in land; hence the underground salt-water wedge will advance landlord. The penetration of seawater into the land will cause the salinization of soils and the damage of the resource of fresh ground water, leading to the waste of good farmlands and the shortage of fresh water.

V. The Response Strategies

The study area is one of the most important economic zones in China. Although they are threatened by sea level rise, anyhow, we must not let them be swallowed up by the sea. The sole option (for us) is to take various possible measures to protect them, especially the city of Tianjin. Today we have adopted the response strategy of limiting the exploitation of ground water in order to slow down ground subsidence and mitigate the calamity caused by the underground intrusion of seawater. As for the problem of future sea-level rise, according to local environmental conditions, we propose a trinity comprehensive measure of treatment, namely, "building seawall to prevent tides - diverting the Huanghe River to settle its sediment loads - raising the constructional base".

1. *Building Seawalls to Prevent Tides*

The length of the coastline in the study area is 289 km. Stony seawalls with the top width of 3 m, the bottom width of 10 m and the height of 6 m should be built, which will cost 1156 million Yuan (1 km costs about 4 million Yuan).

2. *Diverting the Huanghe River to Settle its Sediment Lad on the Coastal Lowlands*

The Huanghe River, which is the highest sediment load river in the world, enters the sea between the Bohai Bay and the Laizhou Bay in the study area. The multiple-year average annual sediment discharge of the Huanghe River is about 1 billion tons. The average sediment content of the river water is 25kg/m^3, with a maximum of 222kg/m^3 (1973.9.7). Based on the average value; 1.6cm-thick of sediment layer can be deposited from 1m-thick of the Huanghe River water. A measure of building the plain reservoir to store water and settle suspended sediment has been adopted in the Huanghe River delta region, which has not only acquired the freshwater, but also silted farmlands. Once the bottom of the reservoir is silted up with sediment to certain height, another lowland will be chosen to build a new reservoir. This measure can be used to silt up the lowlands in the Tianjin-Tanggu region.

The channel of the Huanghe River near the apex of its delta is only 200 km away from Tanggu, much nearer to the North and South Dagang regions to the south of Tianjin City. So the distances of drawing water from the Huanghe River to silt up the coastal lowlands will not be very long. In addition, the Huanghe River is an over ground river. The elevation of the riverbed near Gaoqing upstream from the apex of the delta is 15 m (the ground elevation outside the banks of the river is about 5 m), and the water level of the river is 18 m higher than the ground in Tanggu and Hangu. So the longitudinal gradient of the diversion canal is about 0.01%. If 1/10 of the sediment discharge of the Huanghe

River is drawn to silt up the coastal lowlands, an area of 50 km of the lowland will be silted up for 1 m each year. The area of land under the serious threat of relative sea level rise is 2000 km of Tianjin-Tanggu -Hangu region. If the amplitude of sea level rise by 2100 is 1 m, and 1/10 of the sediment load of the Huanghe River is settled in this region each year, the grounds of the lowlands in Tianjin-Tangu -Hangu region will be silted up for 1 m on the average in 40 years, thus maintaining the relationship between the ground surface of the lowlands and the sea level in this region in the next century the same as at present.

In addition, the Yongdinghe River, which is called "the second Huanghe River in China", enters the sea in the Tianjin-Tanggu region. The sediment load in the lower reaches decreased as the Guanting Reservoir was built at the upper reaches of the river, and on the other hand, the reservoir has been silted seriously. It may be possible to take some technical measures to increase the sediment load of the lower reaches of the Yongdinhe River in order to settle more sediment on the coastal lowland.

There are two routes to choose for the project of diversion canal used to draw water to transport sediment from the Huanghe River to fill in the lowlands in Tianjin-Tanggu region. The first one is from the river section of the Huanghe River near Gaoqing to the coastal lowlands in the Tianjin-Tanggu region by building a diversion canal from south to north along the present coast. The total length of this canal is about 200km (Fig. 4), which is the shortest route. The second one is from the river section of the Huanghe River near Zhengzhou in Henan Province to the lowland in Tianjin by building a diversion canal in the direction of SW-NE, which are 1000km long. From the point of view of long-term interests, the second route is more reasonable, because the project will not only relieve the Tianjin-Tanggu region from the threat of sea level rise, but also improve the conditions of the coastal environment in Tianjin by recharging ground water which will help to slow down the ground subsidence in this region, and improve the ecological environment along the route at the same time.

3. *Raising the Elevation of the Bases of Buildings*

The measures of building seawall and silting up the ground of the lowlands must be combined with the measure of raising the elevation of the bases of large-scale permanent building about 2m. The combined of the three measures can greatly enhance the calamity-resistance power of the Tianjin-Tanggu region. We can not do with the only measure of building seawall without adopting the other two measures. On this point, the lesson of New Orleans of the United States should be kept in mind. The New Orleans is located in the Mississippi Delta where the ground relief is low, and the ground subsides. The city was enclosed by dikes built in early times. But once flooding occurs, the city will be besieged by flood and suffer from flooding calamity. In the future 100 years, the Tianjin-Tanggu region will confront the same predicament as that of the New Orleans at present, and the situation may be even more severe.

Conclusion

With the development of anthropogenic society, the living environment of mankind is getting worse

and the natural disasters are intensifying gradually. The worsening coastal environment of the western Bohai Bay is due to ground subsidence and sea level rise, which results in landlord transgression by sea water, flooding increase and intensity of storm surge and so on. All coastal calamities will be more serious in the next century. We must take effective response measures as early as possible in order to mitigate the loss of the disasters.

Chen Xiqing, 1990, "Sea level changes from 1922 to 1987 in the Changjinag River mouth and its significant" *Acta Geographica Sinica*, 45:4:387-394, (in Chinese).

Chen Zongyong, Huang Yunbe, Zhou Tianhua, Tang Enxing, Yu yifa and Tian Hui, 1991, "A study on mean sea level of the Changjinag River estuary", *Oceanologia et Limnologia Sinica*, 22:4:315-320, (in Chinese).

And You Fanghu, 1981, "The sea level changes along Chinese coast to the western Pacific Ocean", *Oceanologia et Limnologia Sinica*, 12:4:297-305, (in Chinese).

Fang Qiaoying and Shi Ruihai, 1985, "The change of the world sea level in past 100 years", *Marine Science Bulletin* 4: 6:1-5, (in Chinese).

Huang Liren, Hu Huimin and Yang Guohua, 1991, "Sea level change along the western and southern coast of Bohai Sea and recent crustal retrial movement in adjacent area", *Crustal Deformation and Earthquake*, 11:3:1-9, (in Chinese).

Intergovernmental Panal on Climate Change, 1990, "Climate change, the IPCC scientific Assessment" 263-281, Cambridge University Press.

Titus, J.G., R.A. Park, SP Leatherman, J.R. Weggel, M.S. Greene, P.W. Mausel, S. Brown, C. Gaunt, M. Trepan, G. Yohe, 1991, "Greenhouse effect and sea level rise: the cost of hold back the sea", *Coastal Management*, 19:171-204.

Wang Zhihao, 1986, "The sea-level change in 20th century", In: China Sea levels changes, Eds. Qing Yunshan, et al, China Ocean Press, 237-245, (in Chinese).

Yang Huairen and Chen Xiqing, 1988, "Greenhouse effect and impact of sea level rise and climate changes on the nest century", *Journal of Nanjing University*, 24:1:66-74, (in Chinese).

Yu Daoyong, 1986, the trend analysis of changes in sea level during the past 20 years. In: China Sea levels changes, Eds. Qin Yunshan, et al, China Ocean Press, 226-236, (in Chinese).

Zhao Mingcai and Zhang Dachu, 1986, Mean sea level changes in the China sea area for 30 years, Proceeding of the First Symposium on Ocean Tides and Sea Level published by the Institute of Marine Scientific Technological Information, SOA, 119-124, (in Chinese).

On the Solution of the Boundary Layer Equation for the Laminar Boundary Layer between Two Parallel Streams

Li Xinming
Ocean University of Qingdao, Qingdao, 266003
Zhen Li
Horn Point Environmental Lab. University of Maryland System, Cambridge, MD

Abstract In the present paper it will be shown that, by taking the reference frame moving with the velocity of fluid at the interface of two steady parallel streams, the laminar boundary layer flow in the two fluids can be decoupled into two flows. These are exactly the same as the laminar boundary layer flows along a flat plate. And that, by using the existing exact solution of the laminar boundary layer equation for the boundary layer flow along a flat plate and appropriate boundary conditions. An exact solution of the laminar boundary layer equation for the laminar boundary layer between two parallel streams with different densities, viscocities and velocities is given elegantly.

For the cases considered by Lock, the results obtained by the present method are compared with Lock's numerical calculations in detail.

Keywords: boundary layer parallel streams Blasius solution

Ⅰ. Introduction

In the study of the stability of the flow of a fluid stream over a layer of the same fluid at rest, Lessen (1949) has obtained the velocity distribution of steady motion in the free laminar boundary layer separating the two streams. A more general problem, when the two fluids are of different densities and viscosity, was considered and Sir Geoffrey Taylor has already given a simple approximate solution of Von Karman's momentum integral method in an unpublished note. A method for obtaining the exact numerical solutions by the use of asymptotic expansions together with a series expansion has been given by Lock (1951). In the present paper it will be shown that, by taking a reference frame moving with the fluid velocity at the interface, the laminar boundary layer flows in the two fluids can be decoupled into two flows. Those are exactly the same as the laminar boundary layer flow along a flat plate and that, by using the existing exact solutions of the laminar boundary layer equations of the flow along the flat plate and appropriate boundary conditions, an exact solution of the flow system presented above is give elegantly.

Yih(1981) has pointed out that the agreement Lock's results and Reichardt's measurements is

rather less than good. In contrast with this, the present work can predict Reichardt's measurements exactly for the cases mentioned by Yih.

Ⅱ. Boundary Layer Equations

We consider the two – dimensional motion of a stream with a constant velocity U_1, density P_1, and viscosity μ_1, over a parallel stream with a constant velocity U_2, density P_2, and viscosity μ_2. Both fluids are assumed to be incompressible. A case of some generality is that in which two uniform streams of identical fluid, both moving in the same direction but with different speeds U_1 and U_2 (< U_1), come into contact at $\chi' = 0$, $y' = 0$, as shown in Figure 1. When $U_2 = 0$, this can be regarded as a specification of the two – dimensional flow at the edge of a wide slit through which an initially uniform stream is being discharged into the fluid.

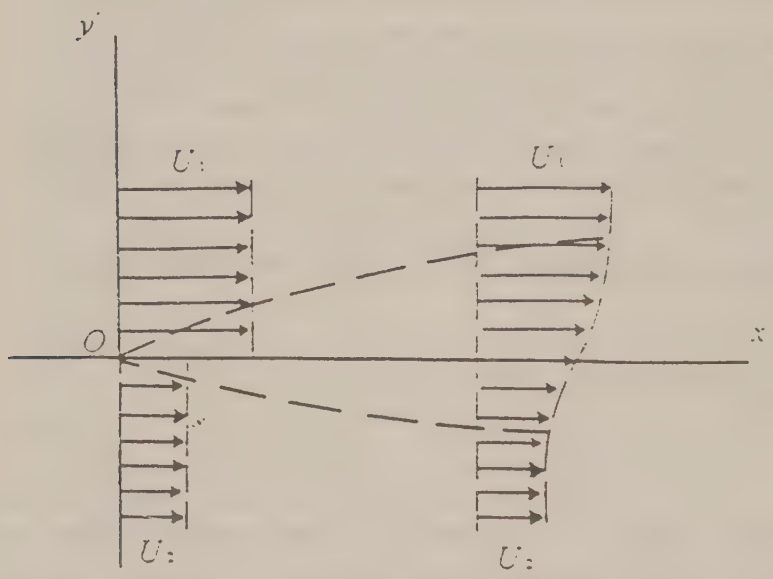

Fig.1 The boundary layer between two parallel stream coming into contact at $x' = 0$, $y' = 0$

As shown by Lock, when $P_1 < P_2$, however, gravity has no effect and the interface is left apparently arbitrary see Lessen (1949). In fact, this dose not materially affects the solution. And according to Batchelor (1967), no part of the upper region of fluid can be accelerated by contact with the lower stream, and no part of the lower region can be decelerated; thus the acceleration is always zero at the interface between the two fluids. In other words, the velocity of the fluids at the interface, U_0, is constant along the flow direction.

Table 1

	$\frac{u_0}{U_1}$		$C_{\tau 0}=\frac{\tau_0}{\rho_1 U_1^2}\left(\frac{U_1 x}{\nu_1}\right)^{1/2}$	
	Exact Solution	R. C. Lock Method	Exact Solution	R. C. Lock Method
$\lambda_1=0, \rho\mu=5.965\times10^4$	0.02495	0.0211	0.31971	0.3318
$\lambda_1=0, \rho\mu=100$	0.17726	0.1727	0.24781	0.3183
$\lambda_1=0, \rho\mu=10$	0.31701	0.3428	0.18743	0.2815
$\lambda_1=0, \rho\mu=1$	0.50000	0.5873	0.11740	0.1996
$\lambda_1=0.501, \rho\mu=1$	0.75050	0.7657	0.04138	0.1219
$\lambda_1=0.25, \rho\mu=1$	0.62500	···	0.07625	···
$\lambda_1=0.75, \rho\mu=1$	0.87500	···	0.01480	···

Based on the conclusions described above, we take the moving coordinates as follows: the x – axis is horizontal, and in the direction of motion of the free streams; the y – axis is vertical upwards; the whole coordinate frame is moving with the velocity at the interface, u_0, but the origin is instantaneously taken to coincide with the point at which the two fluids are supposed first to come into contact, i. e., the moving coordinate frame $O-xy$ moves with the velocity of fluid at the interface but instantaneously coincides with the absolute coordinate frame $O'-x'y'$. The flow pattern observed in the coordinates is shown in Figure 2.

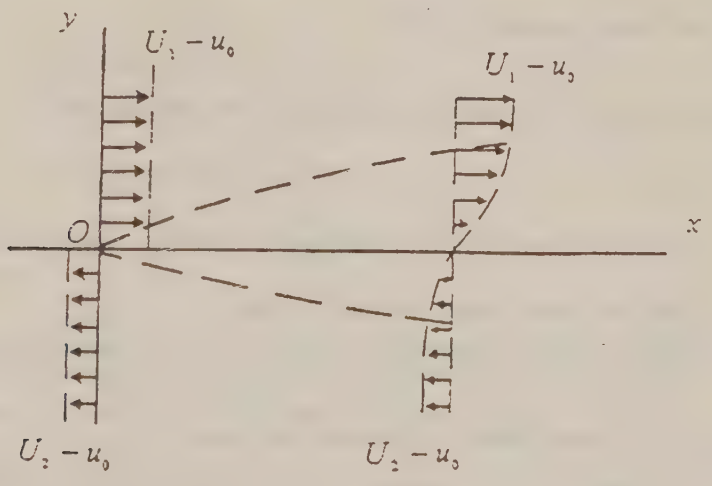

Fig. 2 The flow pattern observed in the moving coordinates

The velocities of the lower and the upper streams in this frame will change to $U_1 - u_0$ separately. U and v represent the corresponding components of velocity of the fluids. It should be noted that in terms of this notation, the real (absolute) velocity components of the fluids would be $u_0 + u$, and v.

The boundary – layer hypothesis and v compare everywhere small with u, the boundary layer equations for the present case are

$$u\frac{\partial u}{\partial x} + v\frac{\partial u}{\partial y} = v_1\frac{\partial^2 u}{\partial y^2} \tag{2.1}$$

for the upper fluid, and

$$u\frac{\partial u}{\partial x} + v\frac{\partial u}{\partial y} = v_2\frac{\partial^2 u}{\partial y^2} \tag{2.2}$$

for the lower fluid, where v1 and v2 are the kinematics coefficients of viscosity of the two fluids separately.

The equation of continuity is

$$\frac{\partial u}{\partial x} + v\frac{\partial u}{\partial y} = 0 \tag{2.3}$$

so that there exists a stream function and

In terms of ψ, Equations (2.1) and (2.2) are written as

$$\psi_y\psi_{xy} - \psi_x\psi_{yy} = v_1\psi_{yyy} \tag{2.4}$$

$$\psi_y\psi_{xy} - \psi_x\psi_{yy} = v_2\psi_{yyy} \tag{2.5}$$

where the subscripts denote the partial derivatives.

In order to solve the Equation (2.4) we introduce the non-dimensional variable

$$\eta_1 = \left(\frac{U_1 - u_0}{v_1 x}\right)^{1/2} y \tag{2.6}$$

and look for a solution in which

$$\psi = (v_1(U_1 - u_0)x)^{1/2} f_1(\eta_1) \tag{2.7}$$

where $f_1(\eta_1)$ is a dimensionless function. This corresponds to

$$u = \frac{\partial \psi}{\partial y} = (U_1 - u_0) f_1'(\eta_1);$$

$$v = -\frac{\partial \psi}{\partial x} = \frac{1}{2}\left(\frac{(U_1 - u_0)v_1}{x}\right)^{1/2}\{\eta_1 f_1'(\eta_1) - f_1(\eta_1)\} \tag{2.8}$$

We are thus led to expect a similarity solution.

Substitution of the expressions (2.7) and (2.6) for ψ into the Equation (2.4) yields

$$2f_1''' + f_1 f_1'' = 0 \tag{2.9}$$

where the prime denotes the derivative with respect to η_1.

In the lower fluid it is convenient to use a different variable η_2 defined by

$$\eta_2 = \frac{(U_1 - u_0)^{1/2}}{(v_2 x)^{1/2}} y, \tag{2.10}$$

so that

$$\eta_2 = \left(\frac{v_2}{v_2}\right)^{1/2} \eta_1 , \tag{2.11}$$

and to put

$$\psi = (v_2(U_1 - u_0)x)^{1/2} f_2(\eta_2), \tag{2.12}$$

where f_2 is also a dimensionless function. Then

$$\begin{aligned} u &= (U_1 - u_0) f_2'(\eta_2), \\ v &= \frac{1}{2}\left(\frac{(U_1 - u_0)v_2}{x}\right)^{1/2} \{\eta_2 f_2'(\eta_2) - f_2(\eta_2)\}. \end{aligned} \tag{2.13}$$

By substituting the expression (2.12) and (2.11) for Δ into the Equation (2.5), we will have

$$2f_2''' + f_2 f_2'' = 0. \tag{2.14}$$

In the moving coordinates, the boundary conditions at infinity are

$$u = U_1 - u_0 , \text{as} \quad y \to \infty ;$$

and

$$u = U_2 - u_0 , \text{as} \quad y \to -\infty ;$$

Then

$$f_1'(\eta_1) = 1 , \text{as} \quad \eta_1 \to \infty ; \tag{2.15}$$

and

$$f_2'(\eta_2) = \frac{U_2 - u_0}{U_1 - u_0} , , \text{as} \quad \eta_2 \to -\infty ,$$

or

$$f_2'(\eta_2) = \lambda , \text{as} \quad \eta_2 \to -\infty ; \tag{2.16}$$

where

$$\lambda = \frac{U_2 - u_0}{U_1 - u_0}. \tag{2.17}$$

If we introduce the $\lambda = \frac{U_2}{U_1}, c = \frac{u_0}{U_1}$。 expression (2.17) for λ may be rewritten as

$$\lambda = \frac{\lambda_1 - c}{1 - c}. \tag{2.18}$$

Since the motion is steady, the interface between the fluids is a streamline, $\psi = 0$, then it is obtained that

$$f_1(0) = f_2(0) = 0. \tag{2.19}$$

The other conditions to be satisfied at the interface are the velocity components in the present coordinates should be continuous and equal to zero and transverse component of stress should be continuous. We therefore have

$$f_1'(0) = f_2'(0) = 0, \tag{2.20}$$

which and the Equation (2.19) ensure that both u and v should be continuous and equal to zero at the interface.

The tangential stress is $\mu \frac{\partial u}{\partial y}$ approximately; using the Equations (2.8) and (2.13), we see that this will be continuous provided that

$$\rho_1 v_1^{1/2} f_1''(0) = \rho_2 v_2^{1/2} f_2''(0). \tag{2.21}$$

It is convenient to put the equations and all boundary conditions together here:

It is easy to see that both the equations and the boundary conditions for the two boundary layers in the two fluids are exactly the same as that for the case of the boundary layer flow along a flat plate. And then any existing results about the boundary layer flow along a flat plate, especially some approximate and exact solutions, may be applied the present study.

Table 2 Solution for the Case

$\rho\mu = 5.965 \times 104, \lambda_1 = 0.$

Lower Fluid

η_2	u/U_1 Exact Solution	u/U_1 Lock's Solution
0	0.02495	0.0211
-2	0.02304	0.0184
-4	0.01966	0.0158
-6	0.01705	0.0134
-8	0.01450	0.0112
-10	0.01206	0.0093
-12	0.00978	0.0076
-14	0.00771	0.0062
-16	0.00589	0.0050
-18	0.00435	0.0041
-20	0.00309	0.0033
-25	0.00111	0.0019
-30	0.00031	0.0011
-35	0.00006	
-40	0.00001	0.0003
-45	0.00000	
-50		0.0001
-60		0.0000

Upper Fluid

η_1	u/U_1 Exact Solution	u/U_1 Lock's Solution
0.0	0.02495	0.0211
0.4	0.15441	0.1537
0.8	0.28306	0.2853
1.2	0.40890	0.4136
1.6	0.52882	0.5353
2.0	0.63901	0.6463
2.4	0.73575	0.7431
2.8	0.81622	0.8228
3.2	0.87918	0.8846
3.6	0.92525	0.9293
4.0	0.95663	0.9594
4.4	0.97648	0.9782
4.8	0.98809	0.9891
5.2	0.99439	0.9949
5.6	0.99754	0.9978
6.0	0.99900	0.9991
6.4	0.99962	0.9997
6.8	0.99987	0.9999
7.2	0.99990	
7.6	0.99999	
7.8	1.00000	

* In Table Ⅱ - Ⅳ u represents absolute velocity.

Ⅲ. Exact Solutions for the Boundary Layer Equations

It will be shown that the Blasius Solution (Blasius, 1908) for the boundary layer along a flat plate can be applied in the present case successfully.

For the upper fluid, in order to find the solution of the Equation (2.9) with the boundary conditions (2.15), (2.19) and (2.20), we suppose that

$$f_1(\eta_1) = A_0 + A_1\eta_1 + \frac{A_2}{2!}\eta_1^2 + \frac{A_3}{3!}\eta_1^3 + \cdots$$

The conditions

$$f_1(0) = f_1'(0) = 0$$

are satisfied provided that

$$A_0 = A_1$$

Since the Equation (2.9) should be satisfied, it may be obtained that

$$A_3 = A_4 = A_6 = A_7 = A_9 = A_{10} = \cdots = 0,$$

and

$$A_5 = -\frac{1}{2}A_2^2, A_8 = -\frac{11}{2}A_2A_5 = -\frac{11}{4}A_2^3, \cdots$$

Hence, if $A_2 = \eta_1$, is taken the solution of Equation (2.9) can be written in the form of

$$f_1(\eta_1) = \sum_{n=0}^{\infty}\left(-\frac{1}{2}\right)^n \frac{\alpha_1^{n+1}c_n}{(3n+2)!}\eta_1^{3n+2}, \tag{3.1}$$

where

$$c_0 = 1, c_1 = 1, c_2 = 11, c_3 = 375,$$

$$c_4 = 27.897, c_5 = 3,817,137, \cdots,$$

$$c_n = (3n-1)!\sum_{i=1}^{n}\frac{c_{i-1}c_{n-i}}{[3(i-1)]!\,[3(n-i)+2]!}, \cdots$$

Here the value of η_1 is to be chosen in such a way as to satisfy the boundary condition $f_1'(\infty) = 1$.

By putting $f_1(\eta_1) = F(\eta_1)$ when $\alpha_1 = 1$, i.e., introducing

$$F(\eta) = \frac{\eta^2}{2} - \frac{\eta^5}{2.5!} + \frac{C_2\eta^8}{4\cdot 8!} - \frac{C_3\eta^{11}}{8\cdot 11!} + \frac{C_4\eta^{14}}{16\cdot 14!} + \cdots,$$

one obtains that

$$f_1(\eta_1) = \alpha_1^{1/3}F(\alpha_1^{1/3}\eta_1) \tag{3.2}$$

Whence, for the boundary condition at $\eta_1 = \infty$,

$$\lim_{\eta_1\to\infty} f_1'(\eta_1) = \alpha_1^{2/3}\lim_{\eta_1\to\infty} F'(\alpha^{1/3}\eta_1)$$

$$= \alpha_1^{2/3}\lim_{\eta_1\to\infty} F'(\eta) = 1,$$

and therefore

$$\alpha_1 = \lim_{\eta_1\to\infty}\left[\frac{1}{F'(\eta)}\right]^{3/2} \tag{3.3}$$

Thus in principle α_1 may be determined by computing $F(\eta)$ from its series for successively increasing

values of η until a sufficiently constant asymptotic value is obtained. For large values of η, however, convergence of the series is slow and it is preferable to compute $F(\eta)$ by numerical integration of the differential equation (Howarth, 1938). In this way it is found that

$$\lim_{\eta\to\infty} F'(\eta) = 2.0854,$$

From (3.3), it is obtained that

$$\alpha_1 = 0.33206$$

For the lower fluid, in order to find the solution of the Equation (2.14) with boundary conditions (2.16), (2.19) and (2.20), we note that if the following function and variable replacements

$$f_3(\eta_3) = -f_2(\eta_2),$$

$$\eta_3 = -\eta_2,$$

are taken, then $f_3(\eta_3)$ will satisfy the following equation and boundary conditions,

$$2\overset{\cdots}{f_3} + f_3 f_3'' = 0,$$

$$f_3(0) = f_3'(0) = 0$$

$$f_3'(\infty) = -\lambda$$

It is clear that, parallel to the same way in which the solution for the upper fluid is obtained, it can be found that

$$f_3(\eta_3) = \sum_{n=0}^{\infty}\left(-\frac{1}{2}\right)^n \frac{\alpha_2^{n+1} c_n}{(3n+2)!}\eta_3^{3n+2},$$

and

$$\alpha_2 = \lim_{\eta\to\infty}\left[\frac{-\lambda}{F'(\eta)}\right]^{3/2} = \left[\frac{-\lambda}{2.0854}\right]^{3/2}$$

Then, for the lower fluid, we have

$$f_2(\eta_2) = -\sum_{n=0}^{\infty}\left(-\frac{1}{2}\right)^n \frac{\alpha_2^{n+1} c_n}{(3n+2)!}(-\eta_2)^{3n+2}, \tag{3.4}$$

where

$$c_0 = 1, c_1 = 1, c_2 = 11, c_3 = 375,$$

$$c_4 = 27,897, c_5 = 3,817,137, \cdots,$$

$$c_n = (3n-1)! \sum_{i=1}^{n} \frac{c_{i-1} c_{n-i}}{[3(i-1)]!\ [3(n-i)+2]!}$$

$$\cdots$$

and

$$\alpha_2 = \lim_{\eta\to\infty}\left[\frac{-\lambda}{F'(\eta)}\right]^{3/2} = \left[\frac{-\lambda}{2.0854}\right]^{3/2} \tag{3.5}$$

From expression (3.3) and (3.5), one obtains that

$$\alpha_2 = \alpha_1(-\lambda)^{3/2},$$

or

$$\alpha_2 = 0.33206(-\lambda)^{3/2} \tag{3.6}$$

The boundary condition (2.21) is satisfied provided that

$$(\rho\mu)^{1/2}(-\lambda)^{3/2} = 1 \tag{3.7}$$

where $\rho = \rho_2/\rho_1$, $\mu = \mu_2/\mu_1$

Note that $\lambda = \dfrac{U_2 - u_0}{U_1 - u_0}$, from (3.7) one obtains the velocity at the interface,

$$u_0 = U_2 + \frac{1}{1 + (\rho\mu)^{1/3}}(U_1 - U_2), \text{if} \quad U_2 > 0 \tag{3.8}$$

or

$$u_0 = U_2 + \frac{1}{1 + (\rho\mu)^{1/3}} U_1, \qquad \text{if} \quad U_2 = 0 \tag{3.9}$$

Table 3 Solution for the Case

$\rho\mu = 100, \lambda_1 = 0$

Lower Fluid

η_2	u/U_1 Exact Solution	u/U_1 Lock's Solution
0.000	0.17726	0.1727
-0.527	0.16286	0.1560
-1.122	0.14663	0.1376
-1.718	0.13048	0.1201
-2.313	0.11459	0.1038
-2.909	0.09910	0.0890
-3.504	0.08427	0.0758
-4.100	0.07027	0.0641
-4.696	0.05738	0.0539
-5.291	0.04580	0.0452
-5.887	0.03565	0.0377
-6.482	0.02704	0.0314
-7.078	0.01993	0.0260
-7.674	0.01426	0.0215
-8.269	0.00990	0.0178
-9.758	0.00346	0.0110
-11.247	0.00099	0.0067
-12.736	0.00023	0.0041
-14.225	0.00004	0.0025
-15.714	0.00001	0.0015
-18.692	0.00000	0.0006
-21.670		0.0002
-24.649		0.0001

Upper Fluid

η_1	u/U_1 Exact Solution	u/U_1 Lock's Solution
0.000	0.17726	0.1727
0.395	0.28512	0.2979
0.789	0.39208	0.4208
1.184	0.49706	0.5381
1.578	0.59704	0.6459
1.973	0.68944	0.7405
2.367	0.77079	0.8193
2.762	0.83911	0.8811
3.156	0.89293	0.9264
3.551	0.93288	0.9574
3.945	0.96041	0.9771
4.340	0.97812	0.9887
4.734	0.98866	0.9951
5.129	0.99454	0.9974
5.523	0.99754	0.9989
5.918	0.99897	0.9996
6.312	0.99960	0.9998
6.707	0.99986	0.9999
7.101	0.99995	1.0000
7.500	0.99998	
8.000	1.00000	

The skin friction coefficient is

$$C_{\tau_0} = \frac{\tau_0}{\rho U_1^2}\left(\frac{U_1 x}{\nu_1}\right)^{1/2} = \alpha_1 (1-c)^{3/2}$$
$$= 0.33206\left(1 - \frac{u_0}{U_1}\right)^{3/2} \tag{3.10}$$

The asymptotic formulas valid for large values of η_1 and η_2 are also found to be

$$f_1(\eta_1) \sim \eta_1 - 1.73 + 0.231 \int_{\infty}^{\eta_1} d\eta_1 \int_{\infty}^{\eta_2} e^{-\frac{1}{4}(\eta_1 - 1.73)^2} d\eta_1, \tag{3.11}$$

for the upper fluid and

$$f_2(\eta_2) = \lambda\left[\eta_2 - 1.73/\sqrt{\lambda} + 0.231 \int_{\infty}^{-\sqrt{-\lambda}\eta_2} d\eta_2 \int_{\infty}^{-\sqrt{-\lambda}\eta_2} e^{-\frac{1}{4}(\eta_2 - 1.73)^2} d\eta_2\right] \tag{3.12}$$

for the lower fluid.

IV. Result and Conclusions

The velocity profiles in the five cases that have been considered by Lock (1951) are recalculated according to (3.1) and (3.11) as well as (3.4) and (3.12) for the upper fluid and the lower fluid separately. Both the present results and the numerical results obtained by Lock are given in Tables Ⅱ – Ⅳ, and plotted in Figures 3 and 4 separately. It can be seen from these tables and Figures that except in the case when $\lambda_1 = 0$, $\rho\mu = 1$, there is larger difference between the velocities at the interface, the velocity profiles given by these two methods have complete agreement. As Yih (1981) has pointed out for the case in which $\lambda_1 = 0$, *and* $\rho\mu = 1$, the calculated value of u_0/U_1 by Lock is approximately 0.6, however, Reichardt's experimental results show that it is about 0.5. In contrast with Lock's results, the present solution shows that for the case described above u0/U1 equals 0.5 exactly. It is clear that our theoretical prediction is in agreement with Reichardt's measurement completely. In addition, in our solutions all flow quantities such as the velocity profiles for the upper and lower fluid layers, the velocity of the fluid particles on the interface, and the skin friction coefficient are given in terms of definite analytical expressions. That is very useful for further application and study.

The values of the velocity ratio u_0/U_1 and the skin friction coefficient $C_{\tau 0}$ for seven cases are calculated according to (3.8) or (3.9) and (3.10) and listed in Table 1. For comparison, the corresponding Lock's numerical results are also included in Table 1.

According to (3.8) or (3.9) and (3.10), it is evident that the values of $u_0 - U_2/U_1 - U_2$ or u_0/U_1 depend only on $\rho\mu$ and the values of $C_{\tau 0}$ depend only on u_0/U_1. Therefor $u_0 - U_2/U_1 - U_2$ or u_0/U_1 and $C_{\tau 0}$ can be plotted against $\rho\mu$ (conveniently, $\rho\mu^{1/3}$) and u_0/U_1 are plotted in Figure 6 separately.

When $U_2 = 0$, the curve of velocities at the interface shown in Figure 5 corresponds to the curve plotted in Figure 3 of Lock's paper. When $\rho\mu = 1$, which implies that both the upper fluid and lower

fluid are the same, by obviously reasoning in this case $\frac{u_0 - U_2}{U_1 - U_2}$ should be equal to 1/2 whether $U_2 = 0$ or not.

Table 4 Solution for the Case

$\rho\mu = 10, \lambda_1 = 0$

Lower Fluid

η_2	u/U_1 Exact Solution	u/U_1 Lock's Solution
0.000	0.31701	0.3428
-0.374	0.29019	0.3096
-0.797	0.25992	0.2730
-1.219	0.22993	0.2383
-1.642	0.20038	0.2061
-2.065	0.17170	0.1767
-2.488	0.14435	0.1504
-2.910	0.11885	0.1273
-3.333	0.09554	0.1071
-3.756	0.07485	0.0897
-4.178	0.05708	0.0748
-4.601	0.04224	0.0623
-5.024	0.03030	0.0516
-5.447	0.02103	0.0427
-5.869	0.01412	0.0353
-6.926	0.00449	0.0217
-7.983	0.00113	0.0133
-9.040	0.00022	0.0081
-10.097	0.00004	0.0050
-11.154	0.00000	0.0030
-13.267		0.0011
-15.381		0.0004
-17.495		0.0002
-19.608		0.0001

Upper Fluid

η_1	u/U_1 Exact Solution	u/U_1 Lock's Solution
0.000	0.31701	0.3428
0.423	0.41290	0.4611
0.846	0.50808	0.5752
1.268	0.60060	0.6802
1.691	0.68821	0.7717
2.114	0.76751	0.8463
2.536	0.83542	0.9031
2.959	0.89027	0.9430
3.382	0.93145	0.9688
3.805	0.96006	0.9842
4.227	0.97835	0.9926
4.650	0.98911	0.9968
5.073	0.99495	0.9987
5.496	0.99783	0.9995
5.918	0.99914	0.9999
6.341	0.99969	1.0000
6.764	0.99990	1.0000
7.000	0.99995	
7.200	0.99997	
7.400	0.99998	
7.600	0.99999	
7.800	0.99999	
8.000	1.00000	

Table 5 Solution for the Case

$\rho\mu = 1, \lambda_1 = 0$

Lower Fluid

η_2	u/U_1 Exact Solution	u/U_1 Lock's Solution
0.000	0.50000	0.5873
-0.286	0.45252	0.5305
-0.609	0.39905	0.4678
-0.932	0.34612	0.4083
-1.254	0.29459	0.3531
-1.577	0.24504	0.3028
-1.900	0.19866	0.2577
-2.223	0.15650	0.2180
-2.546	0.11942	0.1835
-2.869	0.08803	0.1537
-3.192	0.06251	0.1282
-3.515	0.04267	0.1067
-3.838	0.02795	0.0885
-4.161	0.01753	0.0732
-4.484	0.01051	0.0605
-5.291	0.00241	0.0372
-6.099	0.00041	0.0288
-6.906	0.00005	0.0139
-7.714	0.00000	0.0085
-8.521		0.0052
-10.136		0.0019
-11.751		0.0007
-13.365		0.0003
-14.980		0.0001

Upper Fluid

η_1	u/U_1 Exact Solution	u/U_1 Lock's Solution
0.000	0.50000	0.5873
0.360	0.55975	0.6588
0.683	0.61315	0.7205
1.006	0.66586	0.7779
1.329	0.71714	0.8293
1.652	0.76605	0.8734
1.975	0.81154	0.9096
2.298	0.85259	0.9380
2.621	0.88839	0.9592
2.944	0.91842	0.9743
3.267	0.94258	0.9845
3.590	0.96117	0.9911
3.913	0.97482	0.9951
4.236	0.98437	0.9974
4.559	0.99071	0.9987
4.882	0.99471	0.9994
5.205	0.99714	0.9997
5.528	0.99852	0.9999
5.851	0.99927	0.9999
6.174	0.99966	1.0000
6.497	0.99985	
6.800	0.99993	
7.000	0.99996	
7.200	0.99998	
7.400	0.99999	
7.600	0.99999	
7.800	1.00000	
8.000		

Table 6 Solution for the Case

$\rho\mu = 100, \lambda_1 = 0.501$

Lower Fluid

η_2	u/U_1 Exact Solution	u/U_1 Lock's Solution
0.000	0.75050	0.7657
-0.400	0.71737	0.174
-0.800	0.68445	0.6718
-1.200	0.65225	0.6312
-1.600	0.62157	0.5968
-2.000	0.59337	0.5690
-2.401	0.56856	0.5477
-2.801	0.54798	0.5319
-3.201	0.53188	0.5208
-3.601	0.52010	0.5133
-4.001	0.51208	0.5085
-4.401	0.50701	0.5054
-4.801	0.50405	0.5036
-5.201	0.50244	0.5026
-5.601	0.50163	0.5020
-6.001	0.50126	0.5017
-6.401	0.50110	0.5015
-6.801	0.50103	0.5014
-7.202	0.50101	0.5014
-7.602	0.50100	0.5014

Upper Fluid

η_1	u/U_1 Exact Solution	u/U_1 Lock's Solution
0.000	0.7505	0.7657
0.400	0.78363	0.8140
0.800	0.81655	0.8593
1.200	0.84875	0.8991
1.600	0.87943	0.9317
2.000	0.90768	0.9565
2.401	0.93244	0.9741
2.801	0.95302	0.9855
3.201	0.96912	0.9925
3.601	0.98090	0.9963
4.001	0.98892	0.9983
4.401	0.99400	0.9993
4.801	0.99695	0.9997
5.201	0.99856	0.9999
5.601	0.99937	1.0000
6.001	0.99974	
6.401	0.99990	
6.801	0.99997	
7.201	0.99999	
7.601	1.00000	

However, it can be seen that the curve of velocities at the interface given by Lock contradicts the above conclusion. For the same reason, the correctness of Figure 4 in Lock's paper is also open to doubt. If u0 = 0, the upper fluid flow can be considered as a uniform flow over a solid flat plate, and according to (3.10) the skin friction coefficient, $C_{r0} = 0.33206$, which is just the value given by Blasius solution for the corresponding boundary layer problem. Thus, the validity of our solution is confirmed once more. As shown in Figure 6, the curve corresponding to (3.10) is concave-down, however the curve of skin friction coefficient given by Lock's numerical results is concave-up (see Fig.5 in Lock (1951)). By the difference of concavity between these two curves, it is inferable that some error yields in Lock's calculation.

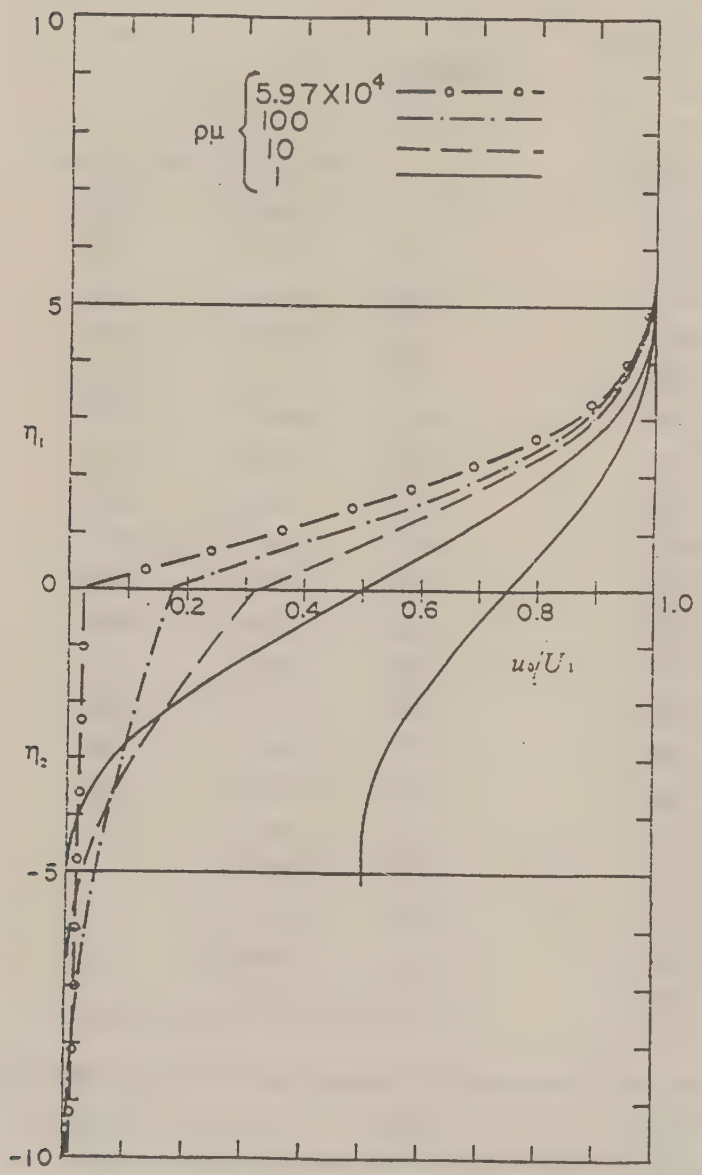

Fig.3 Velocity profiles for 5 special cases discussed by Lock(1951) given by the present exact solution

Acknowledgment The Author is indebted to his colleague Xu Zhaoting for fruitful discussions on this study. Thanks also go to Prof. Y. C. Whang, the Catholic University of America, Washington, D.C. for many helpful and constructive comments.

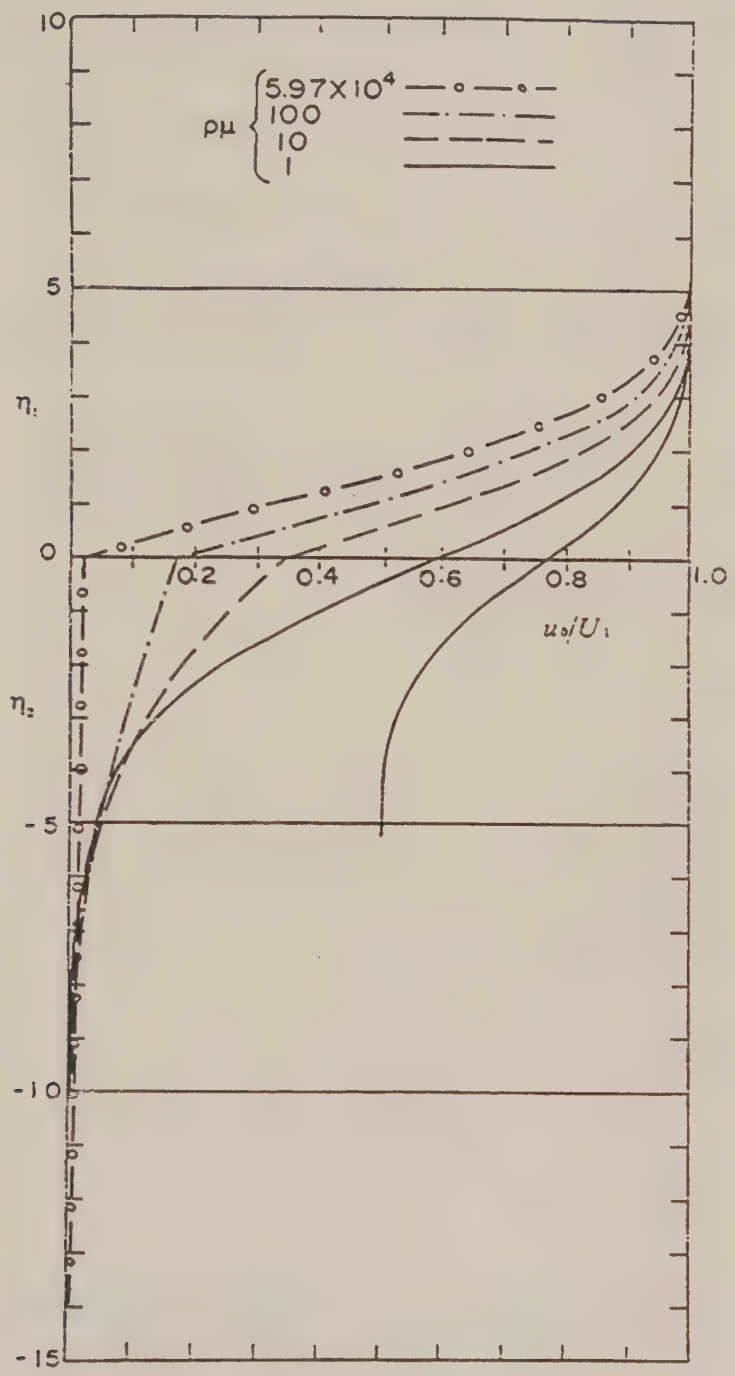

Fig.4 Velocity profiles for the same 5 special cases given by Lock's numerical solution (corresponding to Fig.2 of Lock (1951))

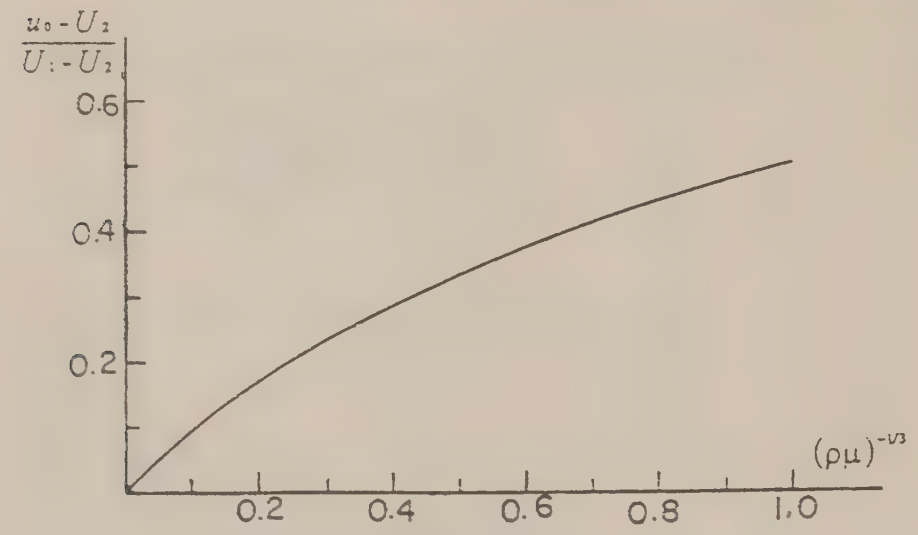

Fig.5 Velocities at the interface

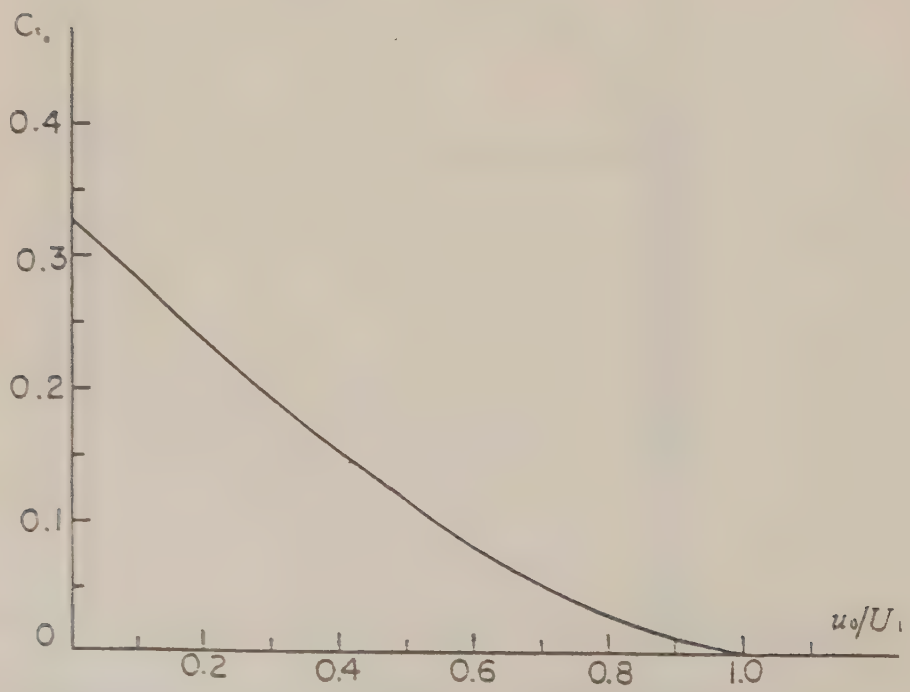

Fig.6 Skin friction coefficients

Batchelor, G. K., 1967, An Introduction to Fluid Dynamics. Cambridge University Press.

Lock, R.C., 1951, The Velocity Distribution in the Laminar Boundary Layer between Paraliel Streams. *Quart. Jour. Mech. and Applied Math.*, Vol.6, pt.1.

Martin Lessen, 1949, On the Stability of the Free Laminar Boundary Layer between Parallel Streams. N. A. C. A. Tech. Note 1929.

Reichardt, H., 1941, Gesetzmaessigkeiten der Freien Turbulenz, *Zeichrift fuer Angewandte Mathematik und Mechanik*, Vol.21, pp257-264.

Schlichting, H., 1968, Boundary Layer Theory. McGraw-Hill, Inc.

Yih, C. S., 1981, Similarity Solutions for Turbulent Jets and Plumes. J. of the Engineering Mechanics D., *Proc. ASCE*, Vol.107, No.Em3, pp455-477.

On Sustainable Development of Marine Resources in Bohai Area

Jiang Tiemin
Shandong Institute for Ocean Economics, Qingdao 266071

Abstract The Bohai, the largest inland sea in China, is abundant in marine resources. However, with the paper economic growth in the Cricum – Bohai Bay Area in the recent years, the environmental pollution in this area has become more and more serious, resulting in a substantial decline and deterioration of marine resources. In view of this critical situation, the method for sustainable development of marine resources in the Bohai Sea is discussed. Practical measures and feasible suggestions are put forward in this paper with the purpose of preventing and controlling environmental pollution as well as natural disasters, and eventually achieving the aim of the sustainable development of marine resources in this area.

Ⅰ. Present Condition and Change of Marine Resources in the Bohai Sea

The Bohai Sea is the largest inland sea in China, one of the twelve-inland seas in the world. It was originally a desert inland basin about 18,000 years ago, and later was inundated with seawater and became a semi-enclosed sea. The Bohai Sea is abundant in marine resources, because of several larger rivers flowing into it, such as the Huanghe River, Haihe River, Liaohe River and Luanhe River, its shallower depth, flat topography, fertile water quality and the larger space suitable for aquaculture. It is a better base for the all-round development of ocean ranching. The Bohai Sea is famous in the world for its functions as a huge fishpond, a salt pond and an offshore oil field. In addition to those marine industrial departments, which directly utilize marine resources, there are quite a lot of industrial enterprises. That indirectly utilize marine resources in the circum-Bohai Sea area, such as sea salt chemical works, marine aquatic products processing plants, marine petrol-chemical works, marine aquatic products processing plants, marine petrol-chemical works, shipyards and ship-repairing works.

In the course of the exploitation of the Bohai Sea, the fishery resources began to decline from the mid-1960s due to overfishing, and the output of fishes, prawns and shrimps has been getting lower and lower. Overfishing and pollution of water environment in this area deteriorate the fishery resources every year. The reasons for this situation are the barriers between the higher and lower levels or between different departments and regions, the ownership of departments and lack of unified policies. At present, among those which are involved in the exploitation and management of the Bohai Sea, there are as many as 10 departments directly subordinate to the central government, plus other relevant provincial, municipal, prefecture and county departments. Hence, the management system with so many and so complicated administrative levels makes it impossible to give full play to their respective features and

superiority and to convert or make up for their respective weak points.

Because no unified regional planning on the exploitation of marine resources in the Bohai Sea area has been formulated, various departments often conduct "blind exploitation" and are beset with numerous contradictions, resulting in a serious deterioration of marine resources in the Bohai Sea area, and particularly the pollution problem. If these problems are not solved timely, the Bohai Sea will eventually become a "dead" sea. At present, the major problems in the exploitation of the Bohai Sea are:

(1) The contradiction between pollution and aquatic products industry as well as tourism;

(2) The contradiction between petroleum exploitation and aquatic products industry;

(3) The contradiction between salt field and fishery;

(4) Contradictions among various industries on the utilization of beaches;

(5) Contradictions among various industries on the utilization of coastal sections (shorelines);

(6) Contradictions between reservoirs, power stations and marine industry.

It is suggested that before implementing the Bohai Sea exploitation plan, an organization called the "Circus-Bohai Sea Exploitation Committee" shall be set up first. The members of this committee shall include authoritative persons from the three provincial governments, and also specialists in marine development. This committee should be directly subordinate to an oceanic administrative department at the central level, but it should be independent of any local government. Under the control of this committee with its unified planning and management, a conceptual change is needed for the exploitation of the Bohai Sea, namely, the classical management method based on mainly experience shall be transformed into the one based on scientific decision-marking. The purely predatory exploitation shall be replaced by the exploitation combined with preservation of resources. And the intelligent exploitation by using chiefly advanced techniques shall be adopted instead of the one by simply extending the production scale.

Ⅱ. Sustainable Development of Fishery Resources in the Bohai Sea

Exploitation and preservation of fishery resources are the two aspects of one problem. Without preservation, sustainable exploitation is impossible. An appropriate method for solving this problem is to adopt measures suitable for local conditions and to divide the area into smaller zones so as to rationally implement exploitation and preservation. The specific opinions are as follows:

1. *Establish the Liaodong Bay Ecological Fishing Zone*

In consideration of its comparatively abundant fishery resources, higher primary productivity, more kinds of resources and larger stocks left, the following measures for the preservation of resources may be adopted:

a) Conducting and strengthening the preservation of the resources of shrimps and small yellow croakers, so as to restore the resources to their historical levels.

b) Setting up proliferation bases for jelly-fish, prawns, portunidae, blood clams and sea cucumbers, and release stations at appropriate sites, and implementing the policy of "whoever releases has

the right to harvest".

c) Taking the Liaodong Bay as a whole, utilizing the waters in three dimensions, thus forming a kind of comprehensive utilization of ecological fishery.

d) Adopting the method of sub-area associated operations for the proliferation, catching, farming and processing industry in this area, and forming an integrated system of services.

2. *Establish the Bohai Bay Comprehensive Development Zone*

The water quality of the fishing ground in the Bohai Bay is fertile because of the outflows of the Huanghe River, the Haihe River and the Daqinghe River, etc. It is a spawning ground as well for small yellow croakers, hairtails, prawns, shrimps, etc. The southern part of this area—Shangdong section can be used as a zone for culture of shrimps and shellfishes. The west section of its southern part is the section of Cangzhou, Hebei Province, suitable for integrated farming and cultivated proliferation of fishes, prawns, crabs and shellfishes. The Tianjin section in the middle part is suitable for establishing this section into a deep-sea fishery base as well as a modernized intensive base for integrated proliferation and farming of fishes, prawns and shellfishes. In the west section of the northern part of the Bohai Sea, the preservation and rational exploitation of resources, such as shrimps and shellfishes, shall be strengthened, and its east section is suitable for the proliferation and culture of sea cucumbers, abalone, oysters, etc.

3. *Establish the Laizhou Bay Ecological Fishing Zone*

Industry and agriculture in this area are well developed, and good conditions exist for the development of fishery. In order to develop ecological fishery, it is necessary to do well in the following aspects:

a) enlisting the initiative of fishermen in developing deep-sea fishery;

b) preserving coastal and near-shore fishery resources;

c) practicing multi-level three-dimensional integrated farming;

d) establishing information services, material supply, products processing and marketing systems.

Ⅲ. Environmental Pollution in the Bohai Sea and Its Prevention and Control

The Bohai Sea has suffered pollution for the last 30 years. Large quantities of farmland water containing chemical fertilizers and pesticides, urban sewage and industrial waste water flow into the Bohai Sea via these rivers, and thus contaminate it. The oil leakage and spill during offshore oil exploitation and transportation in the Bohai Sea causes oil pollution. In the recent years, the pollution along the coast and at the estuaries round the Bohai Sea has already affected the normal life of fishes, prawns, shrimps, crabs and shellfishes, and will finally threaten the health of human beings. The emphasis of the prevention and control of marine pollution shall be placed on the "prevention", and the next is the "control". It takes 16 years for the Bohai Sea to make a total water exchange with the Huanghai Sea.

This means that pollution, having entered the Bohai Sea, if they are those organic chlorine compounds which are difficult to decompose, will flow totally out of the Bohai Sea 16 years later.

The threat of marine pollution to the Aquatic resources in the Bohai Sea and the health of people are now very obvious. For the happiness of our descendants, we must take resolute and effective measures to prevent and control the pollution in the Bohai Sea.

1. *Formulate Special Regulations for the Management of Environmental Protection of the Bohai Sea*

Although there is the "Law of the People's Republic of China on Marine Environmental Protection" and a unified standard for sea water quality, however, considering that the Bohai Sea is a semi-enclosed inland sea, it is absolutely necessary to set a comparatively strict discharge standard and formulate special regulations for the management of environmental protection of the Bohai Sea.

2. *Establish and Improve the Bohai Sea Environmental Management System*

No unified management system for the environmental protection of the Bohai Sea has established now. This work should not only rely on the common efforts from various departments, but also need to set up a coordination department for the purpose of conducting unified planning and management.

a) Strengthen the leadership of environmental protection of the Bohai Sea, set up an environmental protection coordination group, and establish a regional environmental protection organization at a higher level to coordinate the environmental protection work in the Bohai Sea area.

b) Restore the joint meeting system of mayors in the Circus-Bohai Bay Area

It is necessary to adopt or revise the special regulations for the management of environmental protection of the Bohai Sea, the plans for pollution monitoring and the prevention and control of the pollution, and to implement specifically the measures for the prevention and control of pollution in the Bohai Sea.

c) Establish and strengthen the Bohai Sea pollution monitoring and law enforcement agency to effectively carry out the monitoring of pollution events in the Bohai Sea. For the management of environmental protection of the Bohai Sea, the execution of lows must be strictly implemented, which is the key link in the execution of the special regulations. It is necessary to establish the headquarters for the Bohai Sea environmental pollution monitoring and law enforcement.

d) Implement the reporting system for marine pollution events.

3. *Strengthen the Bohai Sea Pollution Monitoring Network*

The Bohai Sea environmental pollution-monitoring network may exist separately as a sub-network of the national marine environmental pollution-monitoring network. It is necessary to rectify the tendency of deficiency in the monitoring of terrigenous pollution in the Bohai Sea and its impact on biological resources, and accomplish the monitoring of the Bohai Sea environment with combined efforts.

4. *Establish an Emergency Force for Coping with Oil Spills in the Bohai Sea*

5. *Strengthen Scientific Research on the Prevention and Control of Marine Pollution in the Bohai Sea*

a) Conduct research on the self-purification ability and environmental capacity of various areas of the Bohai Sea.

b) Conduct research and development of wastewater treatment facilities.

c) Strengthen research on preventive measures against pollution caused by aquatic product farms.

d) Conduct research on soil and water conservation of farmland.

e) Conduct research on the control of pollution caused by village and township enterprises.

f) Pay attention to the research on the protection of wetlands and marshlands along the coast of the Bohai Sea

6. *Control the Pollution in the Critical Sea Water*

Ⅳ. Prevention and Control of Natural Disasters in the Bohai Sea

Major natural disasters occurring in the Bohai Sea, according to the degree of losses caused by these disasters, scope covered and occurrence frequency, are sea water, storm surges, gales and billows at sea, earthquakes and tsunamis, etc. Red tides, land subsidence of coastal cities and the ingress of salt water into underground water-bearing beds in the coastal region may be called as the "man-made natural disasters" because these disasters are formed more or less due to the influence of mankind activities.

To alleviate the regional marine disasters in the Bohai Sea, we must proceed from the overall interests, and take comprehensive measures; while developing production, measures for alleviating disasters shall be implemented simultaneously, and the malignant cycles of environmental ecosystem must be replaced by its benign cycles.

Main Countermeasures for Disaster Mitigation

a) Formulate the Bohai Sea regional disaster mitigation planning as soon as possible

This planning should cover not only the engineering disaster prevention planning for coastal and offshore works, but also the non-engineering disaster mitigation work, such as establishment and improvement of monitoring, pre-warming, salvage, research, publicizing and education of marine disasters.

b) Take the salt-water intrusion and the land subsidence of the coastal region of the Laizhou Bay, the red tide in the nearshore area of the Bohai Sea, etc., such as the key items of disaster prevention and control in the Bohai Sea area.

c) Further improve the Bohai Sea disaster-monitoring network.

d) Strengthen the coastal zone and marine management with the purpose of mainly alleviating the prevention of disasters the key point for the work of alleviating marine disasters.

e) Strengthen scientific and technological research and the development of equipment relating to the disaster alleviation in the Bohai Sea; strengthen publicizing and educational activities for the purpose of disaster alleviation. The key items shall cover seawater, extra-tropical storm surge, intrusion of salt water, land subsidence of coastal area, the prevention and control of red tides, etc.

On the Rational Utilization of Coastal Resources of Shandong Province

Zhao Quanji and Liu Fushou
First Institute of Oceanography, SOA, Qingdao, 266003

Ⅰ. Introduction

From the survey of coastal resources and the functional zoning of the marine and coastal areas of Shandong Province, the authors have collected a good deal of practical data, and at the same time, found out some irrational phenomena in the exploitation and utilization of coastal resources. Taking the coastal area of Shandong Province as an example. This paper makes an analysis on the rational utilization of coastal resources.

Ⅱ. Abundant Coastal Resources in Shandong Province

1. *Harbour Resources*

About two thirds of the coasts of Shandong Province are bedrock-embayment coasts, along which more than 100 bays, large or small, are located. Among them, there are 51 larger bays with the bay area larger than 1 km^2, in which there are 32 sites suitable for seaports with water depth larger than 5m, and 18 sites suitable for seaports with water depth larger than 10m. Along the coasts of Shandong, there are over 160 seaports with 450 berths among which two are 100 kt-grade ones. There are still many coastal sections suitable for seaport site selection. As far as we know, there are 51 sites suitable for deepwater seaports, among which 23 sites are suitable for seaports with deepwater berths of 100 to 200 kt-grade, 14 sits suitable for seaports with deepwater berths of 50 kt-grade and 14 for seaports with berths of 10 kt-grade.

2. *Aquatic Products Resources*

The aquatic products resources in the coastal and marine areas of Shandong Province are abundant both in terms of species and quantity. There are numerous aquatic organisms, both natural and aquacultural, among which there are over 100 species of economic fishes and over 90 species of economic shellfishes. The total natural resource of various shellfishes amounts to 663 kt./a, among which the stock of rare valuable aquatic products is about 7 kt. The potential resources of aquaculture are even more considerable . The main aquacultural products are kelp, scallop, mussel and prawn. The total output of shellfish aquaculture amounts to 318 kt./a, and that of prawn farming 43 kt./a.

3. *Mineral Resources*

Over 100 sorts of mineral products have been found at 1655 orefields in the coastal areas of Shandong Province. And the reserves of 53 sorts of mineral products have been verified at 374 ore fields, among which 27 sorts of mineral products rank in the first 10 places in reserves in the country, and 42 sorts of mineral resources have been mined. The annual output of ore products mined amounts to over 8.8 million tons with an output value of 10.492 billion yuan (RMB).

There are 48 verified oil and natural gas fields with a reservation ares of 1518 km^2 and geologic reserves of oil of 3.1 billion tons and that of natural gas of 23.2 billion m^3. The annual output of petroleum in 1991 amouted to 34 million tons, accounting for 24.3% of the national total (139.6 million tons). The verified coal fields covered an area of 391 km^2 with reserves of coal of 2.18 billion tons, and the present annual output of coal amounts to 2 million tons. The verifies reserves of oil shale are about 300 million tons, and the accumulated reserves (including the potential and verified ones) amount to 8.5 billion tons. The reserves of gold deposits in Shandong's coastal areas accounts for 99.4% of the total reserves in the coastal areas throughout the country. The reserves of molybdenum metal is about 570 000 tons. The beach placers and non-metal mineral products are abundant both in terms of sorts and quantity in Shandong's coastal zone, and most of them are important foreign-exchange earning non-metal mineral products, such as magnesite, graphite and talcum, etc. The coastal area of Shandong Province is also an important salt-producing area. There are 740 km^2 of salt pans, of which 620 km^2 are under production. The output of salt in Shandong in 1990 amounted to 3.07 million tons. There are also undeground brine resources with an concentration of salt 2-6 times higher than the sea water. The distributing area of underground brine water is about 1500 km^2, with gross reserves of brine water of 7.4 billion m^3, which is estimated to contain 810 million tons of salt. And recently some underground brinewater resources have been found in the Jiaozhou area, et alibi.

4. *Tourism Resources*

The tourism resources are also abundant in the coastal areas of Shandong Province. There are numeous places of historic interest and scenic beauty, sceneries with hills and sea view, wonderful peaks and exotic reefs, smooth and soft beaches and the fairylands of islands along the coasts of Shandong Province. In addition, there are convenient tranport facilities, favourable climatic conditions, plentiful delicacies from land and sea, fine handicraft arcticles and unique special local conditions and customs, constituting the wonderful places and paradise for the tourists both from home and abroad. The famous scenic spots of Qingdao, Penglai and Chengshantou Cape are especially excellent and charming.

5. *Renewable Energy Resources*

Renewable energies are cheap potential energies. Furthermore, they do not pollute the environmert.

The coastal areas of Shandong Province is rich in renewable energies, such as tidal energy, tidal

current energy, wave energy, wind energy, and solar energy, etc.

Besides, there are also important resources of land and freshwater, etc.

Ⅲ. Principles for the Rational Exploitation and Utilization of Coastal Resources

In order to exploit and utilize coastal resources in a rational way, it is important to work out the functional zoning plan for the coastal areas. In 1989, the State Oceanic Administration (SOA) and other government departments organised a program of functional zoning for the sea and coastal areas of China. In order to sufficiently reveal the natural properties of the coastal areas and choose the best function and the function order for each coastal section, the function zoning of coastal areas must be conducter based on the four principles: (1) the unification of three (economic, social and environmental)effects, (2) overall consideration and all-round arrangement, (3)scientific rationality and (4)alternater selectivity.

Coastal areas are multiply fitting lands. One coastal section has several functions that can be developed for different purposes. However, considering various social factors, some of the development programs require very strict conditions and can only be carriedout on the coasts or at certain sites of the coast. These development programs are called narrow alternate-selectivity programs. On the other hand, some other programs can cerried our on the coast or in any other places near the coasts. These are calles wide alternate-eslectivity progams. In the practical development of coastal areas, the wide alternate-selectivity programs should give way to the narrow ones so as to make full use of the special value of the coastal resources.

Sometimes the various functions of a single coastal section overlap each other and they all cannot be developed in places away from the coast. In this case, if these functions can be developed simultaneously without serious conflicts , some adjustments are needed to coordinate the different programs of function development. In case that the conflicts between or among different developmental programs of coastal functions cannot be reconciled, i.e., these functions are incompatible, optimization is needed so to give priority to the development of the best function of the coastal section .

Based on the principles mentioned above, the coastal areas of Shandong Province are devided into eight major function of zones according to the superiority of resources, the present situations of development and the land-use planning of various regions (Fig.1). Each major function of zone has its superiority of resources, function order and several main functions. Furthermore, each major function of zone of coastal areas is divided into several subdivisions according to its present situation of development in order to make full use of the coastal resources.

Ⅳ. Some Assurances

The investigation of coastal resources and the function of zoning of coastal areas have founded a scientific basis for the rational exploitation and utilization of coastal resources. However, the following assurances must be available:

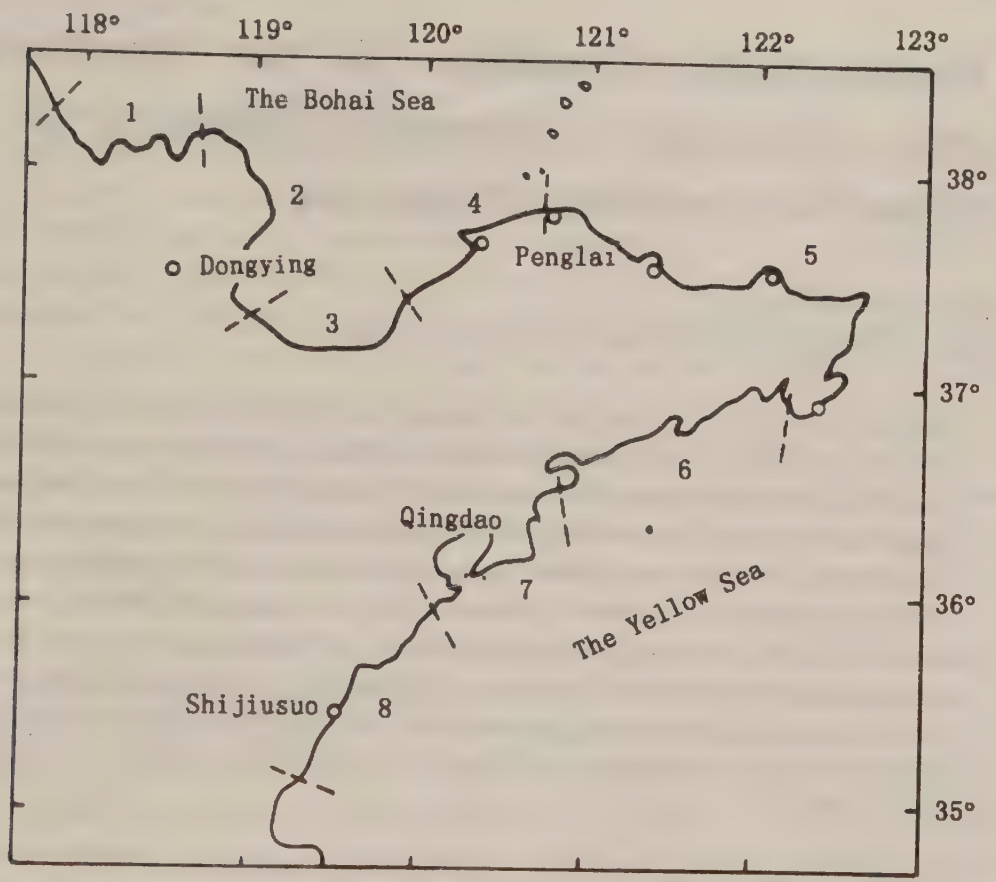

Fig.1 Section divisions of coastal functions and resources of Shandong Province

(1) Working out the plan for the comprehensive development of the coastal zone.

(2) Perfecting oceanic legal system and strengthening coastal management.

(3) Enhancing the consciousness of oceanic territory of the people living and working in the coastal zone.

Oceanographic Condition in the Distribution Areas of Anchovy Engraulis Japonicus in the Yellow Sea and East China Sea

Chen Jufa and Ma Shaosai
Yellow Sea Fisheries Research Institute, CAFS, Qingdao 266071

Abstract Based on the data obtained from the cooperative surveys by China and Norway from 1984 to 1994, this paper deals with the hydrographic characteristics of distribution areas of anchovy in the Yellow Sea and East China Sea from November to May. The relationships between distribution of anchovy and hydrographic environment are also analyzed in this paper. The main research findings are briefly given below. (1) From November to March, the water temperature continually decreases and meanwhile the dense areas of anchovy move from north to south. The high schooling areas of anchovy are mainly distributed in the warm of cold front areas with temperature of 11-13℃. (2) In November and December, the Yellw Sea cold watermass exists roughly between 50m depth and sea bottom. The thermo-halocline is approsimately located at the 30 ~ 50m depth and the anchovy is usually distributed above the thermo-halocline In January and March, the Yellow Sea cold watermass disappears and the fish schools are distributed at the middle and lower depths, even sea bottom.

Keywords: Oceanographic condition, Anchovy, Yellow Sea and East China Sea

Introduction

Anchovy is a kind of small pelagic fish, they are very sensitive to the variation of marine environmental condition and there is a close relationship between the distribution of anchovy and the marine envirommment, particularly the hydrographic environment. This paper mainly deals with the hydrological condition of distribution areas of anchovy in the Yellow Sea and East China Sea from November to May of next year and the impact on behavior and disrtibution of anchovy. This will play a very important part in detemining the dense areas of anchovy and exploring anchovy resource better.

Data Source

During the winter and spring seasons from 1984 to 1994, in the Yellow Sea and East China Sea the surveys of fish resources, especially anchovy, were carried out by the Chinese ane Norwegian scientists, with the acoustic equipment of R/V BEI DOU. The water temperature and salinity were observed at hydrographic stations during the surveys. This paper has been written based on these data and relevant research findings of other persons.

Results and Analysis

1. *The Temperature and Salinity Condition in the Distribution Areas of Anchovy*

1.1 Distribution of water temperature

In November, the temperature and salinity of sea water started to decrease and increase, respectively. The surface temperature in the northern and central Yellow Sea was below 16℃ and anchovy was densely distributed in this area . By contrasting the distribution condition of surface temperature in November from 1985, it can be found that enery year there was a relatively low temperature area in the central area of North Yellow Sea. In general, the minimum values of temperature in cold water areas were not less than 10℃, but there were differences in its scope and strength in different years. In addition, there was a higher temperaturs area to the north of the lower temperature area (Fig.1). In the central Yellow Sea, the surface temperature incerased from north to south. In the southern Yellow Sea and northern East China Sea, the surface temperature changed with variation of latitude and longitude, the lower the latitude is, the higher it was and it increased from coastal area to open sea, In November, in the area north of 37°N the surface temperature varied between 10 ~ 13℃, between 12 ~ 16℃ from 37°N to 34°N and between 16 ~ 23℃ from 34°N and between 16 ~ 23℃ from 34°N to 28°N.

As the cold watermass existed near the sea bottom in the trough area of Yellow Sea, the distribution of bottom temperature in the surveyed area was mainly dominated by the cold watermass, the lowest temperature of cold watermass was 7℃or so. In November, the central position of cold watermass was located at about 37°N, 125°E. If the 10℃ isotherm is regarded as an index for its boundary, more than 60 per cent of the surveyed area was occupied by the cold watermass. In the area west of 126°E, the bottom temperature increased from north to south. Owing to the fact that the sea bottom slope is steep, the temperature increased from west to east and there was a sharp horizontal gradient of temperature at a rate of 0.29℃ per nautical mile in the area east of 126°E. It varied between 7 ~ 16℃ in the Yellow Sea and between 8 ~ 21℃ in the northern East China Sea.

In November, the temperatures were almost the same in the water columm between 0 ~ 30m in the northern and central Yellow Sea, the thermocline was observed below 30m in depth and the temperature changed at a rate of more than 0.3℃ per meter, the cold watermass roughly existed between the 50m depth and the sea bottom(Fig.2). In the southern Yellow Sea and northern East China Sea, the thickness of homogeneous upper layer gradually increased with the reduction of latitude, it was around 75 meters at the section of 30°30′N and reached about 100 meters at the section of 28°30′N. Below the homogeneous layer the temperature decreased with increasing depth.

In December, the upper seawater was further cooled with decreasing air temperature and the surface temperature was below 14℃ in the whole area of Yellow Sea. In the central Yellow Sea the temperature increased from north to south, the southern Yellow Sea and the northern East China Sea were mainly dominated by the Subei Cold Coastal Water and the Yellow Sea Warm Current, due to the opposite flow directions of them the isotherm had a characteristic shape of S. The distribution of bottom temperature in the surveyed area was apparently dominated by three large systems, i.e. the Yellow Sea

Cold Water Mass, the Subei Cold Coastal Water and the Yellow Sea Warm Current(Fig.3). The surface and bottom temperatures in the surveyed area varied between 11 ~ 18℃ and 8 ~ 18℃, respectively.

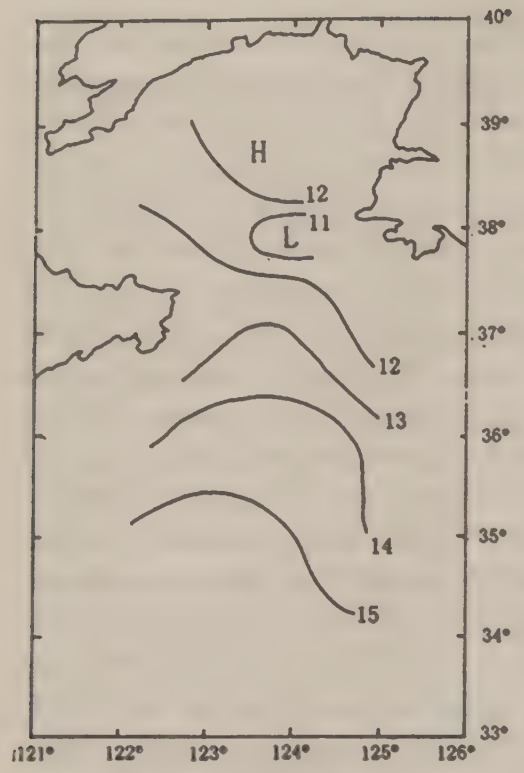

Fig.1 Distribution of surface temperature in the northern and central Yellow Sea in November, 1988

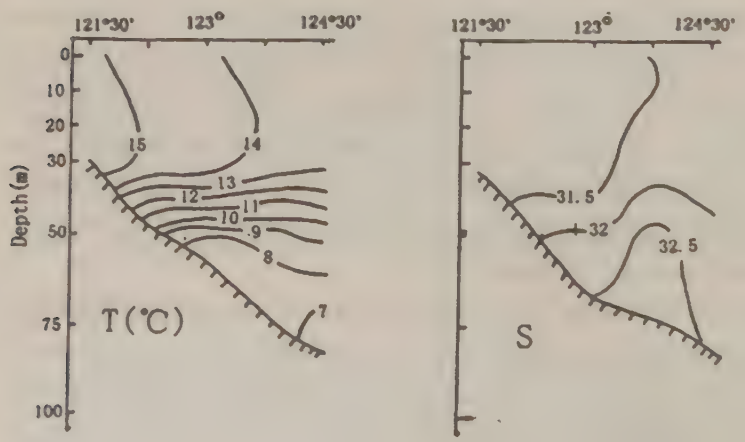

Fig.2 Vertical distribution of temperature and salinity at the section of 35°N in November, 1986

The vertical distribution of temperature at the section of 36°N showed that in December the thickness of homogeneous upper layer already reached around 50 meters in the central Yellow Sea, the strength of thermocline was much weaker than that in November and the upper boundary of cold watermass was below the 60m depth. In the areas uncontrolled by the Yellow Sea Cold Watermass, i.e. the southern Yellow Sea and the northern East China Sea, the temperature was almost homogeneous in the water column from surface to bottom.

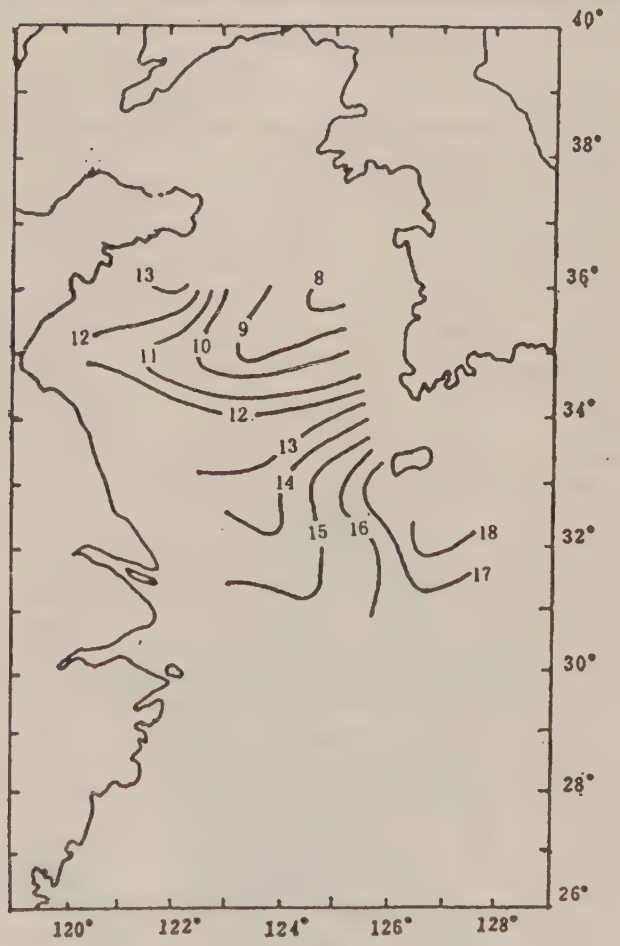

Fig.3 Distribution of botton temperature in the Yellow Sea and northern East China Sea in December, 1985

In January, the water temperature continued to decrease. At the surface the cold water tongue of Subei Coastal Current and the warm water tongue of Yellow Sea Warm Current were fairly strong in strength, the sharp water tongue of Duima Warm Current also existed in the northern East China Sea and the isotherm of 17℃ could extend In northwards to about 32°N, 127°E. The surface temperature

varied between 9 ~ 12℃. Like the surface layer, the distribution of bottom temperature was also dominated by the three large water systems mentioned above and was quite similar to that in the surface. Although in the area north of 34°N the temperature was still lower, the Yellow Cold Watermass no longer existed. The bottom temperature varied between 10 ~ 18℃. In January, the effect of convective and turbulent mixing was strengthened because of the increasing salinity of upper water and the prevailing northern wind . Except in the area north of 28°30′N, the thickness of homogeneous upper layer was 100 meters or so. In the area where depth exceeds 100 meters, the temperature below the homogeneous layer decreased slowly with increasing depth.

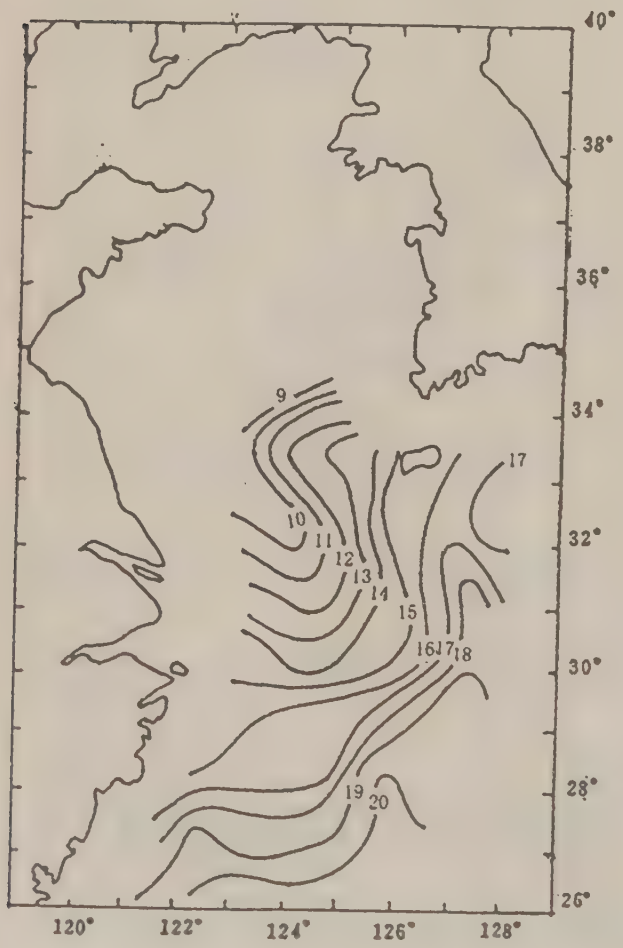

Fig.4 Distribution of surface temperature in the Yellow Sea and East China Sea in January, 1985

In March, the mean temperature was the lowest in a year. Except in a small area dominated by the Yellow Sea Warm Current west of Jizhou Island, in the rest of the southern Yellow Sea the surface

temperature was below 10℃. The Subei Cold Coastal Water normally increased in strength with further decrease of temperature of coastal water and the 10℃ isotherm extended southwards to about 31°N, while the warm water tongue of Yellow Sea Warm Current contracted southwards. In the northern East China Sea the surface temperature increased from north to south and except from coastal area to open sea(Fig.5). In March, the surface temperature in the surveyed area varied between 6 ~ 22℃. The distribution of bottom temperature was very similar to that in the surface, it varied between 7 ~ 18℃.

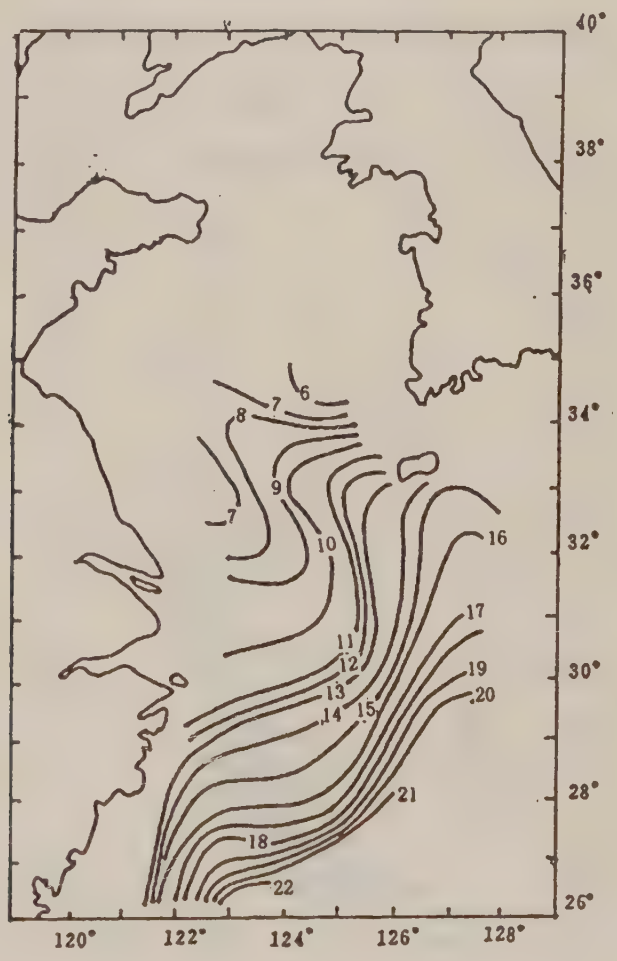

Fig.5 Distribution of surface temperature in the Yellow Sea and East China Sea in March, 1985

In March, the temperatures were homogeneous through the whole water column in the surveyed area, except that at the section of 27°30′N the Jiangzhe Coastal Water flew downwards along the continental shelf and made the Taiwan Warm Current flow just in the upper layer (0 ~ 35m) and conse-

quently the temperature of upper was higher than that of lower layer.

In April, the distribution of surface temperature was roughly the same as that of bottom temperature. In the waters south of Jizhou Island the warm water tongue of Yellow Sea Warm Current had contracted southwards, but the Subei Cold Coastal Water was still strong, especially in the surface (Fig. 6). In April the temperature was slightly higher than that in March and the surface and bottom temperatures varied between 10 ~ 23℃ and between 9 ~ 19℃ respectively.

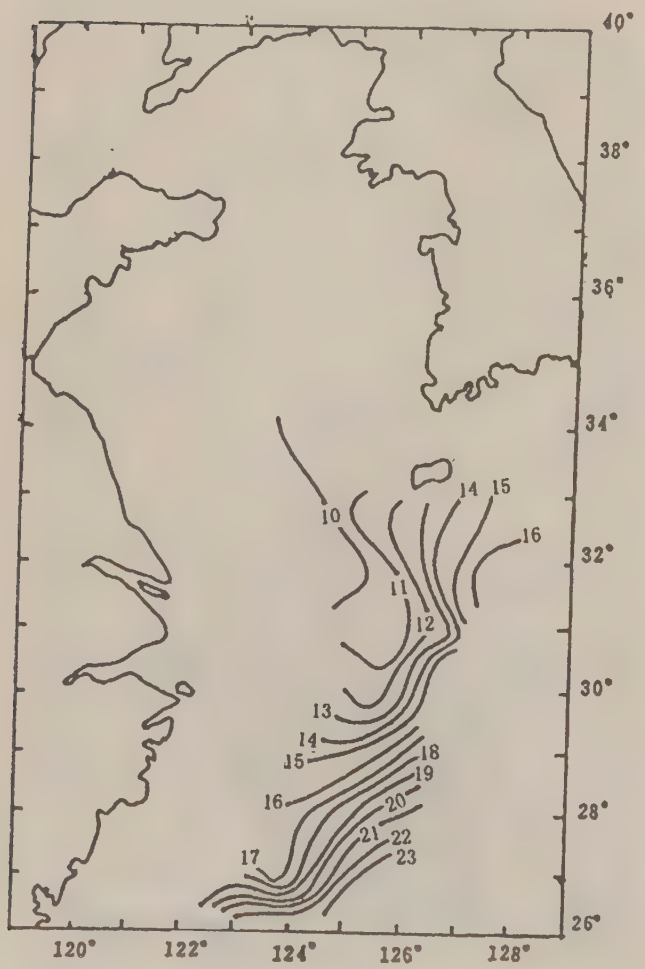

Fig.6 Distribution of surface temperature in the East China Sea in April, 1986

In April there were two types of vertical distribution of temperature in the northern East China Sea. In the waters north of 31°N, the temperatures were almost the same through the whole water column. In the waters south of 31°N, the temperature decreased with increasing depth. As the upper water was warmed and the temperature started to increase, a weak thermocline occurred between the 20m

and 50m depths in the area east of 125°E at the section of 27°N.

In May the surveyed area only covered the coastal waters north of 34°30′N and west of 123°E. The surface temperature was more than 14℃ in the great majority of the observing stations, but pattern of isltherms was still the winter type, i.e. the temperature in the open sea was higher than that in the coastal areas. It can be seen from the distribution of bottom temperature that in May the Yellow Sea Cold Watermass became larger in strength, its center was located at about 35°30′N, 122°E and the lowest temperature was less than 8℃(Fig.7). The bottom temperature in the surveyed area varied between 8 ~ 14℃.

The vertical distribution of temperature at the section of 35°N showed that in May the Yellow Sea Cold Watermass existed between the 10m depth and the sea bottom in the area east of 121°E. The isotherm of 10℃ roughly went in parallel direction with the sea bottom and the thickness of YSCW was 20 meters of so, there was a themocline above the YSCW, and the sharpest thermocline with a rate of around 0.8℃ per meter occurred at 35°N, 121°E(Fig.8).

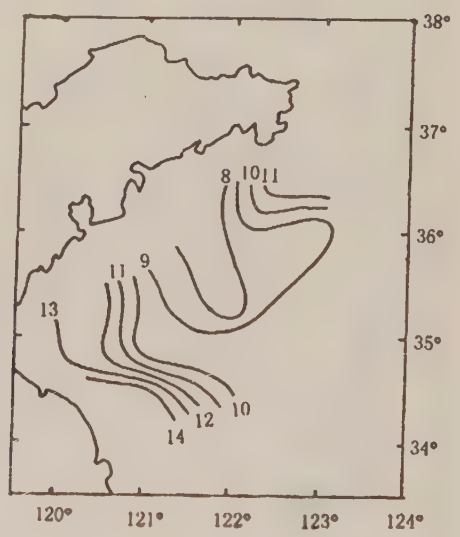

Fig.7 Distribution of bottom temperature in the surveyed area in May, 1991

1.2 Distribution of salinity

Owing to the reduction of rainfall and increase of sea surface evaporation, the salinity started to increase in November in the Yellow Sea and East China Sea . In November, the surface salinity was lower in the coastal areas than that in the open sea varyling between 31 ~ 32 in the northern and central Yellow Sea. The distribution of bottom salinity was similar to that in the surface, the higher salinity was observed in the area dominated by the YSCW and exceeded 33 in the central area of YSCW(Fig. 9).

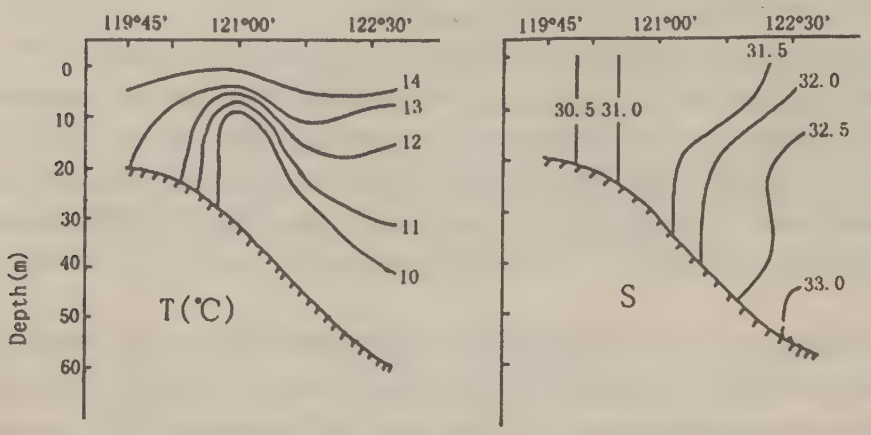

Fig.8 Verical distribution of temperature and salinity at the section of 35°N in May, 1991

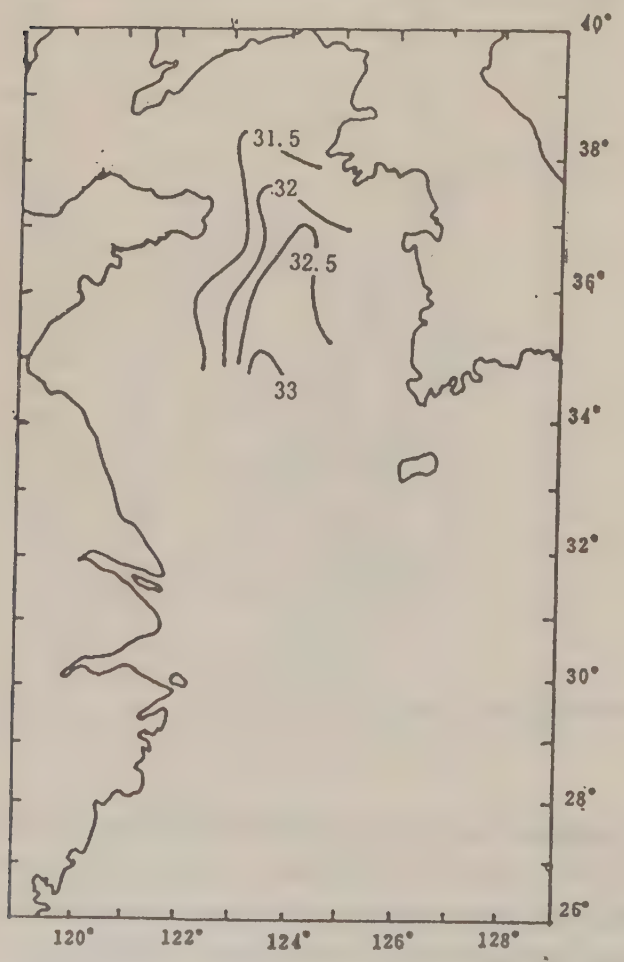

Fig.9 Distribution of bottom salinity in the surveyed area in November, 1986

From December to March, the salinity incereased with reducing latitude and increasing longitude in the southern Yellow Sea and the northern East Chian Sea. In December the surface isohaline of 33 was located in the northern East China Sea and its position was south of 33°N, in January and March it was located in the southern Yellow Sea and extenoled to 35°N in March(Fig.10). Whether in the surface or at the bottom , the distribution of salinity in this area in autumn and spring was dominated by two large water systms, i.e. the higher salinity water system and Yellow Sea Warm Current and the lower salinity water system of Yellow Sea Coastal Current, due to their opposite flow directions the isohalines had a characteristic shape of S. The salinity in the surveyed area varied between 32 ~ 34.5 from December to March.

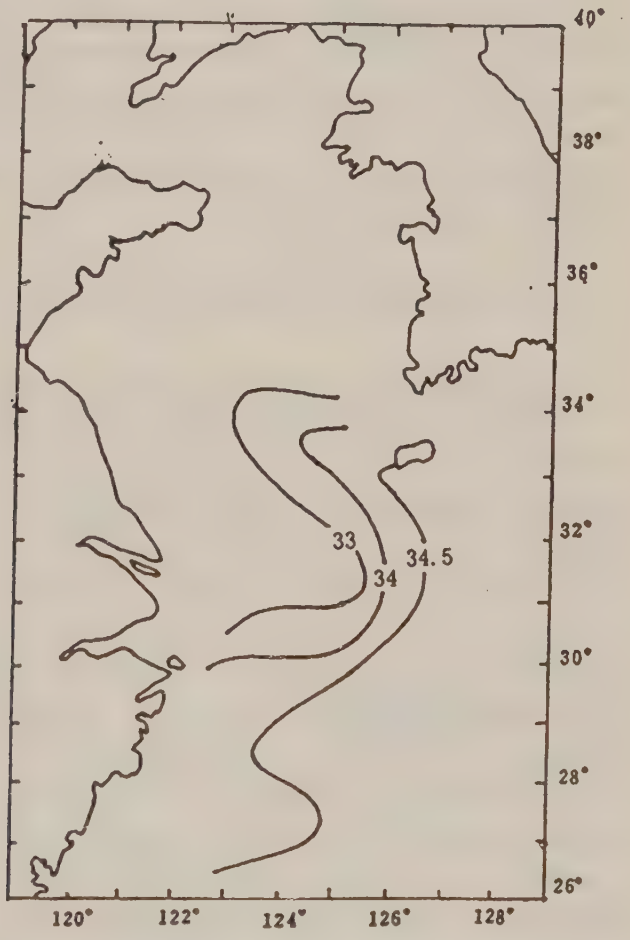

Fig.10 Distribution of bottom salinity in the surveyed area in March, 1985

In April, in the northern East China Sea the distribution of surface salinity was on the whole the same as that of bottom salinity. Although the Yellow Sea Warm Current was weaker in strength than in winter, the strength of Subei Cold Coastal Water with lower salinity was still large and the distribution

of salinity in the surveyed area was mainly dominated by it . The salinity in the area varied between 32 ~ 34.5.

In May, the distribution of surface salinity was consistent with that of bottom salinity. The isohalines roughly went in parallel direction with the coastal line and the salinity increased from inshore to open sea, indicating that the surveyed area was occupied by the coastal water with low salinity. The surface and bottom salinity varied between 30.3 ~ 32.1 and 30.3 ~ 33.1, respectively.

The vertical distributional characteristics of salinity were given below. In November and December a cold water mass existed near the bottom in the Yellow Sea a sharp halocline was observed above it. The depth of halocline was between 30 ~ 50m there were differences in strength in different years and, salinity changed at a rate of more than 0.1 per meter (Fig.2). In the rest of the surveyed area, the same through the whole water column . From January to April, the Yellow Sea Cold Water Mass no longer existed and the surface salinity was approximately equal to that of the bottom salinity. In May, due to the decrease of salinity of the upper water, a weaker halocline already occurred between the surface and the 20m depth in the area where depth is more than 30 meters. However, below the halocline the salinity was still higher like winter.

2. *Relationships between the Migration and Distribution of Anchovy and the Hyerographic Environment*

2.1 Relationship between the dense area of anchovy and the water temperature

Like other pelagic fish species, anchovy is very sensitive to the variation of temperature, and the distribution and schooling of anchovy are mainly restricted by temperature. The position and size of dense areas depended on the distribution of optimum temperature of anchovy. From November to March, the temperature in the surveyed area gradually decreased while the dense areas of anchovy from north to south(Fig.11 ~ 14). In November, the dense areas of anchovy were roughly distributed between 36°30′N ~ 38°15′N and 123°E ~ 124°30′E. In January and March, the dense areas of anchovy were mainly distributed in the front area of Yellow Sea Warm Current with a temperature of 11 ~ 13℃ in the southern Yellow Sea and the front area of Subei Coastal Cold Water with a temperature of 11 ~ 13℃ in the northern East China Sea. In March the dense areas of anchovy in the warm front area in the southern Yellow Sea were slightly east of that in January, while those in the cold front area in the northern East China Sea were closer to the shore and south of that in January.

There are both monthly variation and yearly variation of dense areas of anchovy, and the distribution of dense areas depended on the distribution pattern of isotherms. In November of 1985 and 1987, the temperature in the surveyed area was higher and the position of 11 ~ 13℃ isotherms was in higher latitudes and so were the dense areas of anchovy whose central position was at 37°41′N, 123°40′E in 1985 and at 38°00′N, 123°10′E in 1987 . In November of 1986, the position of 11 ~ 13℃ isotherms was in lower latitudes and the horizontal gradient of temperature was smaller, thus resalting in three dense areas of anchovy in the northern and central Yellow Sea. Except that the central position of the northern one was at 38°10′N, 122°20′E, the remaining two dense areas were south of those in 1985

and 1987, their central positions at 36°55′N, 123°35′E and 36°15′N, 122°55′E respectively. In January and March from 1985 to 1987 the annual variation in the central position of dense areas of anchovy was also very evident. Generally speaking, in a colder year the dense areas of anchovy were to the south and in a warmer year, east of those.

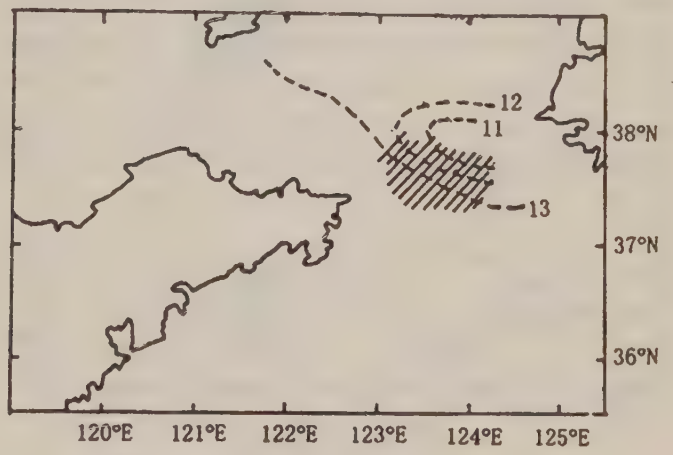

Fig.11 Relationship between the dense areas of anchovy and temperature at the 20m depth in November, 1985

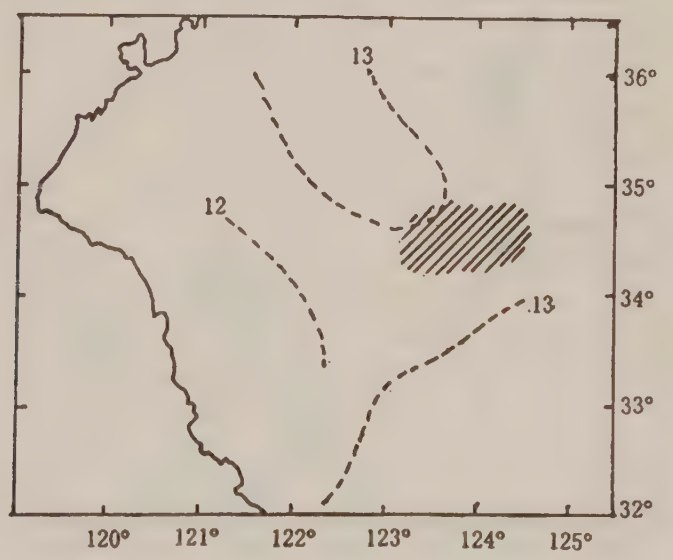

Fig.12 Relationship between the dense areas of anchovy and temperature at the 20m depth in, December 1985

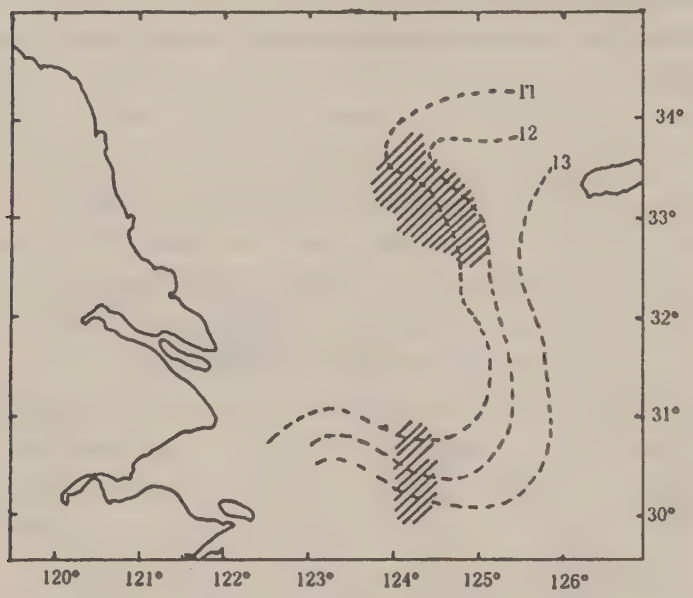

Fig.13 Relationship between the dense areas of anchovy and temperature at the 20m depth in January, 1986

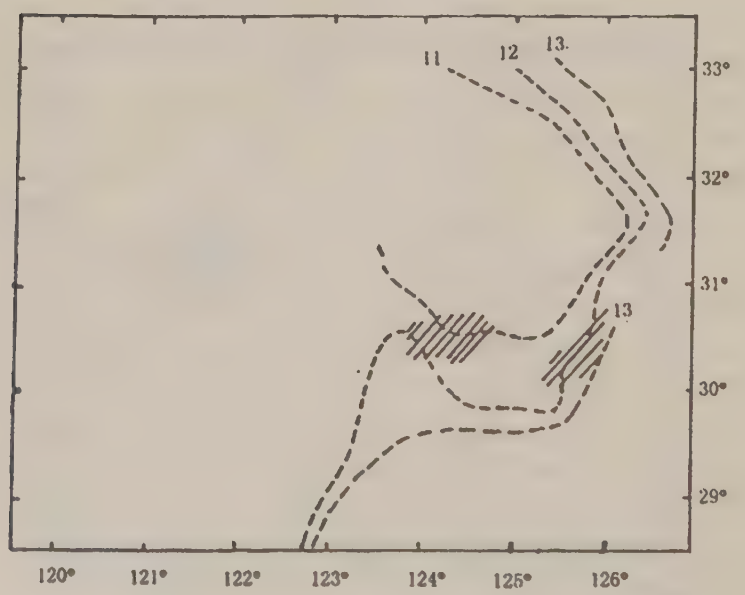

Fig.14 Relationship between the dense areas of anchovy and temperature at the 20m depth in March, 1987

2.2 Relationship between the dense areas of anchovy and the circulation system in the Yellow Sea and East China Sea

The favourable temperature of wintering anchovy was approximately 7 ~ 15℃ and the optimum temperature was between 11 ~ 13℃. Besides the water temperature, the circulation condition and horizontal gradient of temperature have an important effect on the distribution of dense areas of anchovy. In general, the highest concentrations were found in the cold or warm front areas with optimum temperature and sharp horizontal gradient of temperature. In addition, there seems to be a close relationship between the dense areas of anchovy and the whole circulation system in the Yellow Sea and East China Sea in winter(Ma Shaosai, 1989, Zhu Deshan, 1990 and Su Yusong, 1986) and from November to March they were nearly distributed on the current axis of Yellow Sea Circulation(Fig.15).

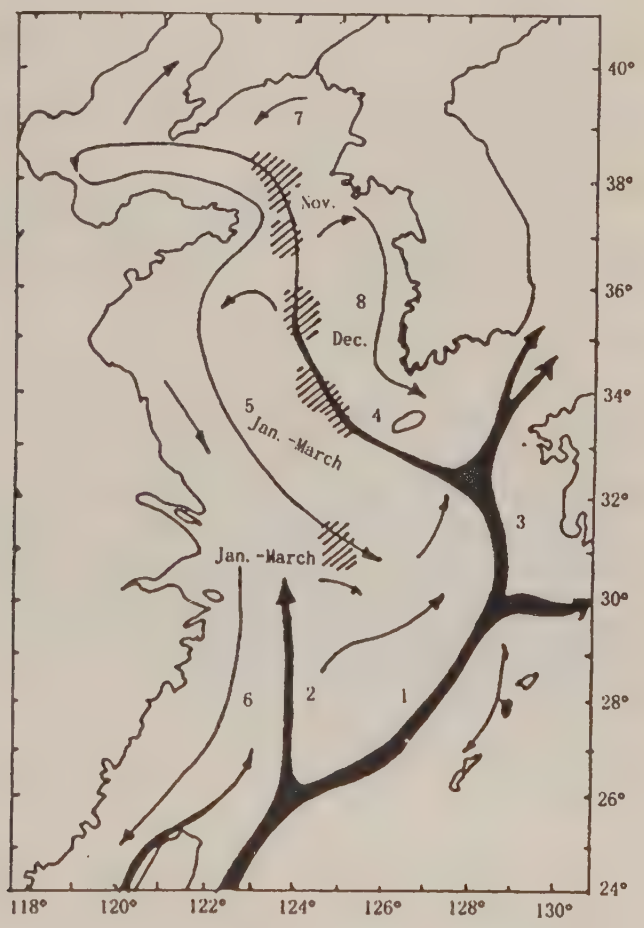

Fig.15 Relationship between the dense areas of anchovy and the circulation systems in winter

2.3 Relationship between the vertical migration of anchovy and the thermo halocline

According to the echo recording of anchovy, it can be seen that during the day and night anchovy had a sharp vertical migration. In the homogeneous areas, in day time anchovy mainly appeared in dense schools at the middle and lower depths or close to the bottom, at nighttime they were scattered in the middle and upper layers. In January and March, in the southern Yellw Sea and northern East China Sea the vertical migration of anchovy basically conformed to the above-mentioned law. However, in the area where a thermo-halocline existed, they were usually distributed above it. In November and December, there was a stronger thermo-halocline in the area dominated by the Yellow Sea Cold Watermass(Fig.2), whether in daytime or at nighttime anchovy seldom passed through the thermohalocline and entered the cold water area colse to the bottom.

He Chengben, et al., 1959. The preliminary study of formation and characteristics of Yellow Sea Cold Watermass, *Oceannologia et Liminologia Sinica*, 2(1):11 ~ 15.

Li Fengqi et al., 1987. Analysis on some characteristics of the warm current in the Yellow Sea, *Transantions of Oceanology and Liminology*, 4:1 ~ 5.

Ma Shaosai, 1989. Relationship between distribution of the wintering anchovy and hydrographic conditions in the Yellow Sea and East China Sea, *Journal of Fisheries of China*, 14(3):201 ~ 205.

Ma Shaosai, 1993. Hydrologic conditions of continental slope waters of East China Sea in the winter and the influence on fisheries, *Marine Fisheries Research*, 14:65 ~ 70.

Su Yusong, 1986. General situation of geographical environment, circulation system and central fishing grounds in the Yellow Sea and East China Sea, *Journal of Shandong College of Oceanology*, 16(1):14 ~ 23

Su Yusong et al., 1989. Formation and seasonal variation of bottom cold water mass in the northern East China Sea, *Journal of Ocean University of Qingdao*, 19(1-2):1 ~ 13.

Wang Sijie et al., 1985. A preliminary analysis of distribution features and variation situation of salinity in the southern Huanghai Sea and northern East China Sea, *Transactions of Oceanology and Liminology*, 4:8 ~ 17.

Wu Yusong, 1989. A survey of geographical environment circulation system in the Huanghai Sea and East China Sea, *Journal of Ocean University of Qingdao*, 19(1-2):145 ~ 155.

Zhu Deshan et al., 1990. Anchovy and other fish resources in the Yellow Sea and East China sea November 1984-April 1988, *Marine Fisheries Research*, 11:1 ~ 141.

Sporopollen Assemblage Characteristics of Surface Sediments in Offshore Area of Western Bohai Sea

Xu Jiasheng[1] and Sun Tingzhi[2]

[1] *First Institute of Oceanography, SOA, Qingdao*

[2] *North Sea Branch of SOA, Qingdao*

Abstract The sporopollen analysis has been made of the 788 samples of the surface sediments collected from the offshore water ares of the western Bohai Sea in this paper. Abundant sporopollen is found and three regions of sporopollen assemblage with distinctive features are identified. They are Pinus-Artemisis-Quercus assemblage region in the sea area of Shanhaiguan-Yanghekou; Pinus-Chenopoeliaceae-Artemisia assemblage region in the sea area of Yanghekou-Nanbao and Chenopodiaceae-Artemisia-Pinus assemblage region in the sea area of Nanbao = Dakouhe. After analysis of and discussion on each assemblage region, it is found that sporopollen assemblages in the sea areas are not only controlled by the coastal vegetation, but also by other natural factors. In this paper emphasis is placed on the influence of the river on sporopollen assemblage. The sporopollen assemblage division proposed in this paper will provide very useful inspiration for dividing the sediment types and studying the hydrodynamic mechanism of the sea area in this area from now on.

Introduction

Belonging to the Cenozoic depressed basin, the west coast of the Bohai Sea is an important sea area for studying the modern sedimentation of China. In this area the sedimentary thickness is greater and the modern sediments are well developed and preserved. In Aug., 1983, a gelolgical and geomorphic investigation was made in the sea area less than 20 m deep of Qinhuangdao City, Shanhaiguan-Dahekou of Huanghua County on the west coast of Bohai Sea. The investigated area amounted to over 3000 km2 and totally 778 samples of the surface sediments were collected. By analysing plentiful sporopollen and algae have been obtained. In order to probe into the distribution pattern of sporollen and algae in the surface sediments in the offshore area of the western Bohai Sea, part of representative samloes (Fig.1) are chosen as main objects of this study.

A Survey of Coastal Vegetation

Firstly, it is necessary to describe briefly the coastal vegetation in order to study the distribution of sporopollen in the sediments in this sea area.

with a high salt content, much mud and the flat relief, the coastal soil of the western Bohai Sea is not favorable for growing trees but herbs and there are few varieties of vegetation. The vegetation on the continental margin og Shanhaiguan-Qinghuangeao-Beidaihe is dominated by the coniferous and broad-

leaf mixed forest consisting of pines and asks. Secondly, some deciduous bush, arbor and other xylophytae which are common in North China are also found. Along the coast, especially on the tidal flat near the high tidal level, there grow some salt-resistant herbs, such as Chenopoeliaceae and *Artemisial*.

The vegetation from Yanghekou to Nanbao is dominated by herbs, with many Gramineae, Chenopoliaceae and Compositae plants. But naturally growing xylophytae are fewer, with only some poplars, willows and elms artificially cultivated as well as some bushes such as false indigo, etc. which are used to keep off sand blown by the wind.

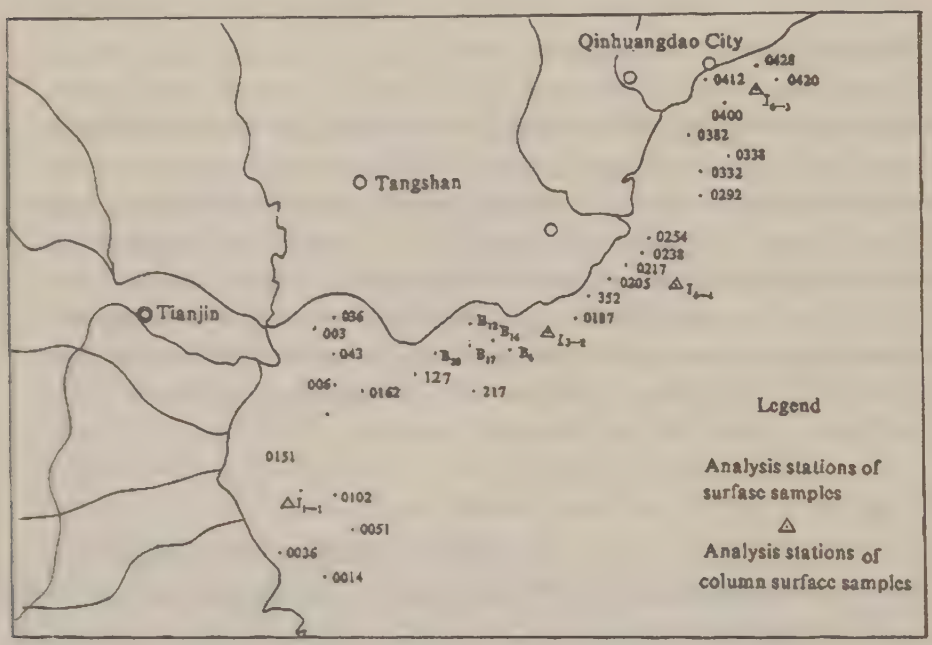

Fig. 1 Stations for sporopollen analysis of nearshore area of the western Bohai Sea

The vegetation from Nanbao to Dahekou is dominated by the salt-resistant herbs such as Chenopodiaceae, Compositae and so on. The alkaline bitter fleabane and wild wormwood are main components, and the mature wormwoos takes up a certain number. Xylophyta is dominated by the artificially-cultivated poplars, Chinese scholartrees, elms and mulberries, which are far from the shore. There is a lush growth of bush such as narrow-leaved oleaster, Chinese tamarisk, etc. on the shell bank from Qikou to Langtuozi.

Division of Sporopollen Assemblage and Its Characteristics

The surface sediments in the offshore area of the western Bohai Sea are rich in sporopollen, and the less content occurs only in a few sedimentary samples. From about the 50 samples of sporopollen

analysed, over 6000 grains of sporopollen and algae, belonging to about 50 different genera and species, are gained in total. From the samples of surface sediments from the entire western Bohai Sea, the main components of sporopollen and algae in this area are: *Pinus*, *Larix*, Cupressaceae, *Betula*, *Alnus*, *Morus*, *Quercus*, *Juglans*, *Tilia*, *Ulmus*, *Pterocarya*, Compositae, Gramineae, Cyperaceae, Chenopodiaceae, *Typha*, Sparganiaceae, *Pediastrum*, *Zygnema*, etc.

Based on the analytical results of sporopollen from the surface sediments, the nearshore area of the western Bohai Sea can be divided into three sporopollen assemblage areas of the northeast, the center and the southwest (Fig.2).

The Norhteast Area, *Pinus-Artemisia-Quercus* Assemblage Area

The main sporopollen and algae of this assemblage are as follows: *Pinus*, Cupressaceae, Taxodiaceae, *Juglans*, *Betula*, *Quercus*, Compositae, *Artemisia*, Chenopodiaceae, Gramineae, *Pteris*, *Pteridium*, Polypodiaceae, *Hystrichosphaera*, etc.

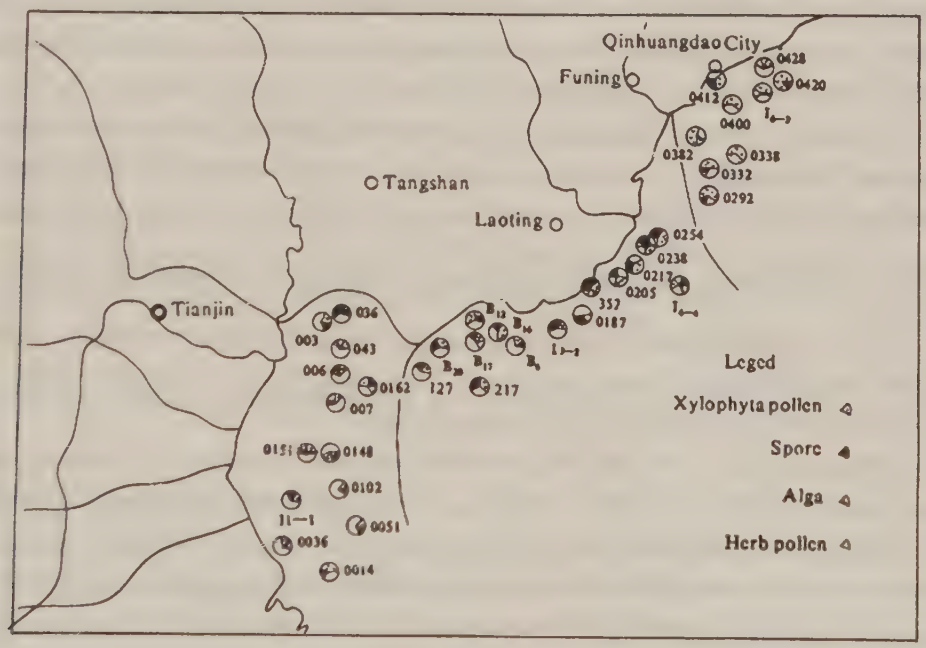

Fig.2 Sporopollen contents and its division in the nearshore area of the western Bohai Sea

As a hill area of the remaining range of Yanshan Mountain, this region is a vegetation area with the coniferous and broadleaf mixed forest and it is dominated by pollen of *Pinus* and *Quercus* (Xu, 1997). The pollen content of xyiophyta is higher, with an average content of 45.3% and the maximum one of 84.6%, and there are more plentiful genera and species. Besides *Pinus* and *Quercus*, Cupressaceae, *Betula*, *Juglans*, *Pterocarya*, *Alnus*, etc. are found. The content of herb pollen in the area

is lower, with an average content of 23.7% and the maximum one up to 40.8%. They are mainly the salt-resistant Chenopodiaceae, Compositae, *Artemisia* as well as Gramineae and others growing on the beach. The sporopollen content in the area ranges from 5.7% to 51.0%, with an average content of about 29.0%, mainly *Peteris* and *Polypodiaceae*. There are only a fewer algae, minly small *Hystricho-sphaera*, in this area. Tts normal content is 0.6-3.2%, with a maximum content of 3.2% and the average one of 1.9%.

From the facts mentioned above, it can be seen that sporopollen assemblage of the surface sediments in this area is characterized by the following:

1. The xylophyta pollen dominated by *Pinus* and *Quercus* is the notable superiority in sporopollen assemblage of the surface sediments in the area.

In the nearshore area of Shanhaiguan, the content of xylophyta pollen amounts to 45.3%, xylophyta in the whole area occupies a dominant position in sporopollen assemblage. Pollen of *Pinus* and *Quercus*, the dominant species, takes up 86.8% in xylophyta.

This is mainly because the coast of this area is located at the hilly country, and under the influence of vegetation of the coniferous and broadleaf mixed forest, the xylophyta pollen is domicant in the surface sediments in this area. This feature is only present in this region which is an only one with a high content of xylophyta pollen in the nearshore area of the western Bohai Sea.

2. The content of herb pollen in this region is lower, generally 28.8% and dominated by the salt-resistant Chenopodiaceae, *Artemisia* and so on. This is mainly resulted from the salt-resistant Chenopodiaceae, Conpositae, *Artemisia* and other herb plants growing on the beach of the region.

The Central Area, *Pinus*-Chenopodiaceae-*Artermisia* Assemblage Region

The assemblage region is distributed in the sea area from Yanghekou to Nanbao, and the Luanhe River with much sand and being apt to change is mainly active in the coast of this region. Several major components in this assemblage region are as follows:

Pinus, Cupressaceae, Taxodiaceae, *Betula*, *Quercus*, Compositae, *Artemisia*, Chenopodiaceae, Granineae, *Pteris*, *Pteridium*, Rubiaceae, *Hystrichospheera*, *Concentricystes*, *Pediastrum*, etc.

In the sporopollen assemblage of the sediments in this area, the herb pollen occupies an obvious dominant position, mainly Chenopodiaceae and *Artemisia*, and its content is up to 40.7%. In this region, the content of xylophyta pollen amounts to 33.2% and the genera and species are more monotonous, mainly pollen of *Pinus*. The content of *Pinus* pollen takes up 70% of that of xylophyta pollen in this region. A little pollen of Cupressaceae is found and so is the pollen of the broadleaf trees. In this region, the spore content is also higher, up to 0.1-28.6%, with an and Polypodiaceae. The pollen of hydrophyte also occupies a certain amount, mainly Sparganiaceae, *Peteris* and other plants growing in the river, lake and marsh. Its content takes up over 1.7-3.5% of that of herb pollen in this region. Algae are in a proper ratio in the region, mainly the sea *Hystrichosphaera* and some river and lake algae, such as *Concentricystes*, *Zygnema* and so on. Its content is about 2.1%.

From the assemblage described above, we can see that this region has the following features:

1. It is obviously dominated by herb pollen, which is resulted from the fact that this region is situated at the salt grassy marshland zone of the northwestern coast of the Bohai Bay. Although herb pollen is dominant in the surface sediments of this region, the content of herb pollen varies greatly because of the different geographic locations of divisions, especially the Luanhe River emptying into the sea from here. This leads to a special feature of the sporopollen assemblage zone, with more hydrophyta pollen and the river and lake-type algae.

2. Since the region is located at the delta area of the Luanhe River, a large amount of sand carried by the Luanhe River empties into the sea, and at the same time, a great quantity of hydrophyta pollen being not apt to hover is continuously carried into the sea, which makes the hydrophyta polen on the land occur in the sediments in the sea area, so the hydrophyta pollen takes up a certain proportion in this region. In the delta area of the Luanhe River, a large amount of hydrophyta pollen is carried into the sea by the river because of influence of the river, and then *Typha*, Sparganiaceae and other hydrophyta pollen are usually found in the beach area off the Luanhe River mouth. Nowadays Caofeidian area is a semi-closed lagoon, but some *Typha*, Sparganiaceae and other hydrophyta pollen are also discovered in the seiments, with a content of 1.7-3.5%. Thus it can be seen that the Luanhe River empties into the sea from Caofeidian, and the hydrophyta pollen is the trace left by the river.

In the sporollen assemblage of this region, the content of the land algae is higher, and the river- and lake-type algae are mainly the following three varieties: *Concentricystes*, *Pediastrum* and *Zygnema*. They are mainly distributed in the estuarine area, with a content of 1.1% generally. In the discarded Luanhe mouth and Caofeidian area, their content is up to over 2.5%, which also indicates that Caofeidian was once closely related to the Luanhe River. The more plentiful hydrophyta pollen and the river-and lake = type algae occurring in this region reflect the characteristics of deposition of the Luanhe River mouth, which forms and obvious feature of sporopollen assemblage in this region.

The Southwestern Region, Chenopodiaceae-*Artemisia-Pinus* Assemblage Area

This region is located in the sea area from Nanbao to Dakouhe, and this assemblage mainly includes the following several sporopollens:

Pinus, Cupressaceae, *Betula*, *Quercus*, *Gramineae*, Compositae, *Artemisia*, Chenopodiaceae, Amarantheae, Polypodiaceae, *Pteris*, *Pteridium*, *Hystrichospheara*, *Concentricystes*, etc.

This region is dominated by herb pollen, with an average content of 56.6% and the major components are the saly-resistant Chenopodiaceae and *Artemisia*. The content of xylophyta pollen in this region is much lower, mainly *Pinus* whose content amounts to 12.2% in the region. The content of the broadleaf trees' pollen is even more lower, with a littel *Quercus*, *Juglans* and *Betula*. Besides, it is discovered that the content of xylophyta pollen is higher in the area far from the coast and lower near the coast. The content of pteridophyta's spore in this area is closer to that of *Pinus* pollen, up to 13.9%. And it is dominated by the redeposited *Pteris* and Polypodiaceae. The content of algae, on an average, is up to 2.2% in the region, mainly the marine *Hystrichosphaera*. The content of algae obviously changes with the depth of water, that is, it increases with the increasing of the water depth, so it

amounts to 15.9% in the deepest area.

To sum up, this assemblage has the following features:

1. It is absolutely dominated by Chenopodiaceae and *Artemisia*, and there is a little other herb pollen. Since the region is a plain of the Huanghe and Haihe Rivers' delta, the relief is extremely flat, with a broad tidal flat. On the coast there are all the saline herb communities, there is little xylophyta, and the artificially-cultivated xylophyta grows sparsely only in the area far from the coast. Therefore, sporopollen assemblage is dominated absolutely by Chenopodiaceae and *Artemisia*, with an average content of 56.6%, and the content of pollen of xylophyta is very low.

2. The farther is the distance from the coast, the lower is the content of herb pollen. This is because it is difficult for the pollen to be waved for a long distance, but it is only carried into the offshore area and deposited there under the processes of river and wind. The xylophyta pollen increases with tje increasing of the distance from the coast. The content of spore, on an average, is up to 27.3% in this region, mainly *Pteris*, Polypodiaceae and *Pteridium*.

3. The content of pollen is lower in the estuarine area with the rapid sedimentation. Because of the influence of silty sedimentation of the Huanghe River, the silt is rather rapidly accumulated in the esuaries of the rivers with much silt, such as the Haihe River and Zhangweixing River. Thus, the content of sporopollen is much lower, even absent, which is an important feature of variation of sporopollen assemblage in this region. The xylophyta pollen, however, is easy to go with wind, especially *Pinus* pollen, and its output is very high. In pollen texture, *Pinus* pollen is different from others. With two air sacs and a light specific gravity, it not only goes with wind to a very far area, but also drifts with the current for a long thim when it falls on the sea surface. *Pinus* pollen, therefore, increases with the increasing of the distance from the coast (Fig.3). This is the reason that there are not many pine trees, but with a higher content of *Pinus* pollen, on the coast of this region.

4. In the surface sediments of the western Bohai Sea as a whole, the content of algae is more abundant, with a maximum one of 15.9%. The following four algae, *Hystrichospheara*, *Zygnema*, *Concentricystes*, *Pediastrum*, are mainly counted up in this paper. However, the one with a maximum content in the whole area is *Hystrichospheara* wgucg us a common alga. In general, the size of *Hystrichospheara* is 8 to 60 m, dominated by the samll *Hystrichospheara* with a short thorn and its individual is 10-15 m. In some samples a few big and middle ones are also found (Wang et al., 1980). *Dinoflagellate* with a body length of 60-80 mm is also discovered in the sea area 20 m deep.

Hystrichospheara is extensively distributed in the western Bohai Sea, and its content amounts to 2.5 around in the sea area with a water depth less than 15 m. For example, there occurs a high value in the Luanhe mouth and Caofeidian. The most common ones in this sea area are small and medium *Hystrichosphaera*. In the region, it is very senstitive for *Hystrichosphaera* to indicato the environment. Its content varies with the change of the water dopth, that is to say, the quantity increases in the deep area but decreases in the shallow area, reflecting the heightening of marine environment. In the water depth from 2 to 20 m, the contents range from 1.2 to 12.2 (Tables 1 and 2), which basically corresponds to the distribution law in the East China Sea and Huanghai Sea (Wang et al., 1979).

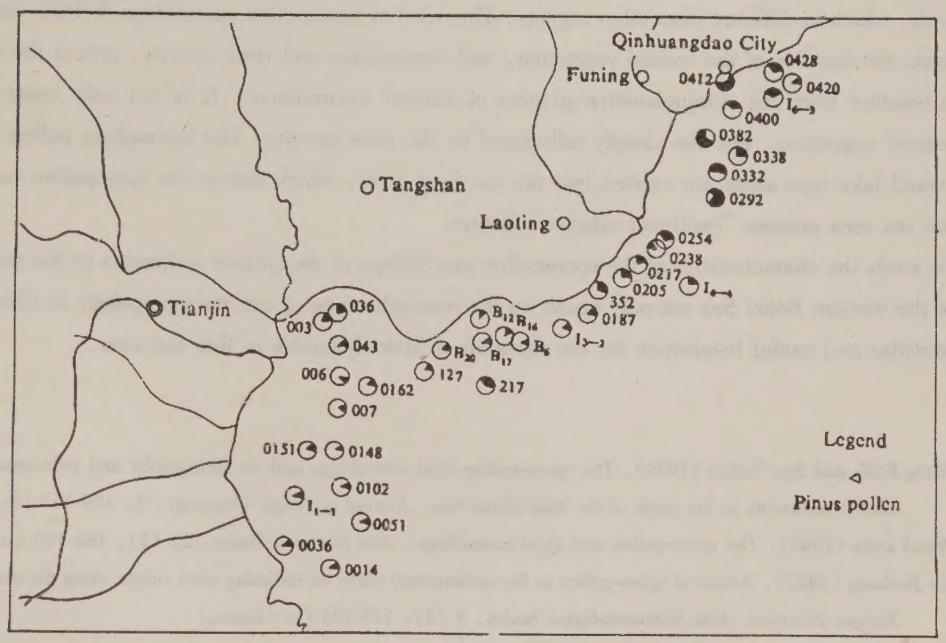

Fig.3 A map showing the content of Pinus pollen in the offshore area of the western Bohai Sea

Table 1 A relationship of distribution of algae and water depth from profile of Luanhe mouth

Station no.	0238	0254	0292	0382	0400	14-4
Depth of sea water	8.0	10.3	12.0	14.1	15.0	20.0
Contents of Hystrichosphaera(%)	1.2	2.1	4.3	5.9	6.0	12.2

Table 2 A relationship of distribution of Hystrichosphaera and water depth from profile of Caofeidian

Station no.	B12	B17	B16	352	0148	0162
Depth of sea water	2.4	3.1	3.5	ɔ.0	10.0	15.0
Contents of Hystrichosphaera(%)	1.4	1.9	2.2	3.1	3.6	4.0

From the above-mentioned analysis, it can be concluded that sporopollen in the surface sediments in the offshore area of the western Bohai Sea can be divided into three different assemblage regions with their own features. The sporopollen assemblage in the northeastern aea area from Qinhuangdao to Yanghekou is characterized by the maximum content of xylophyta pollen in the whole area; in the sporopollen assemblage in the central area from Yanghekou to Nanbao there occur more abundent hydrophyta pollen and the river-and lake-type algae which attracts people's attention, and the sporopollen assem-

blage in the southwestern sea area from Nanbao to Dakou he is characterized by the high content of herb, which is different from other regions. This kind of sporopollen assemblage division objectively reflects the features of the coastal vegetation, soil composition and river activity, and at the same time it is resulted from the comprehensive process of natural environment. It is not only controlled by the coastal vegetation, but also deeply influenced by the river activity. The hydrophyta pollen and the river-and lake-type algae are carried into the sea by a river, which makes the sporopollen assemblage in the sea area possess "continent-relative" feature.

To study the characteristics of the sporopollen assemblage in the surface sediments in the nearshore area of the westorn Bohai Sea not only opens up the research scope of marine sporopology in China. but also provides and useful inspiration for the research of hydrodynamics in this sea area.

Wang Kaifa and Sun Yuhua (1979). The spore-pollen-algal assemblage and its stratigraphy and palaeogeography in the marine sediments in the north of the East China Sea, *Journal of Tongji University*, 2: 129-152 (in Chinese).

Wand kaifa (1980), The spore-pollen and algal assemblage, *Acta Botanica Sinica*, 22 (2): 182-190 (in Chinese).

Xu Jiasheng (1987), Action of spore-pollen to the sedimentary study on radiating sand ridges along the coast of northern Jiangsu Province, *Acta Sedimentologica Sinica*, 5 (4): 147-158 (in Chinese).

Marine Science Bulletin

Marine Science Bulletin publishes papers on marine science and technology including physical oceanography, chemical oceanography, marine biology, marine geology, environmental oceanography, estuarine & coastal sciences, marine technology, digital ocean, coastal zone management, ocean engineering, marine economics, etc., and aims to promote international academic exchange.

Editor-in-Chief : Hou Wenfeng (侯文峰)
Deputy Editor-in-Chief : Lin Baofa (林宝法) Yang Ying (杨 鹰)
Executive Editor : Deng Zhiwen (邓志雯) Lu Mingsheng (卢明生)

Marine Science Bulletin (Vol.1 No.1 May 1999)

Responsible Institution:
State Oceanic Administration of China
Edited and Published Semi-annually by :
National Marine Data and Information Service
Address : 93 Liuwei Road , Hedong District , Tianjin 300171 , China
E-mail : msb@netra.nmdis.gov.cn

ISSN1000-9620
CN12-1182/N

Price: $30.00 per year